

**IMPINGEMENT HEAT TRANSFER DUE TO CIRCULAR  
AIR JET OVER ROUGH FLAT SURFACES.**

by



**Md. Nurul Islam.**

This thesis submitted to the Department of MECHANICAL ENGINEERING in partial fulfillment of the requirements of the award of the degree of,

**Master of Engineering**

in

**MECHANICAL ENGINEERING**

**Bangladesh Institute of Technology. Khulna.**

August, 2000.

**BANGLADESH INSTITUTE OF TECHNOLOGY, KHULNA.**

**DEPARTMENT OF MECHANICAL ENGINEERING**

We hereby recommend that the project report prepared by

**Md. Nurul Islam**

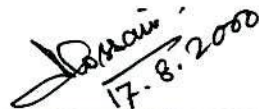
entitled "**Impingement heat transfer due to circular air jet over rough flat surfaces.**" be accepted as fulfilling this part of the requirements for the degree of Master of Engineering (Mechanical engineering ).

  
17/8/2000

**Prof. Dr. Naseem Ahmed**

Head of the Department (Mechanical Engineering)  
Bangladesh Institute of Technology, Khulna.


**Chairman**

  
17-8-2000

**Dr. Khandker Aftab Hossain**

Associate Professor ( Mech.)  
Mechanical Engineering Department  
Bangladesh Institute of Technology, Khulna

**Member (Supervisor)**

  
17-8-2000

**Prof. Dr. Nawsher Ali Moral.**

Mechanical engineering Department  
Bangladesh Institute of Technology, Khulna.

**Member**

  
17/8/2000

**Prof. Dr. M. Abu Taher Ali.**

Mechanical Engineering Department  
Bangladesh University of Engineering and Technology,  
Dhaka.

**Member (External)**

August, 2000

## Certificate of Research

This is to certify that the work presented in this thesis is out come of the investigation carried out by the candidate under the supervision of Dr. Khandker Aftab Hossain, Associate professor in the Department of Mechanical Engineering of B.I.T. Khulna, Bangladesh.

*D. Hossain*  
17.08.2020


SUPERVISOR

*[Handwritten Signature]*  
29/8/2020  
CANDIDATE

## DECLARATION

This is to certify that this work has been done by me and it was not submitted elsewhere for the award of any degree or diploma or for any publication.

Countersigned by,

  
17-8-2000  
(SUPERVISOR)

Author,

  
29/8/2000  
(MD. NURUL ISLAM)

## ACKNOWLEDGEMENT

The author is deeply indebted and much obliged to Dr. Khandkar Aftab Hossain, Associate Professor, for his valuable suggestions, inspiration, guidance and constant encouragement in carrying out this research work .

The author is very much grateful to Professor Dr. Naseem Ahmed, Head of the department Mechanical Engineering ,for his kind help at various stages of this research work and for the helpful discussion. The author is very much indebted to Professor Dr.NawsherAli Moral for his inspiration and for the helpful discussion .The author also wishes to thank Professor Dr. K.A.Kazim, Dr. A. N.M. Mizanur Rahman, Associate professor, Mr.Towhidul Islam Khan, Asstt. professor, and Mr. Ahsan Reza choudhury, lecturer (Mech.) for their inspiration.

Thanks are also due to Professor Dr. M. A. Samad, Director, B.I.T.Khulna.

Appreciation also goes to Mr. Monirul Azim , Mr. Md. Tabarak Hossain and other staff member in the department for their kind help in different stages of this project work. At last the author expresses his sincere gratitude to his wife and daughters for their encouragement and kind help during this work.

And above all, the author gives thanks to Almighty Allah for allowing him to complete his work.

Date. ..17/8/2000

Author.

DEDICATED  
TO MY PARENTS

## ABSTRACT

An experimental investigation was carried out to investigate the pressure distribution and the local and average Nusselt number due to impinging of a circular air jet over uniformly heated rough and flat surfaces. The present investigation shows the dependence of the pressure on jet exit Reynolds number, relative roughness of the surfaces and nozzle-to-surface spacings. It was observed that the overall pressure co-efficient,  $c_p$  increases with the increase of jet exit Reynolds number and decreases with the increase of surface roughness and nozzle-to-surface spacings. It also observed that the co-efficient pressure at the stagnation point remains constant for the lower values of surface roughness but increases beyond a specific value of surface roughness.

In this investigation the nature of dependence of heat transfer on various parameters namely, jet exit Reynolds number, relative roughness of the surface and nozzle-to-surface spacings are identified. Jet exit Reynolds numbers of 6000, 8700, 16520 and 23400, relative surface roughness of smooth, 0.01306, 0.01338, 0.01806, and 0.01952 and dimensionless nozzle-to-surface spacings of 1.61, 2.41, 3.22, and 4.03 are considered for the investigation. It was observed that the local Nusselt number increases with the increase of jet exit Reynolds number and surface roughness, but decreases with the increase of nozzle-to-surface spacings. It also observed that the stagnation point Nusselt number remains constant for the lower values of surface roughness but increases beyond a specific value of surface roughness, which predicts that there is a critical value of surface roughness.

The average Nusselt number was calculated and a correlation developed in terms of jet Reynolds number, relative roughness of the surface and nozzle-to-surface spacings. The correlation yields  $\pm 10\%$  accurately in context with experimental findings, however shows singularity for smooth surface.

Experimental results provided useful information which have significant of potential industrial applications regarding the radius of the heat transfer area, nozzle-to-surface spacing and surface roughness for maximizing the average Nusselt number.

# PREFACE

Air jet impingement is a common method of heating or cooling the solid surfaces. Considerable works have been done on impingement heat transfer due to air jet on flat smooth or modified surfaces but comparatively little work is found to exist on rough surfaces. For this reason, this problem was selected as project work for partial fulfillment of the requirements of the degree of Master of Engineering.

The materials presented in this report is based on the author's research experience.

However, the materials presented in this report are as follows :

In chapter-1, Introduction, motivation to select the problem, outline of the research work, jet description and surface characteristics are presented.

In chapter-2, Theory on jet and surface roughness and their measuring processes are described.

In chapter-3, the literature concerned with the impingement jet are described.

Chapter-4, is concerned with the experimental setup and experiment procedure.

Chapter-5, is concerned with the results and discussion.

Lastly, Chapter-6, is concerned with conclusion.



## CONTENTS

CHAPTER-1	INTRODUCTION.	1
1.1	General discussion	1
1.2	Objectives	2
CHAPTER-2	THEORY	3
2.1	Fluid mechanics of jet.	3
2.2	Flow phenomena of impinging jet.	4
2.3	Surface roughness and its measurement.	5
CHAPTER-3	LITERATURE REVIEW	8
3.1	General discussion	8
CHAPTER-4	EXPERIMENTAL SETUP & PROCEDURE.	13
4.1	General discussion	13
4.2	Experimental Setup	13
4.2.1	Air jet & pressure measuring arrangement.	13
4.2.2	Jet support arrangement	13
4.2.3	Transverse mechanism of impingement surface	14
4.2.4	Heater assembly including test surface	14
4.2.5	Temperature measuring arrangement	14
4.3	Experimental Technique	15
CHAPTER- 5	RESULTS AND DISCUSSION	17
5.1	General Discussion	17
5.2	Pressure Distribution	17
5.3	Heat transfer characteristics	19
5.4	Correlation of Average Nusselt number	21
CHAPTER- 6	CONCLUSION	22
6.1	General Discussion	22
6.2.1	Conclusion for pressure distribution	22
6.2.2	Conclusion for Heat Transfer characteristics	23
6.3	Scope of further work	23
Appendix-A	Sample calculation	76
REFERENCES		78

## NOMENCLATURE

A	Heat transfer area, in $m^2$ .
H	Dimensionless nozzle-to-surface spacing, $h/d$ .
L	Total radial distance over which heat transfer considered (m)
$Nu_x$	Local Nusselt number, $q.d/k_f(T-T_j)$ .
$Nu$	Average Nusselt number,
$P-P_a$	Measured pressure, $kN/m^2$ .
$Pr$	Prandtl number $\mu C_p/k_f$
R	Dimension less radial distance from stagnation point, $r/d$ .
$Re$	Reynolds number based on the diameter of the jet, $vd/v$ .
$R_o$	Dimensionless radius on heat transfer surface, $r_o/d$ .
$R_a$	Center line average roughness, in $\mu m$ .
$T_j$	Temperature of air jet ( $^{\circ}K$ ).
$T_w$	Local temperature of the heat transfer surface ( $^{\circ}K$ ).
T	Local temperature after jet impingement ( $^{\circ}K$ ).
$T_1$	Temperature of heated surface at point 1.
$T_2$	Temperature of heated surface at point 2.
$c_p$	Pressure co-efficient, $(P-P_a)/0.5\rho v_j^2$ .
d	Jet diameter in m.
$d_x$	Distance between points on rough surface (m).
$\epsilon$	Dimensionless relative roughness, $R_a/d$ .
h	Nozzle-to-surface distance in m.
$k_f$	Thermal conductivity of fluid (air). ( $W/m \cdot ^{\circ}K$ )
$k_s$	Thermal conductivity of surface .
q	Surface heat flux ( $k W/m^2$ )
r	Radial distance from stagnation point, in m.
$r_o$	Radius of the jet, in m.
v	Velocity of air jet in m/sec.
$U_x$	Shear velocity of fluid.
<b>GREEK ALPHABETS</b>	
$\theta$	Dimensionless temperature, $(T-T_j)/(T_w-T_j)$ .
$\rho$	Air density in $kg/m^3$ .
$\mu$	Dynamic viscosity of air in $kg/m \cdot sec$
$\nu$	Kinematic viscosity of air in $kg/m \cdot sec$ .
$\gamma$	Specific weight of manometric fluid of manometer in $N/m^3$ .

## LIST OF FIGURES

Figure No.	Figure
2.1	Schematic diagram of a free impinging jet system
4.1	A schematic diagram of the Experimental setup.
4.2	Instrumented test section and thermocouple arrangement
4.3	Photographic view of the Experimental setup.
5.1.1-5.1.4	Distribution of pressure co-efficient $C_p$ over surfaces of different roughness for a Reynolds number and at nozzle-to-surface spacing, $H=1.61$ .
5.1.5-5.1.7	Distribution of pressure co-efficient $C_p$ over surfaces of different roughness at various Reynolds numbers and at various nozzle-to-surface spacings
5.1.8-5.1.12	Distribution of pressure co-efficient $C_p$ for different Reynolds numbers over various surfaces for a specific nozzle-to-surface spacing.
5.1.13-5.1.15	Distribution of pressure co-efficient $C_p$ for various Reynolds numbers over a surface and for a nozzle-to-surface spacing.
5.1.16-5.1.20	Distribution of pressure co-efficient $C_p$ for different nozzle-to-surface spacings over a surface of a specific roughness and for a specific Reynolds number
5.1.21-5.1.23	Distribution of pressure co-efficient $C_p$ for different nozzle-to-surface spacing over a surface of a specific roughness and for a Reynolds number.
5.2.1-5.2.4	Distribution of Nusselt number over surfaces of different roughness for a Reynolds number and for a specific nozzle-to-surface spacing.
5.2.5-5.2.7	Distribution of Nusselt number for a specific Reynolds number over the surfaces of different roughness and for different nozzle-to-surface spacings.
5.2.8-5.2.12	Distribution of Nusselt number for different Reynolds number over a surface and for a specific nozzle-to-surface spacing.
5.2.13-5.2.15	Distribution of Nusselt number for various Reynolds number over a surface of specific roughness, $\epsilon = 0.01338$ and at a nozzle-to-surface spacing.
5.2.16-5.2.20	Distribution of Nusselt number for different nozzle-to-surface spacings over a surface and at a specific Reynolds number, $Re=16500$ .
5.2.21-5.2.23	Distribution of Nusselt number for different nozzle-to-surface spacings over a surface of specific roughness, $\epsilon = 0.01816$ and at a Reynolds number.
5.3.	Calculated Average Nusselt Number Vs. Measured Average Nusselt Number plot.
5.4.	Calculated Average Nusselt Number Vs. Measured Average Nusselt Number comparison curve.

**CHAPTER- ONE**  
**INTRODUCTION**

# CHAPTER ONE

## INTRODUCTION

### 1.1. GENERAL

Jet impingement is a common method of heating or cooling the solid surfaces. Heat transfer under impinging jet is generally superior to that of conventional methods. Because, fluid flow in the form of jet impingement drastically increases its momentum. In turbulent flow, the molecules in the flowing fluid move in a random manner. The molecules of flowing fluid transfer momentum and energy from one place to another by mixing of the fluid particle, typically termed as eddy mixing. Generally the rate of heat transfer is high in turbulent flow because of increased and random mixing. Thus, most practical application of jet impingement occur in industries, where the heat transfer requirements have exceeded the capacity of ordinary heating and cooling techniques. Industrial jet impingement includes, drying of paper, textiles and veneer, tempering of glass, annealing of metals and cooling of gas turbine blades, electronic components and drying of films in film industries, vapor deposition on cylindrical surface in combustion chamber, exhaust of effluents in power plants.

Numerous investigations have been reported in last few decades emphasized on various aspects of fluid mechanics and heat transfer of impinging jet. However, most of the earlier studies are confined with jet impingement on smooth surfaces. Recently, jet impinging on arrays of block mounted on other flat surfaces has attracted considerable attention. Many investigators have observed that relatively high heat transfer characteristics of impinging jet is associated with high turbulence levels in the flow of fluid.

A variety of turbulence promoting schemes have been used to enhance heat transfer. The new investigation of jet impingement combined with extended and modified surfaces have shown promising results. The present study has been encountered to investigate the pressure distribution and heat transfer characteristics due to impingement of circular air jet over flat smooth and rough surfaces. In this case, heat transfer between uniformly heated rough flat surfaces and impinging circular air jet was investigated experimentally to determine the values of local and average Nusselt numbers and pressure distribution. Different jet exit Reynolds numbers, nozzle-to-surface spacings and roughness of sheet surfaces have been considered to identify their influence on pressure distribution and heat transfer.

## 1.2. OBJECTIVES

The study of impingement heat transfer due to circular air jet is important due to its numerous practical engineering applications. In previous significant amount of work has been done on impingement heat transfer due to jet of air on flat smooth or modified surfaces. In the literature no remarkable work is found related to distribution of pressure and heat transfer over rough surfaces. This is one of the prime motivations behind the present investigation. The objectives of the present investigation are as follows :

1. Investigation of the pressure distribution for impinging jet of air over smooth and rough surfaces at various nozzle-to-surface spacings, jet exit Reynolds numbers and surface roughnesses and compare the obtained results with smooth surface.
2. Investigation of the local temperature of each sheet at various nozzle-to-surface spacings, jet exit Reynolds numbers and surface roughnesses.
3. To calculate the local and average Nusselt numbers over rough surfaces.
4. To develop a correlation for average Nusselt number in terms of surface roughness of the impingement surface, jet exit Reynolds number and nozzle-to-surface spacings.

**CHAPTER-TWO**

**THEORY**

# CHAPTER TWO

## [THEORY]

**2.1. Fluid Mechanics of Jet:** A jet is created by the flow of fluid through an orifice or nozzle into the stagnant reservoir or co-current stream of fluids. Jets are of three types, namely,

1. Confined or Bounded jet
2. Wall jet
3. Free jet

**2.1.1 Confined or Bounded jet:** In the case of bounded jet the fluid is discharged from a nozzle or an orifice into a confined region bounded by solid surface. So, no entrainment will add to the main stream.

**2.1.2 Wall jet:** When fluid flows from an opening over the solid surface along the axis of the jet and parallel to the solid surface than a wall jet is formed. Entrainment will add to the main flow stream. Therefore, momentum of the main flow will increase.

**2.1.3 Free jet:** It forms when the jet flows in an infinite fluid reservoir having no influence or contact of solid surface. Entrainment will influence the main flow stream. Free jets are:

**2.1.3.1. Plane jet:** Fluid is discharged from a plane nozzle of large length into a large stagnant mass of the same fluid.

**2.1.3.2. Axisymmetric jet:** Fluid is discharged from a circular nozzle, orifice or pipe into a large stagnant mass of the same fluid. The jet spreads axially and radially in the surrounding fluid only.



**2.1.3.3. Cross flow jet :** Any free jet when discharged in a moving stream of fluid whose direction is other than parallel to the axis of the jet.

**2.2. Flow phenomena of impinging jet :** When a free jet impinges on a flat solid surface as shown in Figure 2.1, the entire flow field is conventionally divided into four regions,

- 1) the potential core region
- 2) the free jet region,
- 3) the stagnation region
- 4) the wall jet region.

1) **Potential core region :** In this region, the velocity at every point have the same magnitude as the nozzle exit velocity are considered as the inviscid fluid. The velocity of jet is self-preserving. This region retains 5 to 6 times the jet diameter from the nozzle exit.

2) **Free jet region :** In the free jet region, the jet flows freely after potential core region . In the free jet region, the fluid mixes with the surrounding fluid and the flow is considered as inviscid flow. But jet spreads slightly laterally and becomes thicker.

3) **Stagnation region:** In the stagnation region, the jet strikes the solid surface and the velocity of flow grows rapidly from zero at the stagnation point to the jet velocity within one jet diameter. The radial dimension of the stagnation region is of the order of the jet radius  $r_0$  and the boundary layer thickness is of the order of  $(\sqrt{\nu r_0 / U_0})$ , where  $\nu$  is the kinematic viscosity of the fluid.

4.) **Boundary layer region:** In the boundary layer region, where the radial distance is greater than  $r_0$  . In this region, the velocity outside the boundary layer remains constant and the flow is of the boundary layer type.

5) **Transition region:** In the transition region where the boundary layer becomes as thick as the whole fluid layer. The boundary layer reaches the free surface and the viscous stresses become important for the whole flow field. In this region the Blasius type velocity profile does not exist.

6) **Similarity region:** In the similarity region where the whole flow is of the boundary layer type and there exists a similarity solution to the velocity field. In this region, the flow becomes independent of the way in which it originated, that is, the influence of jet geometry and initial condition completely vanishes.

The impinging jet behaves essentially like a free jet ahead of stagnation point. The pressure does not remain constant. Pressure increases as the flow approaches the stagnation region. The mixing induced turbulence, penetrates towards the center of the jet. The potential core extends up to 5 to 6 times the nozzle diameter for a circular jet. The turbulence intensity has two peaks as either sides of the jet exit. As the width of potential core decreases, the peaks move closer to the axis of the jet. A turbulent jet has fully developed turbulence at the end of potential core region and the turbulence intensity reaches a peak value. The centerline velocity beyond this point in turbulent jet, decays as  $(x/d)^{-1}$  for a circular jet. Ultimately a wall jet region is formed.

**2.3. Surface roughness and its measurement :-** A little consideration will show that surfaces produced by different machining operations are of different characteristics. They show a remarkable variation when compared with each other. The variations are judged by the degree of smoothness. A surface produced by super finishing is the smoothest while that by planing is the roughest. In the assembly of two mating parts, it becomes absolutely necessary to describe the surface finish in quantitative terms which is the measure of micro-irregularities of the surface and expressed in microns.

**Classification of Rough surfaces:** The surface roughness encountered in practice vary in their shape, size, distribution and arrangement, micro-scopical surface property, characteristics behavior with flow etc. For convenience they are classified as follows.

The roughness formed by sand particles or stone chips are called sand roughness. Nikurades [33] described the sand roughness from technical point of view. The average absolute protrusion height of the roughness elements or the relative roughness heights with respect to some significant length are used to describe such roughness.

Rib roughnesses are employed by putting rectangular or cylindrical ribs on the surface transverse to the flow direction. Depending on the ratio of the height of the roughness ribs and pitch, such roughness can be divided into D- type and K-type roughness. When the error in the origin is proportional to the height of the roughness elements then the roughness is called K-type or sand grain roughness. For a D-type roughness the error in origin is a linear function of the distance in the downstream direction. For specific engineering purposes the roughness elements for different geometrical shape are sometimes used, these are defined by their characteristic length. Another type of roughness termed as “tuft roughness” are also sometimes encountered. The examples of these types of roughness are grassy lands, green bushes, cornfields, green mosses grown in the ship hull. The behavior of these types of roughness varies with the flow velocity and hence their analysis becomes complicated. The tuft roughness elements may show sticking character due to capillary action of narrow space present in between the fibers.

Different types of roughness can again be divided into two types, depending on how the surface roughness change is brought about. If the crest of the roughness elements lie above the preceding smooth surface, it is termed as upstanding surface roughness and if the crests lie below the smooth surface it is termed as the depressed type surface roughness.

The surface roughness of all types can again be expressed in terms of “equivalent sand grain roughness” as proposed by Nikuradse.

A surface is said to be hydraulically smooth when the roughness protrusions are contained within the laminar sublayer and it is said to be rough when the protrusions are partly outside laminar sub layer. This is indicated by the roughness Reynolds number,  $k_s v / \nu$ .

$0 < (K_s U^* / \nu) < 5$	hydraulically smooth regime
$5 < (K_s U^* / \nu) < 70$	transition regime
$(K_s U^* / \nu) > 70$	hydraulically rough

There are many ways of calculating the surface roughness mathematically, but the following two methods are commonly used:

1. Centerline Average Method (C.L.A.method)
2. Root Mean Square Method (R.M.S.method)

**Center line average method**:- The center line average method is defined as the average value of the ordinates between the surface and the mean line, measured on both sides of it. The surface finish is measured in terms of C.L.A. value and it is denoted by Ra. Mathematically, C.L.A.or

$$R_a \text{ (in microns)} = \frac{h_1+h_2+h_3+\dots+h_n}{n}$$

where,  $h_1, h_2, h_3, \dots, h_n$ , are the ordinates measured on both sides of the mean line and 1, 2, 3, ..., n, are the number of ordinates.

This method is conventionally used to measure or calculate the surface roughness.

**Root mean square method** :- The root mean square method is defined as the square root of the arithmetic mean of the square of the ordinates. Mathematically,

$$R.M.S. \text{ (in microns)} = \sqrt{\frac{h_1^2+h_2^2+h_3^2+\dots+h_n^2}{n}}$$

where,  $h_1, h_2, h_3, \dots, h_n$  are the ordinates measured on both sides of the mean line and n is the number of ordinates.

**CHAPTER-THREE**

**LITERATURE REVIEW**

# CHAPTER-THREE

## LITERATURE-REVIEW

### 3.1.GENERAL.

The body of impingement jet literature is large. Most early works concentrated on jets impinging on smooth flat surfaces. Jet impingement on smooth, curved surfaces also has been investigated.

Gardon and Akfirat [10], have investigated the effect of turbulence on local heat transfer coefficient of impinging jets. They concluded that the heat transfer characteristics of impinging jets couldn't be explained in terms of velocity and position dependent boundary layer alone, but by accounting for the influence of turbulence. They later appeared to be uniquely dependent on the jet Reynolds number.

Goldstein et al.[12] experimentally investigated the heat transfer between a single circular air jet impinging on a heated flat plate that is 0.2405m wide and 0.107m long. In these high Reynolds number experiments( $6.2 \times 10^4 \leq Re \leq 1.24 \times 10^5$ ), the maximum stagnation Nusselt number(at  $R=0$ ) occurred at  $H \sim 8$ , which is slightly higher than earlier values,  $H \sim 6-7$ , by Gardon[11] and  $H \sim 6$  by Tataoka[41].

Jambunathan et al [24] did a detailed survey on the impingement cooling of a single air jet. They concluded that the simplest correlation's for local convective heat transfer co-efficient is a function of the Reynolds number,  $h/d$ ,  $r/d$  and the Prandtl number.

Bouchez and Goldstien [5], Investigated the impingement cooling of a circular jet with/without a cross flow. It was found that as the jet- to- crossflow mass flux ratio decreases within a moderate range, the stagnation point will be deflected by the cross flow; consequently the stagnation point moves down stream. As the jet-to-cross mass flux ratio increases a recirculation and mixing zone was visualized. In the experiment the surface heat flux was in the

range of 320-1200  $\text{w/m}^2$  and the jet spacing to-diameter ratio was arranged to be 6 and 12 respectively, since the surface heat flux is low and the jet spacing to- diameter ratio is high. The convective heat transfer co-efficient was found to be almost irrelevant to the surface heat flux.

Sparrow et al [37], investigated the heat transfer of a vertical confined impinging circular jet with a crossflow. The velocity of the crossflow was fixed at 12 m/s and the jet mean velocity was varied. It was found that the convective heat transfer coefficient with jet impingement can be ten times higher than that without an impinging jet. In the result the convective heat transfer coefficient was represented as a function of the jet to cross flow mass flux ratio, the location and the jet spacing to diameter ratio. For a mass flux ratio more than eight, an optimum jet spacing-to-diameter ratio was clearly observed. The optimum ratio corresponds to a peak value of the convective heat transfer coefficient. For the condition of jet spacing-to-diameter ratio less than the optimum value, the jet is in a potential core. If so, the intensity of turbulence intensity decreases as the jet spacing to diameter ratio decreases. Thus the peak convective heat transfer coefficient descends. Alternatively as the jet spacing-to-diameter ratio is greater than the optimum value, the peak convective heat transfer coefficient also decreases due to a strong mixing effect.

The heat transfer of an unconfined jet impinging on a flat surface with low Reynolds number and nozzle-to-surface spacing to jet diameter ratio was investigated by several investigators , as

Huang and ElGank [15], the heat transfer of an unconfined jet impinging on a flat plate with low Reynolds number and nozzle-to-surface spacing to jet diameter ratio was investigated by them. In this work the average Nusselt number was found to be proportional to  $\text{Re}^{0.76}$ . The measurement of the heat transfer of an unconfined impinging jet with the nozzle-to-surface spacing to jet diameter ratio less than 1.0 was performed by Lytle and Webb[45]. For a nozzle-to-surface spacing less than 0.25 times the jet diameter the effect of fluid acceleration between the nozzle wall and impingement surface was seen; this results in a clear observation of the secondary maxima in the Nusselt number.

Huber and Vistanta [16], investigated the effect of jet to sheet spacing on convective heat transfer to a confined impinging jet array. A thermochromatic liquid crystal technique was used to visualize and measure the isotherms on the impingement plate. They found that, for a high separation distance between the jet and impingement plate, the adjacent jet interference before impingement will cause significant degradation of the convective heat transfer coefficient. The effect of a spent air arrangement on the heat transfer was also investigated. It was found that the spent air results in a heat transfer enhancement by minimizing adjacent jet interference in the wall jet region.

The diameter dependency on the Nusselt number for a jet impinging on an isothermal plate was investigated by Hollworth and Gero[17], They investigated that , for the cases with values of  $h/d$  greater than 10, the jet diameter has no effect on the Nusselt number. Due to the limitation of the measurement, this experiment did not varify this point for cases with a lower value of  $h/d$  Stevens and Webb[38] investigated the local heat transfer coefficient for a free liquid jet impinging normally on a uniform heat flux surface. The ratio of mean jet velocity to jet diameter was proposed, in the correlation, to vanish the nozzle size dependency.

The local heat transfer from a small heat source to a normally impinging, confined and submerged liquid jet was experimentally investigated by Garimella and Rice[13], they investigated that the nozzle-to-heat source spacing, jet Reynolds number and nozzle diameter, were explored as variables. The results indicate that at the stagnation point, for a given Reynolds number and nozzle-to-heat source spacing, the smaller nozzle produces a lower Nusselt number. The correlation for the stagnation point and area-average heat transfer coefficient were expressed in terms of jet Reynolds number, fluid prandtl number, nozzle-to-heat source spacing and nozzle aspect ratio.



Jung-Yang san, Chih-Hao Huang and Ming-Hong shu [25], investigated the local Nusselt number of a confined circular air jet vertically impinging on a flat plate. The aspect ratio of the jet orifice was 1.0. four different jet hole diameters, namely 3.0, 4.0, 6.0 and 9.0 mm were considered individually. The Reynolds number, the surface heating width and the surface heat flux, on the heated area were the variables in the measurement. It was intended to realize the effect of the jet hole diameter on the heat transfer of a confined jet impingement, for various operating conditions.

Very recently, jet impinging on arrays of blocks mounted on otherwise flat surface (simulated electronic packages) have attracted considerable attention. [18-19].

A number of investigators have observed that the relatively high heat transfer characteristics of impinging jets are related to high turbulence levels in the fluid flow as found in the references 7,14, 29,32 & 36 . A variety of turbulence promoting scheme have been used to enhance jet impingement heat transfer with varying degree of success.

A few investigations of jet impingement combined with extended surfaces have reported generally promising results.

Ali Khan et al. [1] positioned a punched plate with circular holes upstream of a heated surface. Hrycak [20], studied heat transfer for a jet impinging on a smooth plate modified with spike and concentric ring proturbulances.

Obot and trabold [34], investigated arrays of jets impinging on surfaces having repeated square ribs with transverse flow of the spent air.

Hensen and Webb [21] , have performed an experiment to characterize heat transfer to a normally impinging air jet from surfaces modified with arrays of fin-type extensions. Heat transfer enhancement for six fin geometries was evaluated by comparison with results for a smooth, flat surface. Average Nusselt number and overall system effectiveness are reported as functions of fin type, jet Reynolds number, and nozzle-to-surface spacing for two nozzle

diameters. Enhancement of the absolute rate of heat transfer, as compared to the smooth surface, was demonstrated by a factor ranging from 1.5 to 4.5. The system effectiveness as a function of  $Re$  exhibited strong fin type dependence due to significant variations in the total surface area and average Nusselt number. The fin type dependence of  $Nu$  as a function of  $Re$  was found to be a result of variations in the turbulence level, fluid velocity, and the percentage of total surface area exposed to normal, oblique, and parallel flow. The average Nusselt number correlated well in the form  $Nu = C \cdot Re^m$ . For the modified surfaces, the system effectiveness decreased monotonically with increasing  $z/d$  in contrast to the smooth surface behavior.

Pressure distribution over surfaces by impinging jet has been observed by some investigators,

Hossain. K.A. and Arora. R.C. [22], described that impinging jet behaves essentially like a free jet ahead of stagnation point. The pressure does not remain constant. Pressure increases as the flow approaches the stagnation region. In the stagnation region, the center line velocity decreases to a zero value and pressure approaches to the maximum at the stagnation point.

Ali. M.A.T., Hasan.A and Islam. M.T. [2], described that, at the beginning of the rough surface the wall static pressure suddenly dropped from its smooth wall pressure gradient. Wall shear stress was found to increase more or less proportionately with the roughness height. At smooth rough junction, the roughness height caused the near wall flow to deflect upwards resulting in the production of secondary current which died out quickly away from the wall.

**CHAPTER-FOUR**

**EXPERIMENTAL SETUP**

**AND**

**PROCEDURE**

# CHAPTER-FOUR

## EXPERIMENTAL SET-UP AND PROCEDURE

### 4.1. General

The experimental program comprised with airflow, static pressure and temperature measuring devices. The details of the experimental facilities were discussed later in this chapter.

**4.2. Experimental set-up.** : The experimental set-up is shown in Figure 4.1. The different parts of the experimental setup are as follows.

- 1) Air jet and pressure measuring system.
- 2) Jet support frame.
- 3) Impingement surface with traverse mechanism.
- 4) Heater and test surface arrangement.
- 5) Temperature measuring system.

**4.2.1. Air jet and Pressure measuring arrangement.**:- The air jet was issued from a circular copper tube of inside diameter 6.2 mm. The length of the tube was 320 mm which was sufficiently larger than hydraulic diameter (120 ID) to ensure fully developed flow [9]. The jet system and its different views are shown in Figure 4.1. Photographs taken from different angles are shown in Figure 4.3.

The jet arrangement consisted of an air blower (1.5 hp) , a variac, a filter cum settling chamber, a flow straightner, a pitot tube, an inclined manometer for air, a converging nozzle and a 6.2 mm diameter copper tube.

**4.2.2. Jet support arrangement** : The jet support frame was used to adjust the elevation of the jet exit from the heated impingement surface and to maintain the jet in vertical position.

**4.2.3. Traverse mechanism of Impingement surface:** The transverse mechanism was used to hold the heater and impingement surface arrangement at suitable upper or lower position in perfectly flat position and also for center the jet with the center of the rough surface.

**4.2.4. Heater assembly including test surfaces:** The heated plate was of 0.195 mm thick (34 gage) M.S. sheet, measuring 140 mm $\times$ 140 mm ( $k = 54$  w/m.K). The sheet was laid perfectly flat on a 25.4mm thick Bakelite slab ( $k=0.23$  w/m.K ) over laid on 25.4 mm. thick cork sheet ( $k=0.42$  w/m.k) and on a temper glass sheet and the perimeter of the M.S. sheet and Bakelite was insulated by the cork sheet. The M.S. sheet was heated uniformly using two plate type heaters of 150 W, 220 v each. Heaters were connected with 220 volt a.c. supply in series. (Figure 4.2.).

Investigations were performed on 5 (five) test surfaces . One of them was smooth and others were of different roughnesses. Surfaces were artificially roughened by scribing the surfaces by scribers of various sizes in random manner. Surface roughness was measured by Dial gauge indicator and roughness was calculated by using the Center Line Average method (C.L.A method).

**4.2.5. Temperature measuring-arrangement:** Surface temperatures of the sheets were recorded by digital temperature recorders. These recorders were connected with sheets as shown in Figure 4.2.a and Figure 4.2.b. Thermocouple leads were of K-type (Cromel-Alumel) couple [26]. The thermocouple leads were inserted through the upper surface of the Bakelite slab and the ends of the thermocouple wire were soldered to maintain in a good contact with the underside of the heated sheets during the experiments.

**4.3 Experimental Technique:** Throughout the experiments the jet was centered with the center of the surface, airflow was adjusted by rotating the knob of the variac. Then velocity of the airflow was measured by Pitot tube and manometer (by which velocity of air and jet Reynolds number was calculated). Then the nozzle-to-surface spacing ( $h$ ) between the surface and nozzle exit was adjusted. At this position, pressure distribution over sheet surface due to jet of air impingement was recorded. Then heater turned on to heat the sheet and after attaining steady state condition, sheet surface temperature (before impingement), air temperature at nozzle exit, ambient temperature and sheet surface temperature (after impingement) were recorded by digital temperature recorders.

The procedure was followed for each surface (smooth,  $\epsilon = 0.01306$ ,  $\epsilon = 0.01338$ ,  $\epsilon = 0.01806$  and  $\epsilon = 0.01952$ ) at nozzle-to-surface spacing, 10 mm, 15 mm, 20 mm and 25 mm and Reynolds numbers were 6000, 8700, 16500 and 23400.

**TABLE: 1****Specification of the Instruments.**

NAME	MANUFACTURER	SPECIFICATION
1. Air Blower	Alldays & Onion Ltd. Birmingham,	hp. -1.5, Rpm-5200. Amp-1.2, Volts-220/250. 50Hz.
2. Variac	The Electric Apparatus Ltd England.	Volts-60/200, Ohm-500. Amp. -45.
3. Pitot tube	Airflow development Ltd High Wycomb, G.B.	one way
4. Inclined manometer for air.	Airflow development Ltd. High Wycomb, G.B.	Range- 0-2.5 kN/m <sup>2</sup> .
5. Plate type heater	Made in india	150 W (2 Nos.), 220 volts
6. Digital Temperature Recorder.	KKK-MC-03230240 Made in Taiwan.	0 <sup>0</sup> C - 800 <sup>0</sup> C.

**TABLE-2****Nominal Experimental Condition:**

1. Ambient temperature and pressure: 30<sup>0</sup> C ; 101.325 kN/m<sup>2</sup>.
2. Jet diameter : 6.2 mm.
3. Sheet specifications : 140mm. × 140 mm × 0.195mm.
4. Reynolds number : 6000 , 8700 , 16500 & 23400.
5. Fluid : Air at 30<sup>0</sup>C and of thermal conductivity is 0.026 w/m.K.

**CHAPTER-FIVE**

**RESULTS  
AND  
DISCUSSION**



## CHAPTER-FIVE

### RESULTS AND DISCUSSION

**5.1. General:** In the present study the pressure distribution and heat transfer over smooth and rough surfaces due to impinging circular air jet was investigated. Experiments were performed for jet Reynolds numbers 6000, 8700, 16500 and 23400 for jet diameter of 6.2 mm. The dimensionless nozzle-to-surface spacings were 1.61, 2.42, 3.22 and 4.03 and surfaces were of relative roughness, smooth, 0.01306, 0.01338, 0.01806 and 0.01952.

**5.2. Pressure Distribution :-** The pressure distribution over the surfaces of different roughness was plotted for different Reynolds number and at different nozzle-to-surface spacings, in Figure 5.1.1 to Figure 5.1.23.

**5.2.1. Effect of surface roughness on Pressure distribution:** In Figures 5.1.1 to 5.1.4, the effect of surface roughness on coefficient of pressure  $c_p$  distribution is presented at nozzle-to-surface spacing,  $H = 1.61$  and at different jet Reynolds numbers such as 6000, 8700, 16500 and 23400 with radial distance  $R$ . It was observed that the coefficient of pressure was maximum at the stagnation point for different rough surfaces and gradually decreases with the increase of radial distance from the stagnation point as shown in the Figure 5.1.1. It also observed that the coefficient of pressure,  $c_p$  was decreased with the increase of surface roughness for a particular jet exit Reynolds number and nozzle-to-surface spacings due to loss of energy of the flow. At a particular radial distance  $R = 2.5$  all the curves coincide in a single point and beyond radial distance  $R = 2.5$  all the lines coincides in a single and diffuses completely. Similar trends followed by the curves for  $Re = 8700, 16500$  and 23400.

Figures 5.1.5 to 5.1.6, presented the variation of coefficient pressure,  $c_p$  with radial distance,  $R$  at nozzle-to-surface spacing,  $H = 2.42$  and at different Reynolds numbers. It was also observed that the coefficient of pressure decreases with the increase of Reynolds number.

**5.2.2 Effect of Reynolds number on pressure distribution :** Figure 5.1.8 to 5.1.12 shows the variation of coefficient pressure,  $c_p$  with radial distance,  $r/d$  at different Reynolds numbers for smooth and rough surfaces at nozzle-to-surface spacing,  $H = 1.61$ . the coefficient of pressure,  $c_p$  showed the maximum value at the stagnation point and decreases with the increase of Reynolds numbers. The coefficient of pressure,  $c_p$  decreases with the increase of jet exit Reynolds number and at radial distance  $R = 2.5$  all the curves coincide in a single point and the fluid flows rest of the distance with same energy. Variation of surface roughness does not affect coefficient of pressure,  $c_p$  at the stagnation point.

Figure 5.1.11 and Figure 5.1.13 to Figure 5.1.15 shows the variation of coefficient of pressure,  $c_p$  with radial distance,  $r/d$  at surface roughness  $\epsilon = 0.01806$  at different Reynolds number and different nozzle-to-surface spacings. It was observed that the coefficient of pressure  $c_p$  at the stagnation point decreases with the increase of nozzle-to-surface spacing at a particular Reynolds number. It occurs due to the increased rate of mixing of the surrounding fluid with the main stream of jet.

**5.2.3 Effect of nozzle-to-surface spacing on pressure distribution:** Figure-5.1.16 shows the distribution of coefficient pressure,  $c_p$  for smooth surface and at  $Re = 16520$  at different nozzle-to-surface spacings. It was observed that the coefficient of pressure decreases at the stagnation point with the increase of nozzle-to-surface spacings. at radial distance  $R = 2.5$  all the curves coincide on a single point and gradually goes to zero. Figure 5.1.16 to Figure 5.1.20 shows the distribution of coefficient of pressure,  $c_p$  at different nozzle-to-surface spacings for various

rough surfaces and jet exit Reynolds number,  $Re = 16520$ . Comparing these curves it was observed that the coefficient of pressure,  $c_p$  at the stagnation point did not affect by increase of surface roughness. But away from the stagnation point and within radial distance  $R = 2.5$ , the coefficient of pressure,  $c_p$  affected by the increase of surface roughness.

Figure-5.1.21 to Figure-5.1.23 presented the distribution of coefficient pressure,  $c_p$  with radial distance  $r/d$  at Reynolds numbers,  $Re = 6000, 8700$  and  $23400$  and at surface roughness,  $\epsilon = 0.01806$  for different nozzle-to-surface spacings. Similar trends were observed for these curves.

**5.3. Heat transfer characteristics:** The experiment was performed to study the heat transfer characteristics over the surfaces of various roughness for different Jet Reynolds numbers,  $Re$  and different nozzle-to-surface spacing,  $H$  and then measured Nusselt number,  $Nu$  over the surfaces of different roughness was plotted for different nozzle-to-surface spacing and jet Reynolds number in as shown Figures 5.2.1 to 5.2.23.

Figure 5.2.2 shows the distribution of Nusselt number with radial distance  $R$  for different roughness at jet exit Reynolds number,  $Re = 8700$  and at nozzle-to-surface spacing  $H=1.61$ . Similar trends are observed in the Figures 5.2.1 to 5.2.4. Comparing these Figures it is observed that the Nusselt number increases with the increase of jet Reynolds number.

Figures 5.2.5 to 5.2.7 show the distribution of Nusselt number with radial distance at Reynolds number  $Re = 16500$  and at different nozzle-to-surface spacings. Comparing Figures 5.2.3 and 5.2.5 to 5.2.7, it is observed that the Nusselt number decreases with the increase of nozzle-to-surface spacings.

Figure 5.2.8 shows the distribution of Nusselt number,  $Nu$  with radial distance for smooth surface and nozzle-to-surface spacing,  $H = 1.61$ . It is observed that heat transfer increases with the increase of jet exit Reynolds number but it decreases with radial distance.

Figures 5.2.8 to 5.2.12 show the variation of heat transfer characteristics with radial distances for different surface roughness at nozzle-to-surface spacing,  $H = 1.61$ . Comparing these Figures, it is observed that Nusselt number at stagnation point remains same for lower values of surface roughness but increases for the higher values of surface roughness due to increase of more heat transfer area of the surface.

Figure 5.2.10 and 5.2.13 to 5.2.15 show the distribution of Nusselt number at different Reynolds number at surface roughness  $\epsilon = 0.01338$  with radial distance for various nozzle-to-surface spacings. Comparing these Figures, it is observed that the Nusselt number at stagnation point decreases with the increase of nozzle-to-surface spacings and heat transfer decreases gradually with the increase of radial distance.

Figure 5.2.16 to 5.2.20 show the distribution of Nusselt number with radial distances at various nozzle-to-surface spacings at jet Reynolds number,  $Re = 16520$  for various surface roughness. It is observed that the Nusselt number decreases with the increase of radial distances. It is also observed that the Nusselt number remains constant at stagnation point for lower values of surface roughness but shows higher value at the more rough surfaces, this is because of increased heat transfer area at higher rough surfaces.

Figure 5.2.19 and 5.2.21 to 5.2.23 show the distribution of Nusselt number with radial distance for various nozzle-to-surface spacings and jet exit Reynolds numbers at surface roughness  $\epsilon = 0.01806$ . The Nusselt number at the stagnation point increases with the increase of jet exit Reynolds number and decreases with the increase of nozzle-to-surface spacings. The Nusselt number also decreases with the increase of radial distances.

**5.4. Correlation for Average Nusselt number:-** The experimental values of local Nusselt number,  $Nu_x$  were used to calculate the Average Nusselt number,  $\overline{Nu}$  based on the local temperature difference, as a function of radial distance, using the relation,

$$\overline{Nu} = \frac{\sum Nu_x \cdot x}{L} \quad [1]$$

The Correlation for Average Nusselt number has been developed in terms of jet Reynolds number ( $Re$ ), relative roughness ( $\epsilon$ ) and nozzle-to-surface spacing ( $H$ ), but not applicable for smooth surface. The exponents in equation (2) were determined, using the least square curve fit method based on the experimental data. The present correlation for  $Nu$  is as follows,

$$\overline{Nu} = 15(Re)^{0.43}(\epsilon)^{0.60}(H)^{-0.45} \quad [2]$$

However, as shown in Fig- 5.3 & Fig-5.4, the agreement of correlation was within  $\pm 10\%$  accuracy of the experimental data covering the complete range of parameters.

**CHAPTER-SIX**

**CONCLUSION**

## CHAPTER - SIX

### CONCLUSION

**6.1. General:-** In this concluding chapter, the high-light of the findings of the present investigations have been presented. The scope of extension of the present research facility is also outlined with a view to acquire more knowledge from the same situation.

**6.2. Conclusions:-** In light of the discussion of results the following conclusions were drawn as a consequence of present work.

**6.2.1. Conclusion for pressure distribution :** Variation of pressure distribution due to impinging air jet over a surface depends on surface roughness, jet Reynolds number and nozzle-to-surface spacing in the following manner.

1. Co-efficient of Pressure is maximum at the stagnation point for all surfaces, Reynolds numbers and nozzle-to-surface spacings.
2. Co-efficient of Pressure increases with the increasing of jet Reynolds number and jet Reynolds number has significant effect on pressure distribution.
3. Co-efficient of Pressure over surface decreases when nozzle-to-surface spacing increases..
4. Co-efficient of Pressure over surface decreases with the increase of surface roughness but pressure is independent of surface roughness at the stagnation point. Co-efficient of pressure at the stagnation point remains constant for the lower values of surface roughness but increases beyond the surface roughness,  $\epsilon = 0.01338$  which predicts that there is a critical value of surface roughness in between  $\epsilon = 0.01338$  and  $\epsilon = 0.01806$ .

**6.2.2 Conclusion for Heat Transfer characteristics:** Heat transfer due to circular air jet over rough surfaces depends on relative surface roughness,  $\epsilon$  jet Reynolds numbers,  $Re$  and nozzle-to-surface spacings,  $H$  in the following manner.

1. Nusselt number increases with the increase of roughness of the surface.
2. Nusselt number decreases with the increase of nozzle-to-surface spacings.
3. Nusselt number increases with the increase of jet Reynolds number.
4. The stagnation point Nusselt number increases with the increase of surface roughness. The stagnation point Nusselt number remains constant for lower values of surface roughness but increases beyond the roughness  $\epsilon = 0.01338$  which predicts that there is a critical value in between  $\epsilon = 0.01338$  and  $\epsilon = 0.01806$ .
5. A correlation has been developed for calculating the average Nusselt number,  $Nu$  with in  $\pm 10\%$  accuracy based on experimental data.

**6.3. Scope of further work:-** the following suggestions are put forward as an extension of the present investigation.

1. The same work can be repeated with more different size of rough surfaces and at higher jet Reynolds number.
2. The same experiment can be repeated by using the wall jet.
3. The same experiment can be repeated by using the oblique jet.



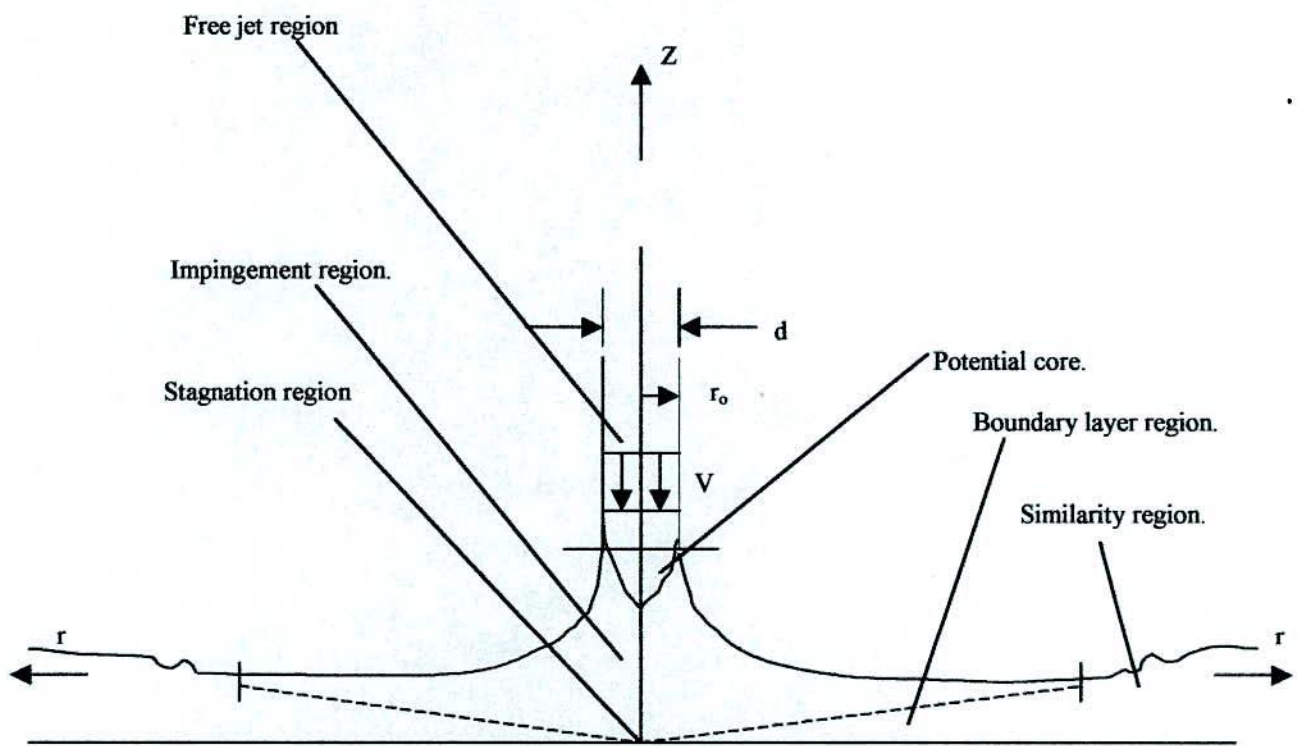


**Fig.- 2.1. : Schematic Diagram of a Free Impinging Jet System.**

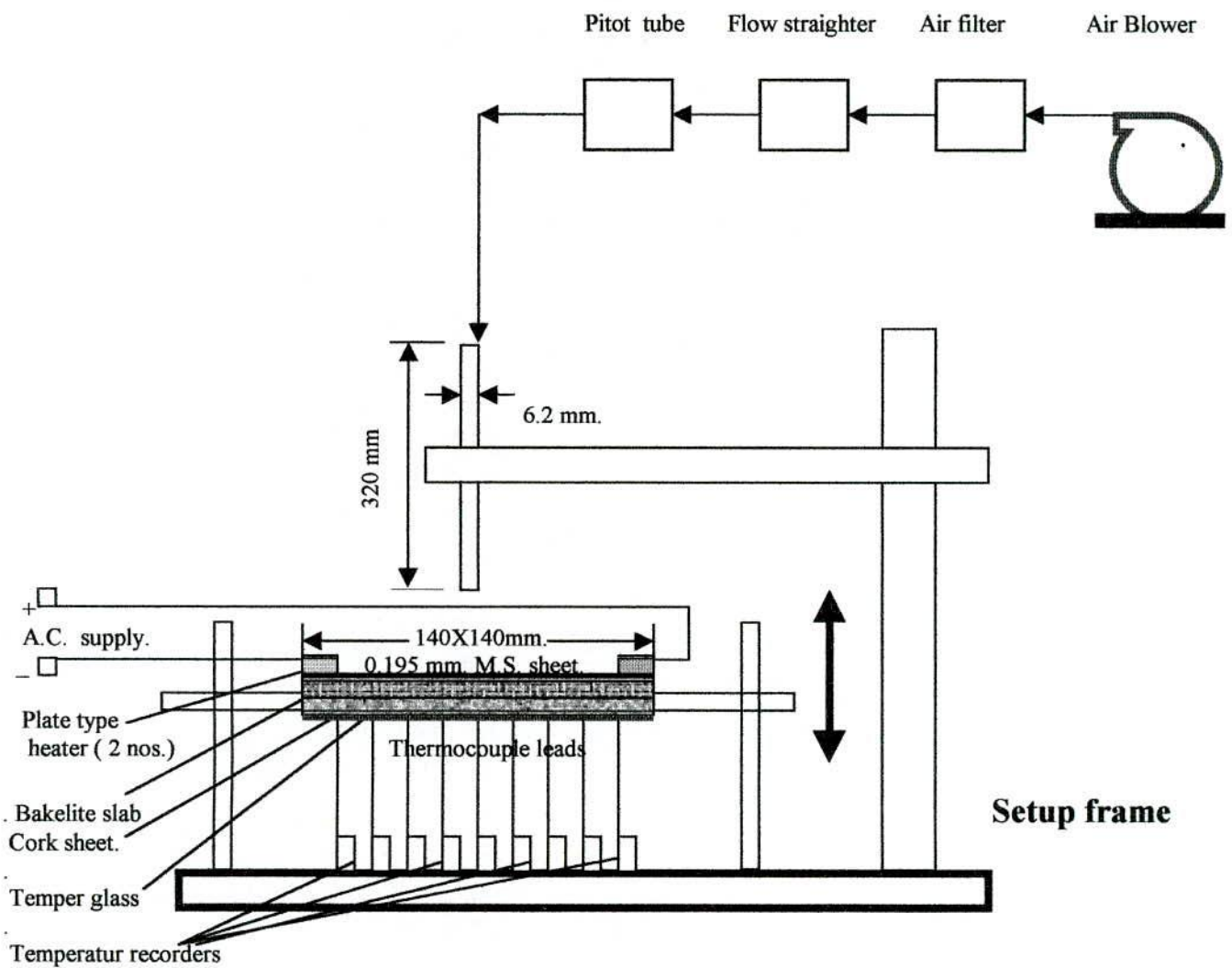


**Fig.-4:1. - A Schematic of Experimental Setup**

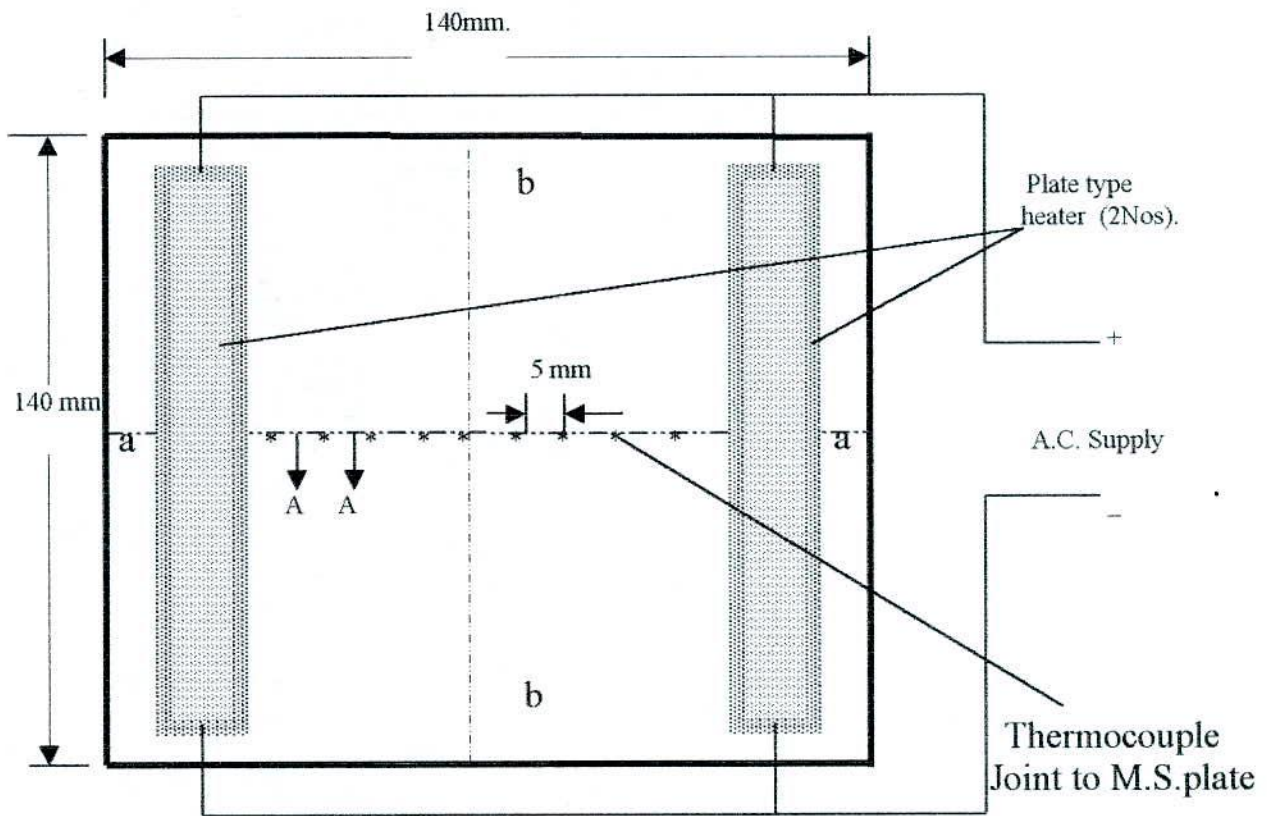


FIG. 4.2.a :- M.S. Sheet (.0192mm. thick) test section.

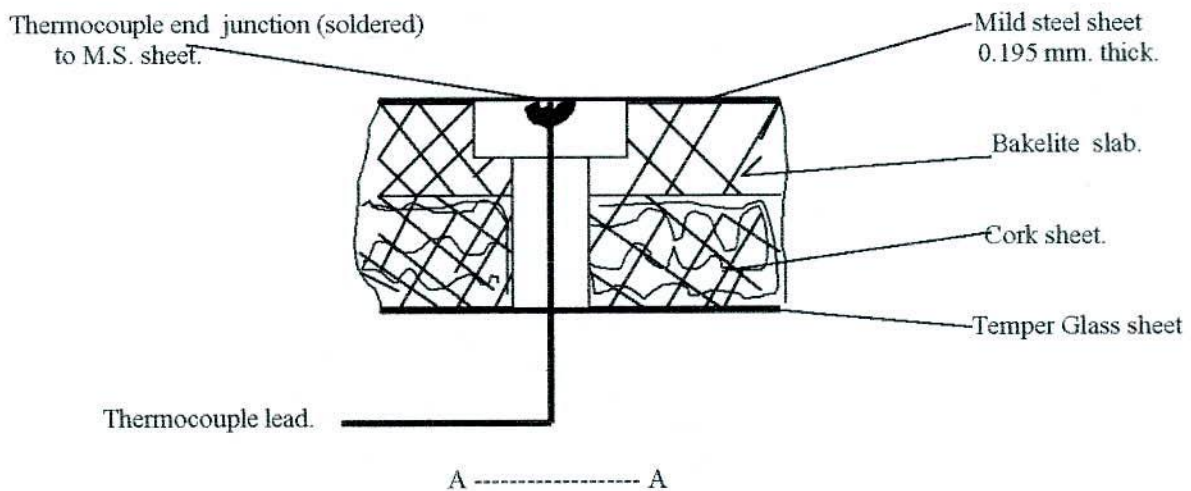
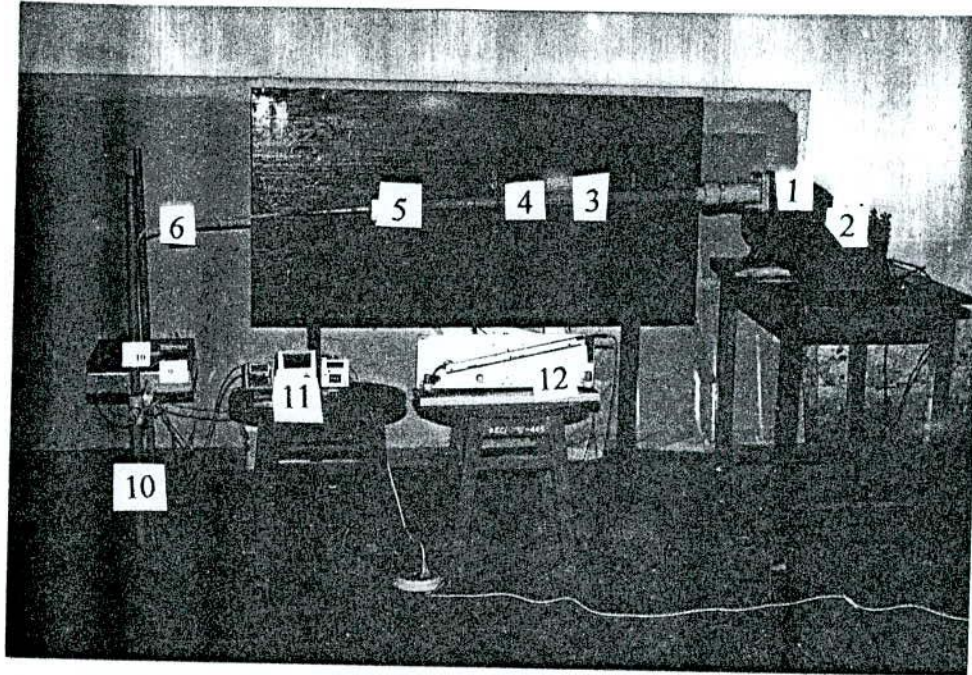


Fig. 4.2 .b: Cut-away view of thermocouple setting

Fig. -4:2. Instrumented test section and thermocouple arrangement.



1. Blower. 2. Variac 3. Air filter 4. Flow straightner. 5. Converging nozzle
6. Jet tube (Copper tube ) 7. M. S. sheet (140 mmX140 mm, 0.195 mm thick)
8. Plate type heater (2 nos) 9. Bakelite slab +Cork sheet +Tempered glass
10. Plate elevating stand 11. Digital temperature recorders 12. Manometer for airflow.(Type- 5) with Pitot tube connection

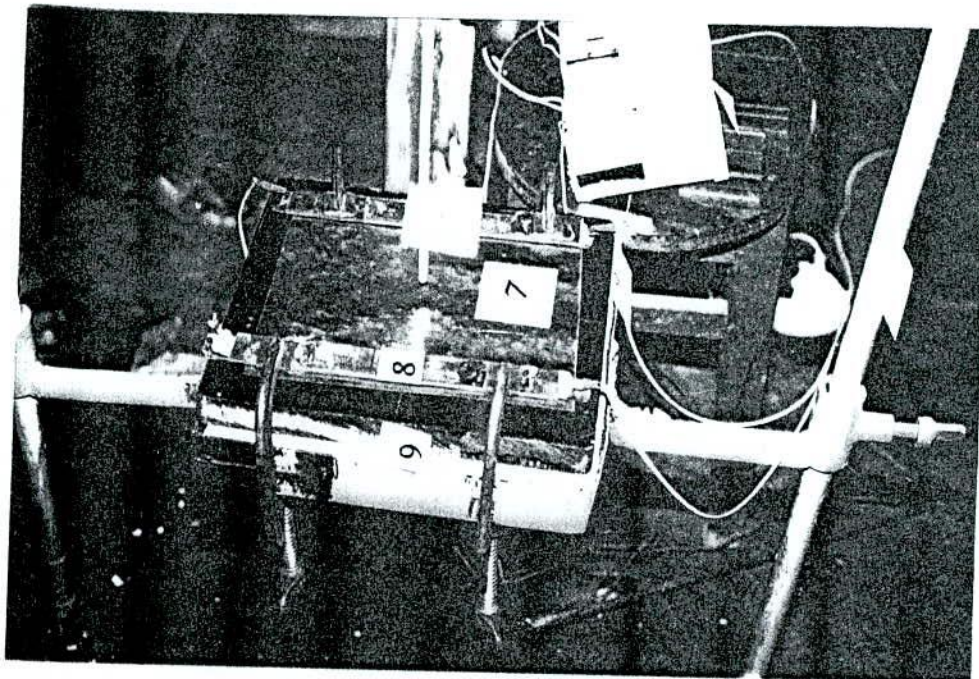


Fig. 4.3. : Photographic view of the Experimental setup.

## PRESSURE DISTRIBUTION

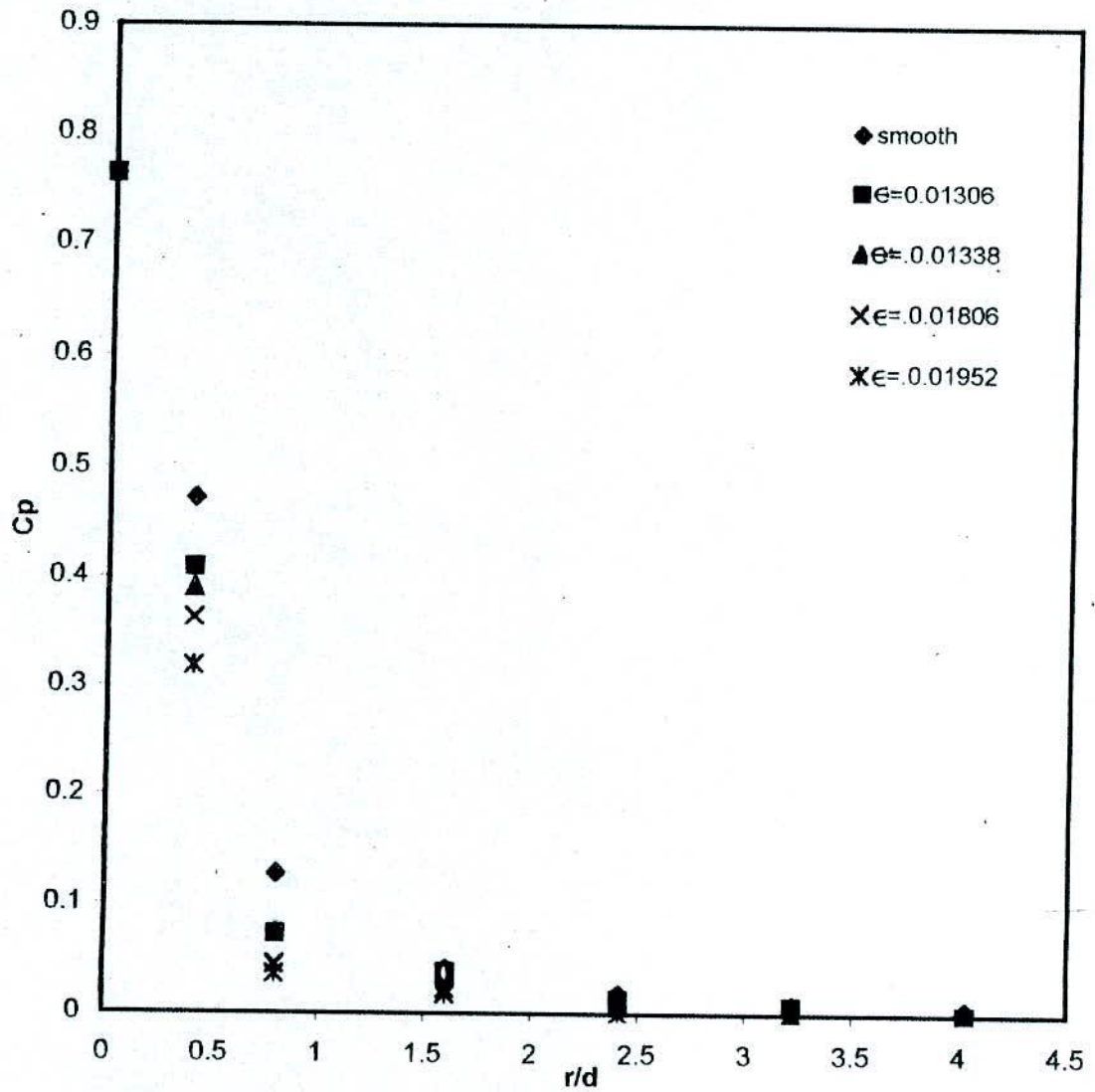


Fig.-5.1.1. Distribution Of Pressure on Surfaces of different roughness at  $Re=6000$  and jet-to-plate spacing  $H=1.61$ .

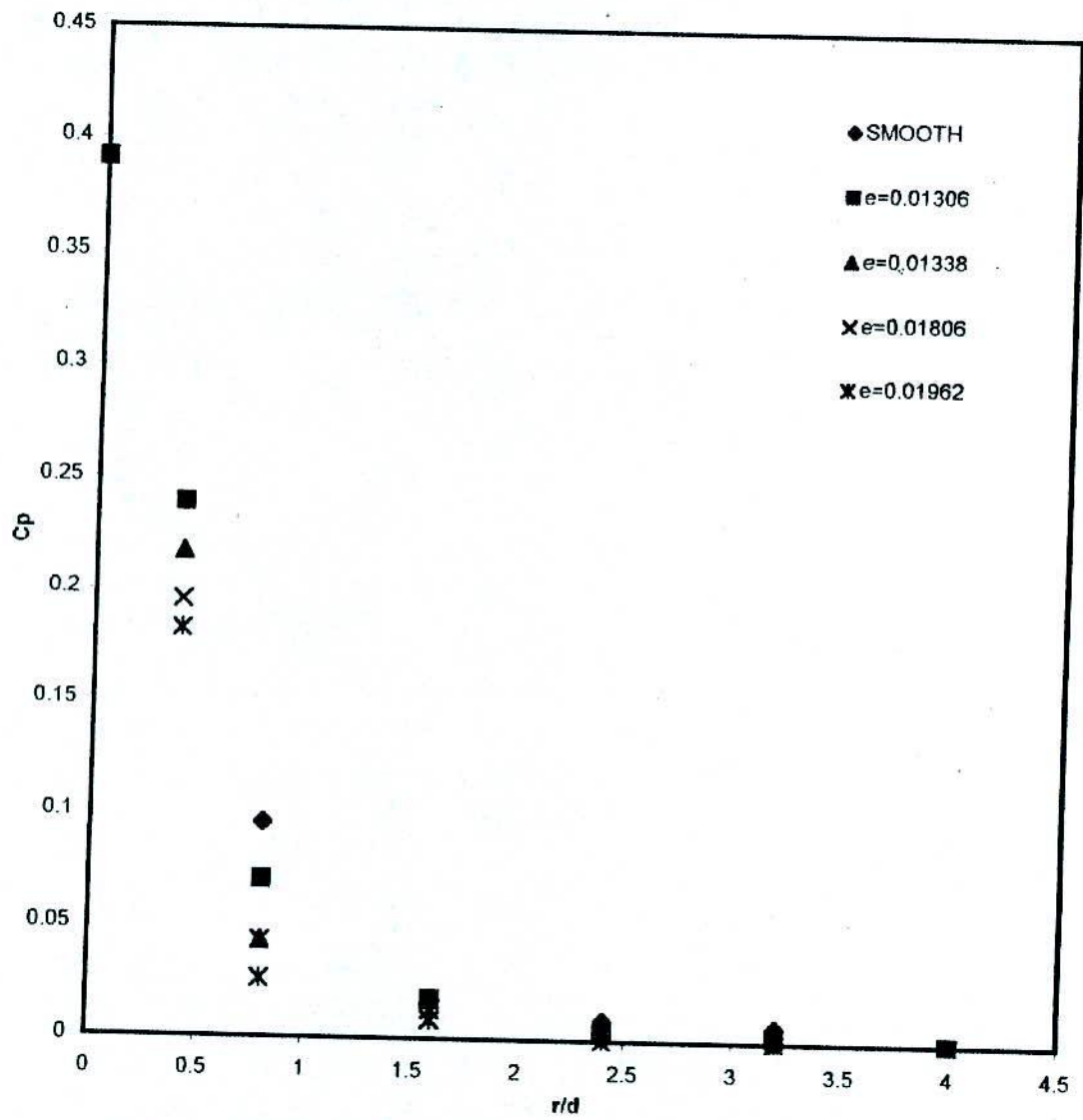


Fig.-5.1.2. Distribution of pressure on surfaces of different roughness at  $Re=8700$  and at Jet-to-plate spacing,  $H=1.61$ .

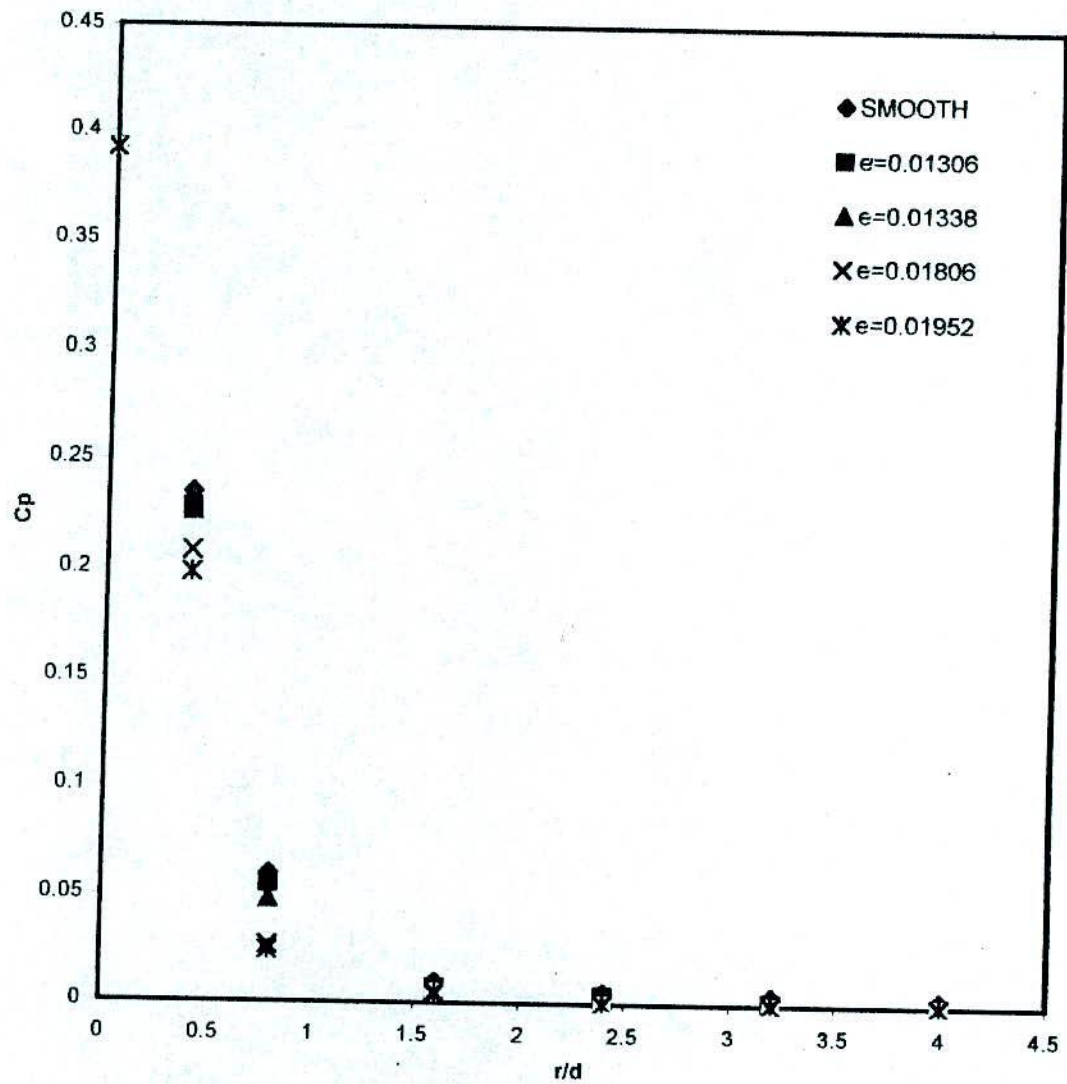


Fig. - 5.1.3. Distribution of pressure on surfaces of different roughness at  $Re=16520$  and at jet-to-plate spacing,  $H=1.61$ .

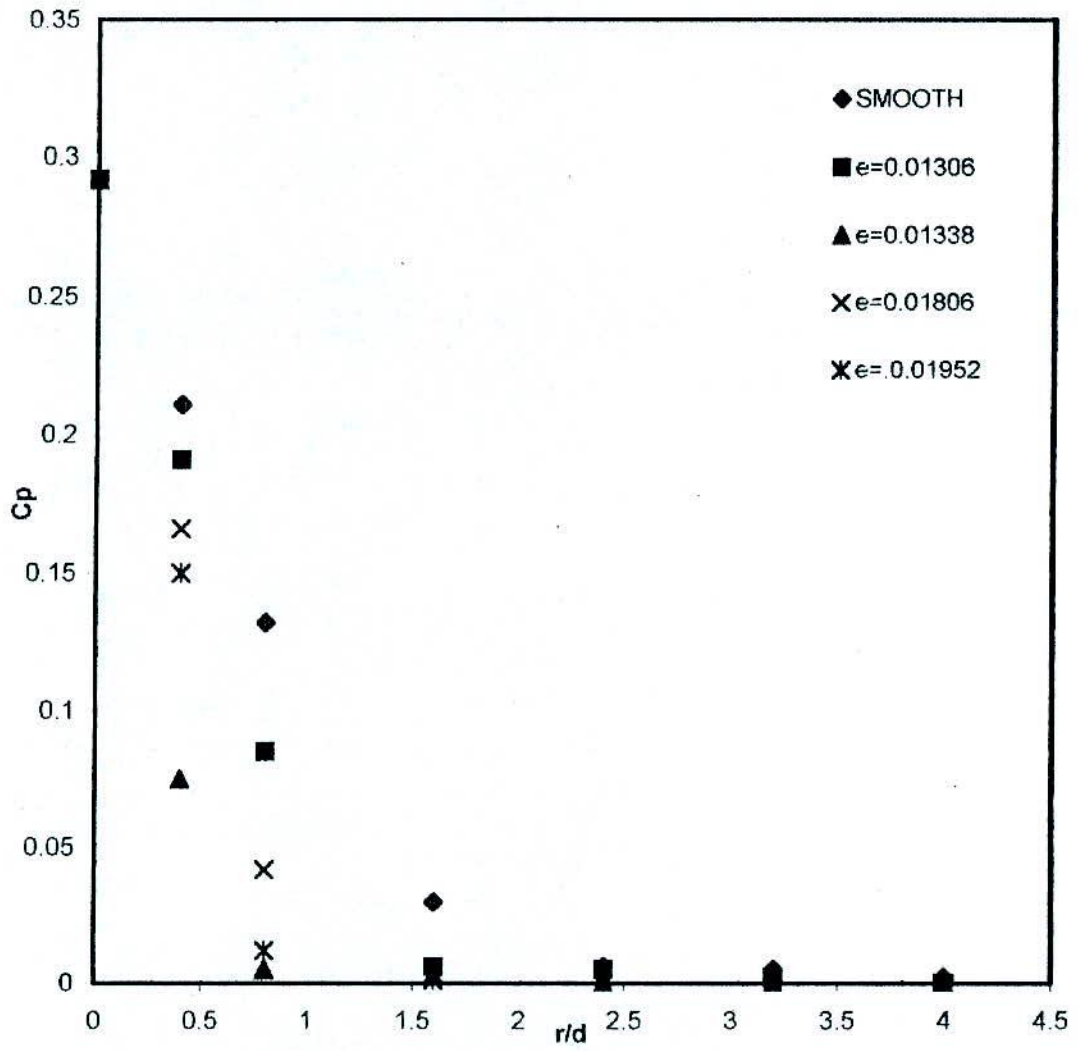


Fig.- 5.1.4. Distribution of pressure on surfaces of different roughness at  $Re= 23400$  and at Jet-to-plate spacing ,  $H= 1.61$ .



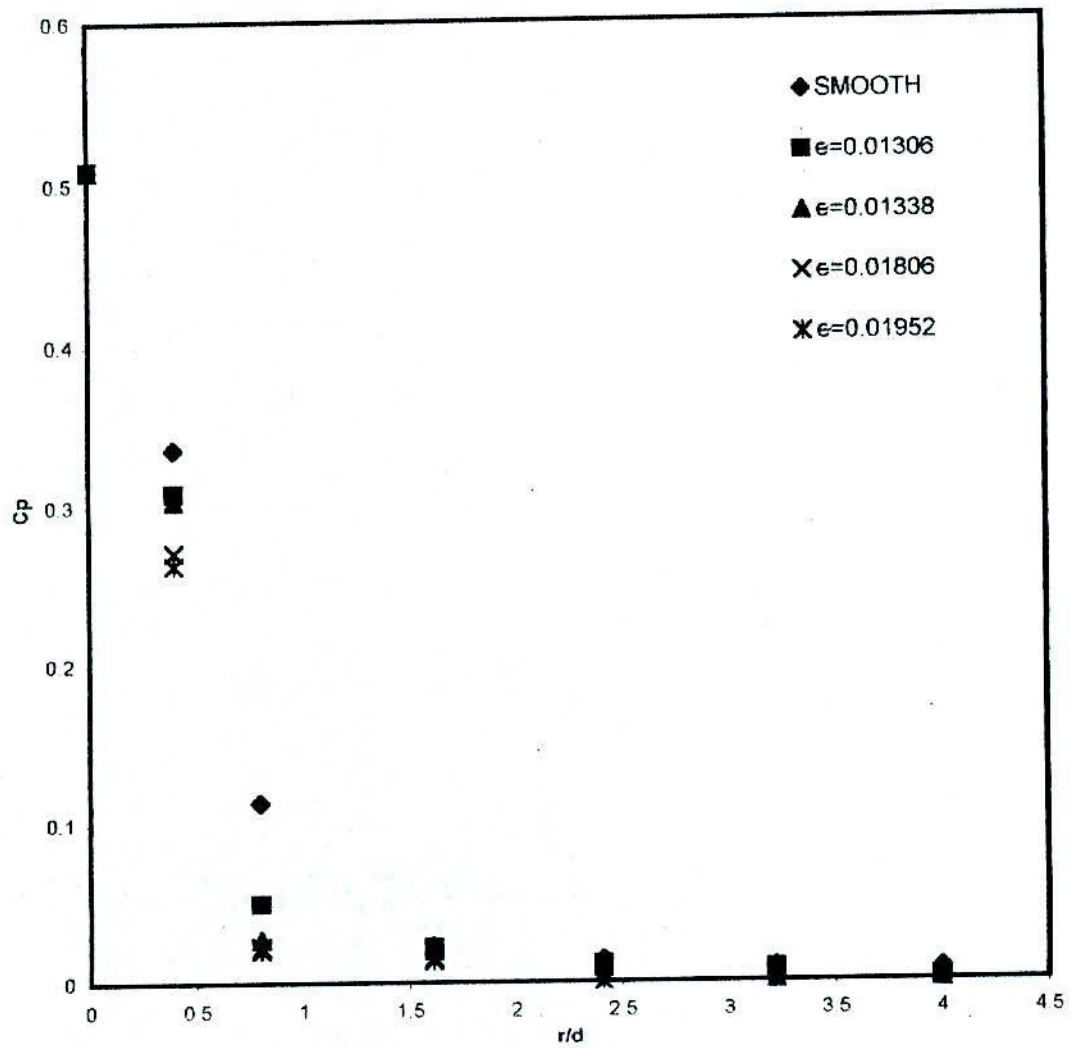


Fig. 1.5. Distribution of pressure over surfaces of different roughness at  $Re=6000$  and at Jet-to-plate spacing,  $H=2.42$ .

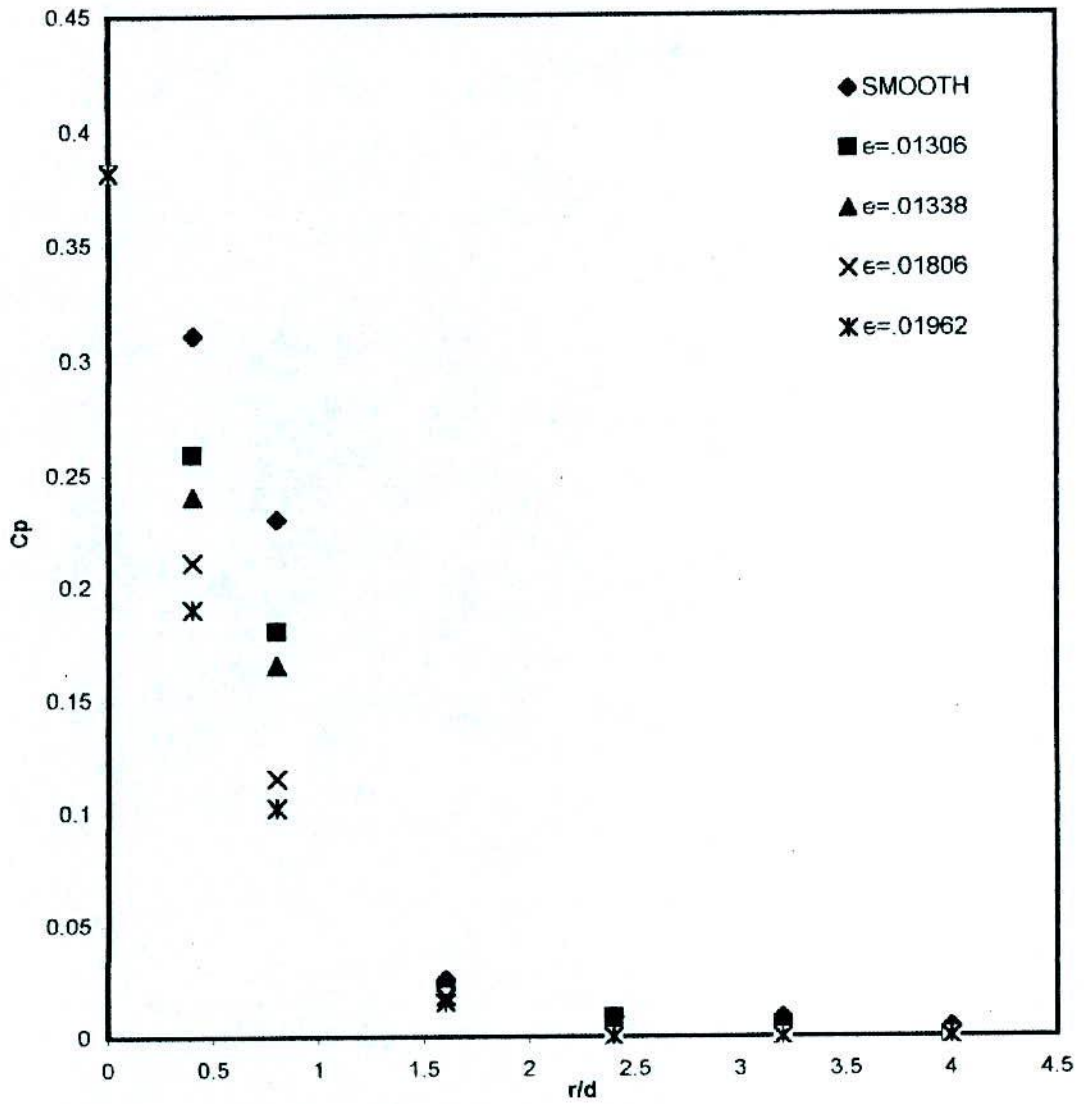


Fig.-5.1.6. Distribution of pressure over surfaces of different roughness at  $Re=8700$  and at Jet-to-plate spacing,  $H=2.42$ .

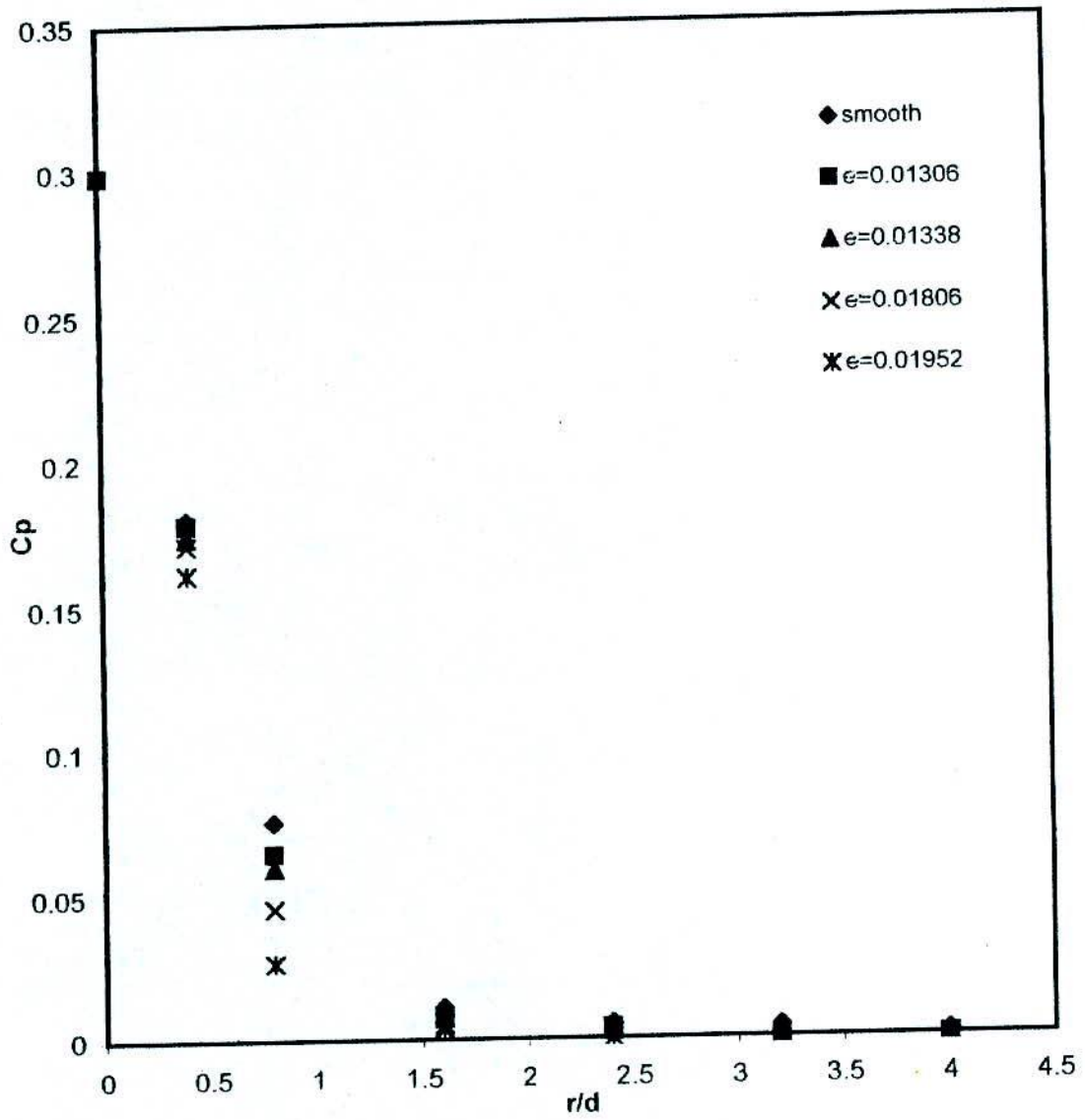


Fig.- 5.1.7, Distribution of pressure over surfaces of different roughness at  $Re=16520$  and at Jet-to-plate spacing,  $H=4.03$ .

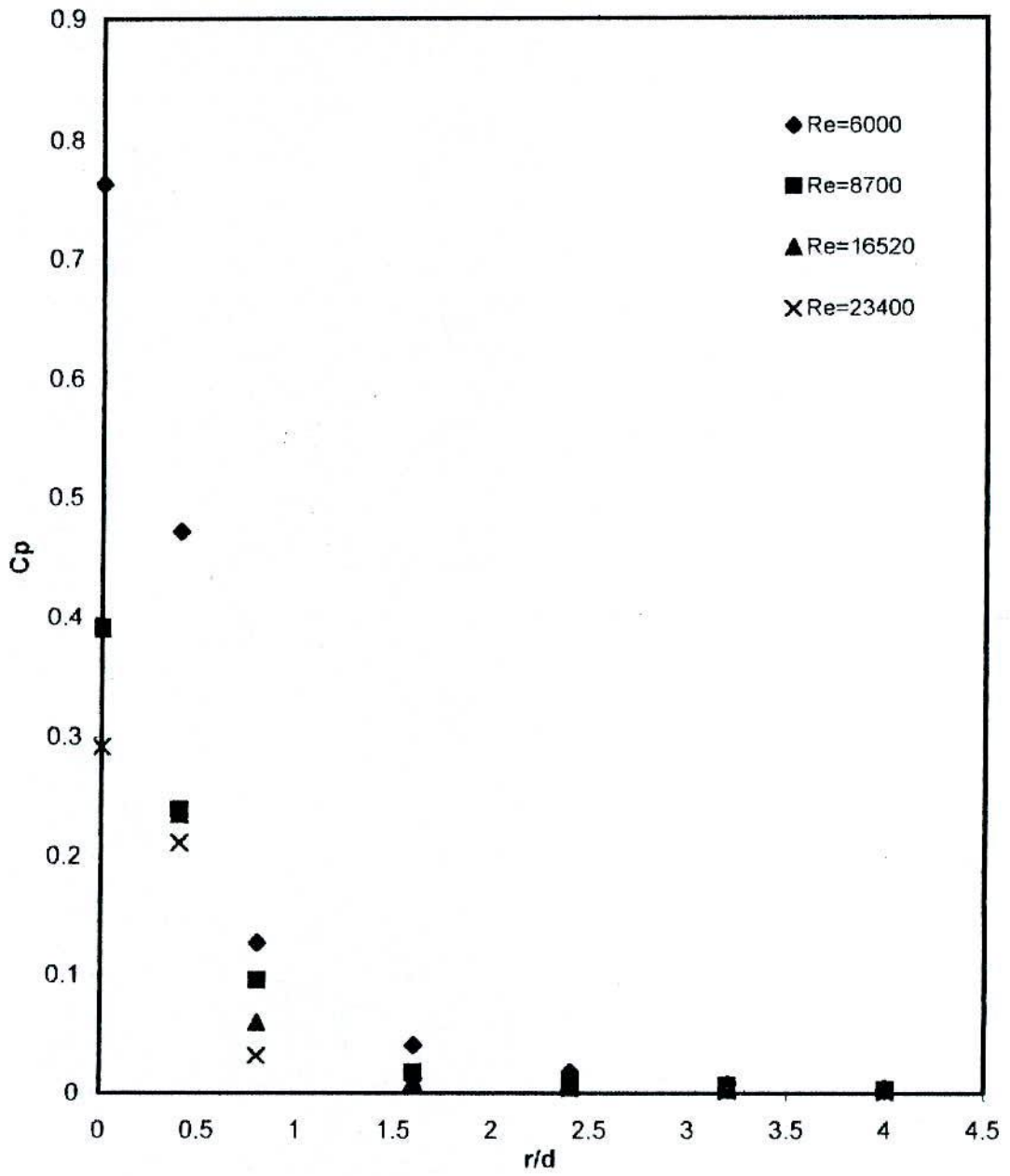


Fig5.1.8. Distribution of pressure over smooth surface for different Reynolds number at Jet-to-plate spacing,  $h=1.61$ ,

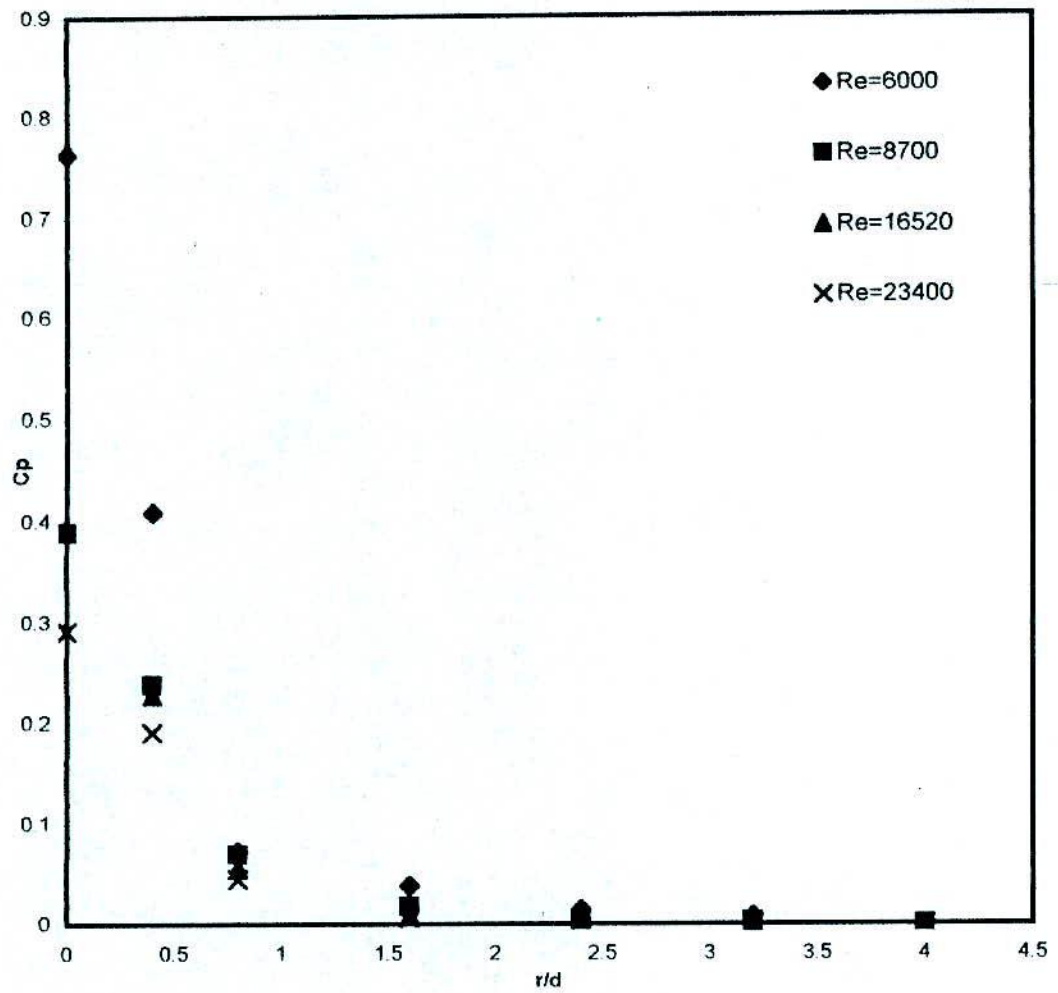


Fig.-5,1,9, Distribution of pressure over a surface of roughness,  $e=,01306$  for different Reynolds number and at Jet-to-plate spacing,  $H=1,61$ ,

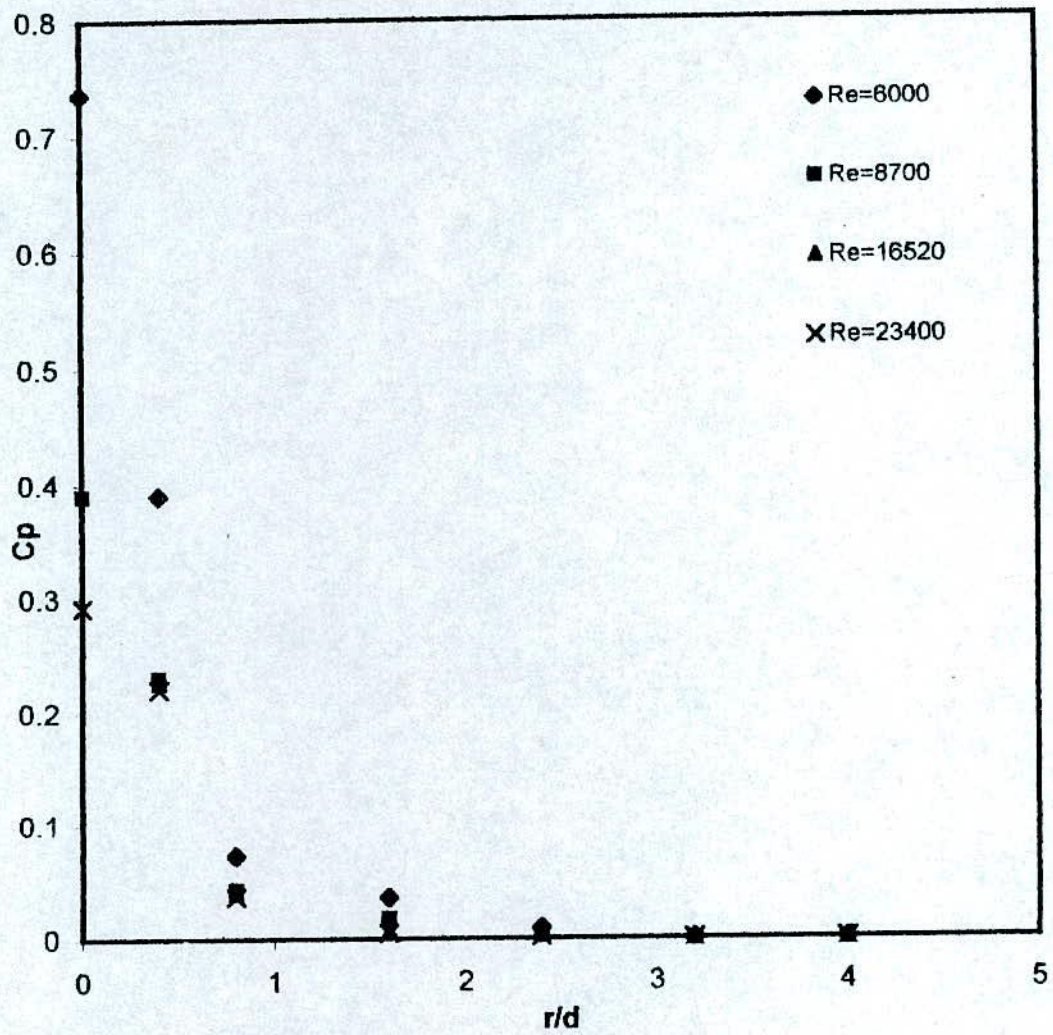


Fig.-5, 1, 10, Distribution of pressure over a surface of roughness,  $\epsilon=0.01338$  for different Reynolds number and at Jet-to-plate spacing,  $h=1.61$ ,

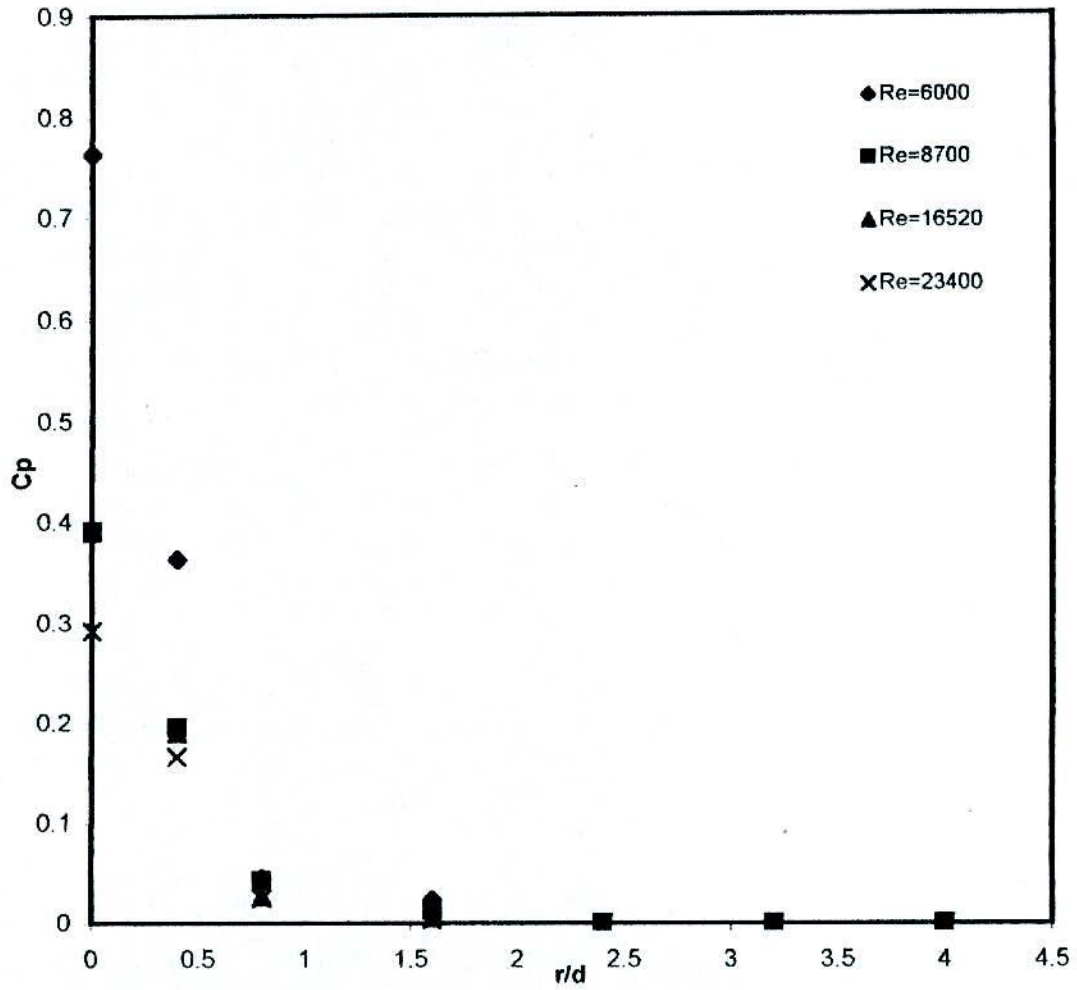


Fig.-5,1,11, Distribution of pressure over a surface of roughness,  $\epsilon=0,01806$  for different Reynolds number and at Jet-to-plate spacing,  $H=1.61$ .

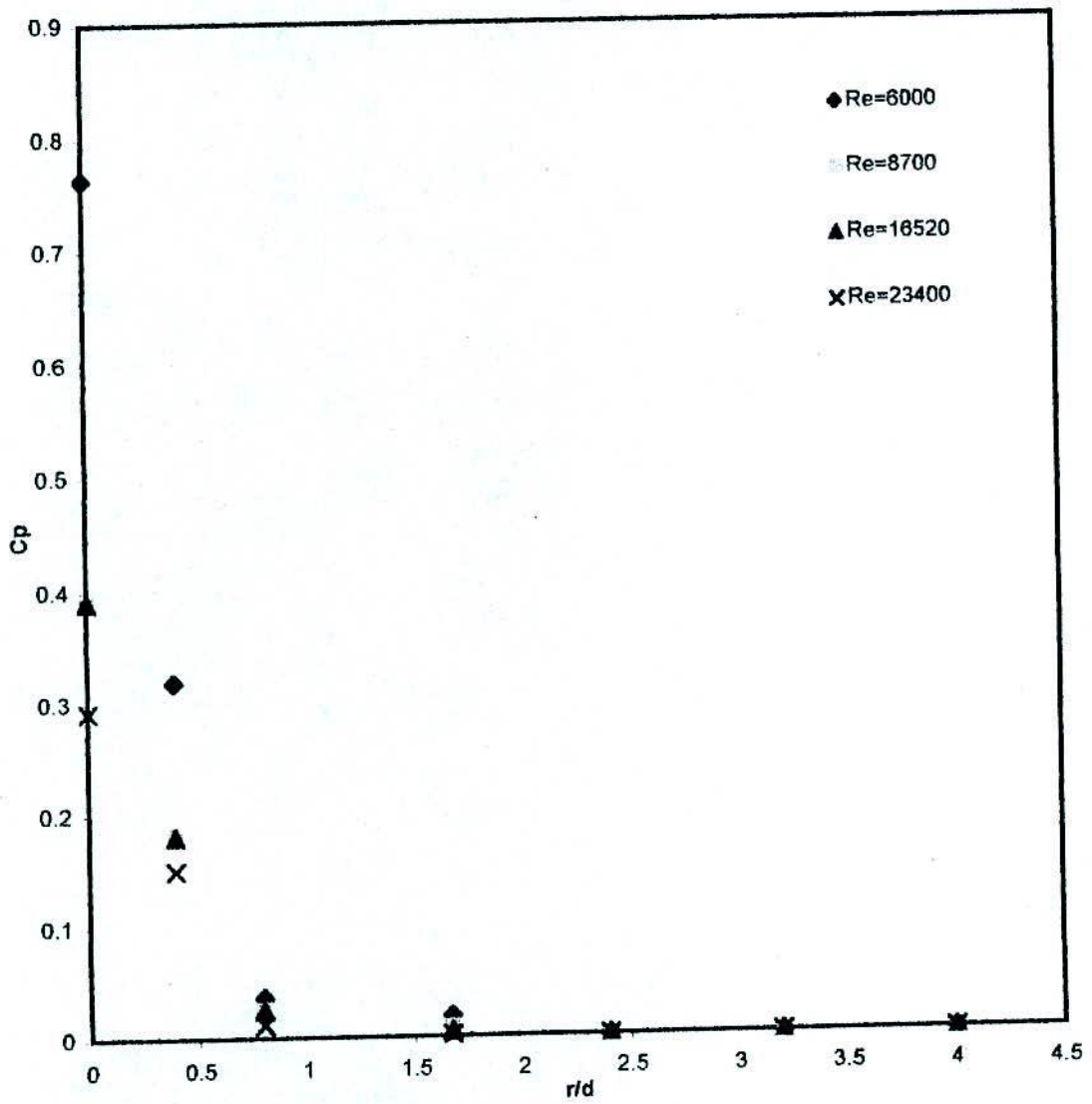


Fig.-5, 1, 12, Distribution of pressure over a surface of roughness,  $\epsilon=0.01952$  at different Reynolds number and at Jet-to-plate spacing,  $H=1.61$ ,



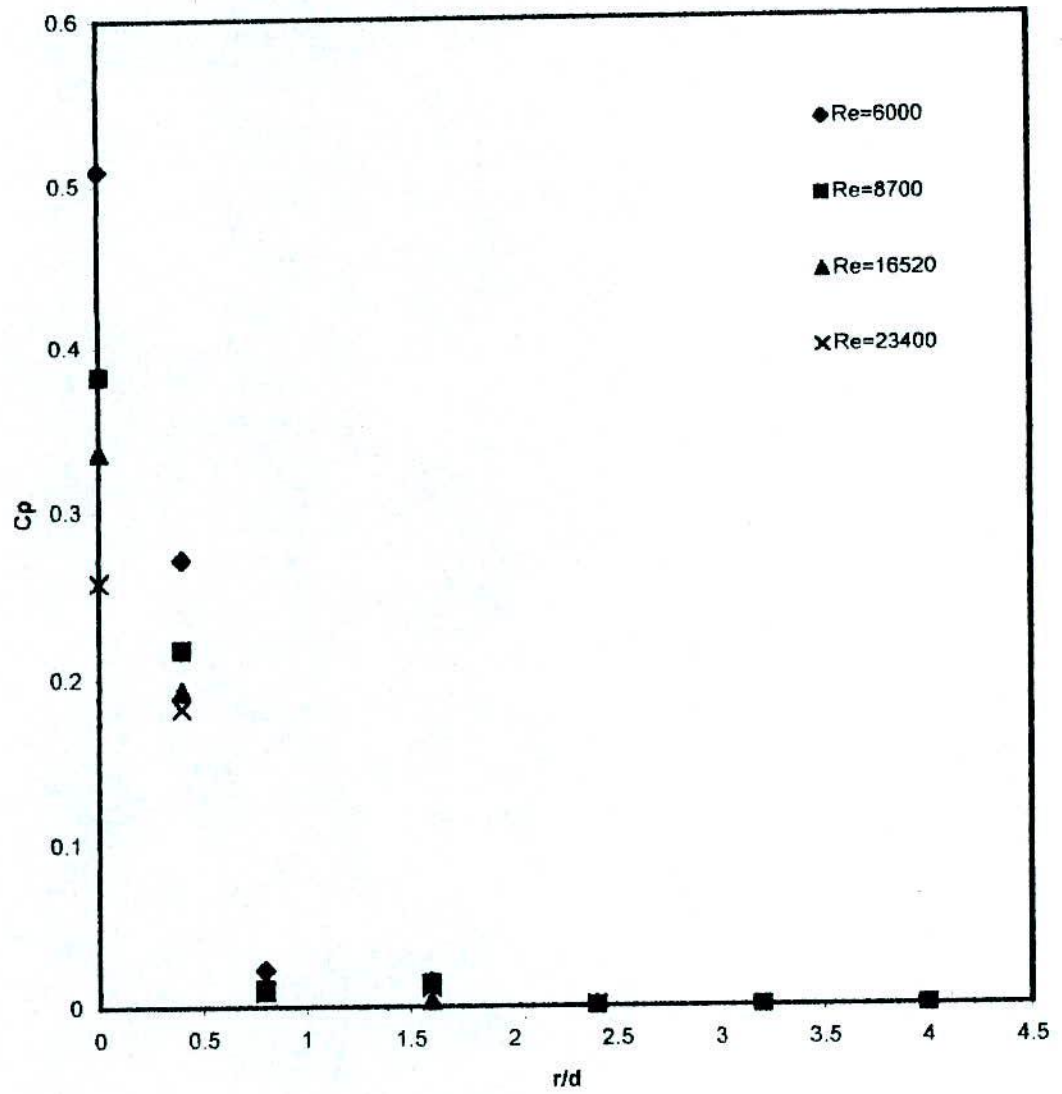


Fig.-5,1,13, Distribution of pressure over a surface of roughness,  $\epsilon=0.1806$  at different Reynolds number and at Jet-to-plate spacing,  $H=2.42$ ,

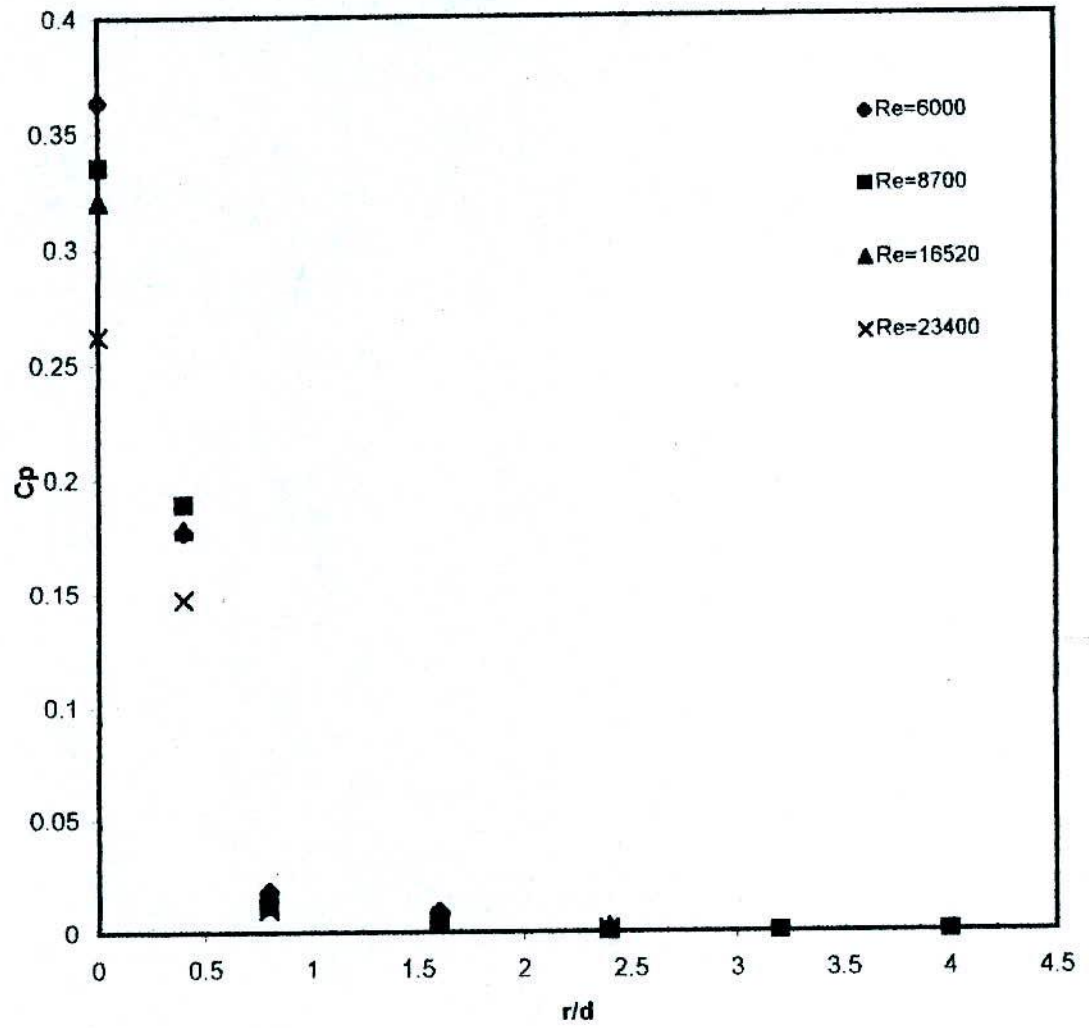


Fig.-5.1,14, Distribution of pressure over a surface of roughness ,  $e=,01806$  at different Reynolds number and at Jet-to-plate spacing , $H=3,22$

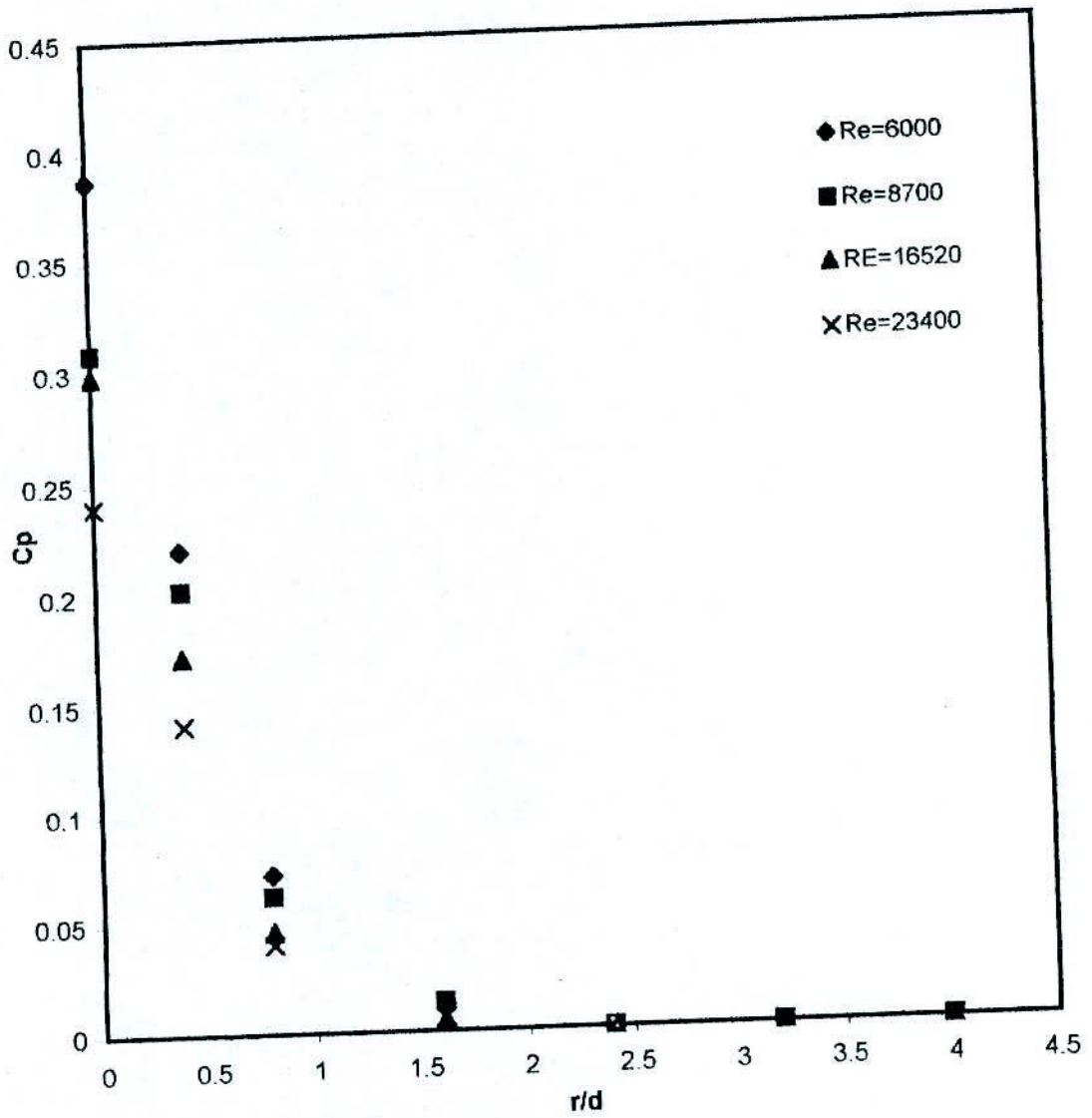


Fig.-5,1,15, Distribution of pressure over a surface of roughness,  $\epsilon=0.01806$  at different Reynolds number and at Jet-to-plate spacing,  $H=4.03$ .

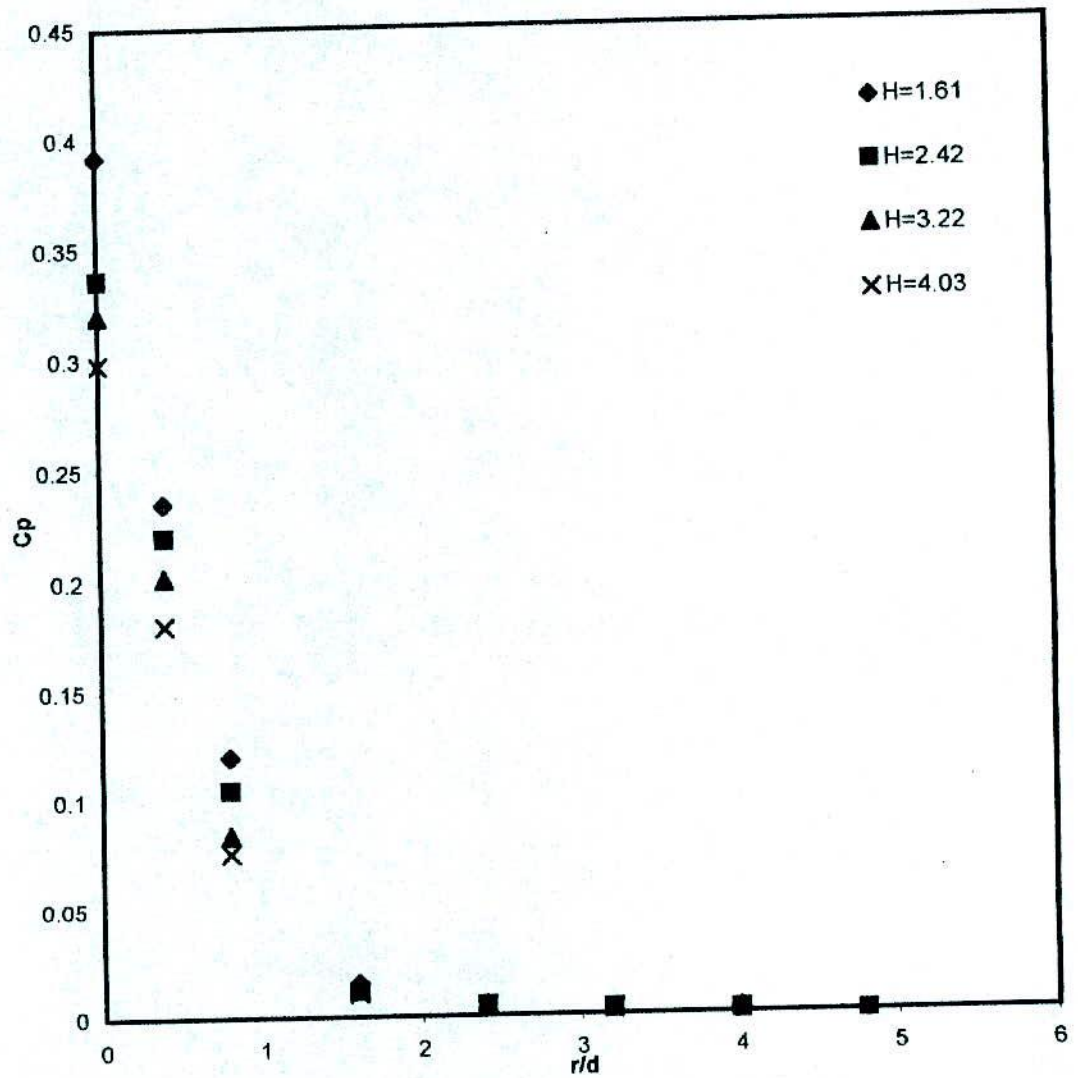


Fig.-5,1,16, Distribution of pressure over a smooth surface for different jet-to-plate spacing and at  $Re=16520$ .

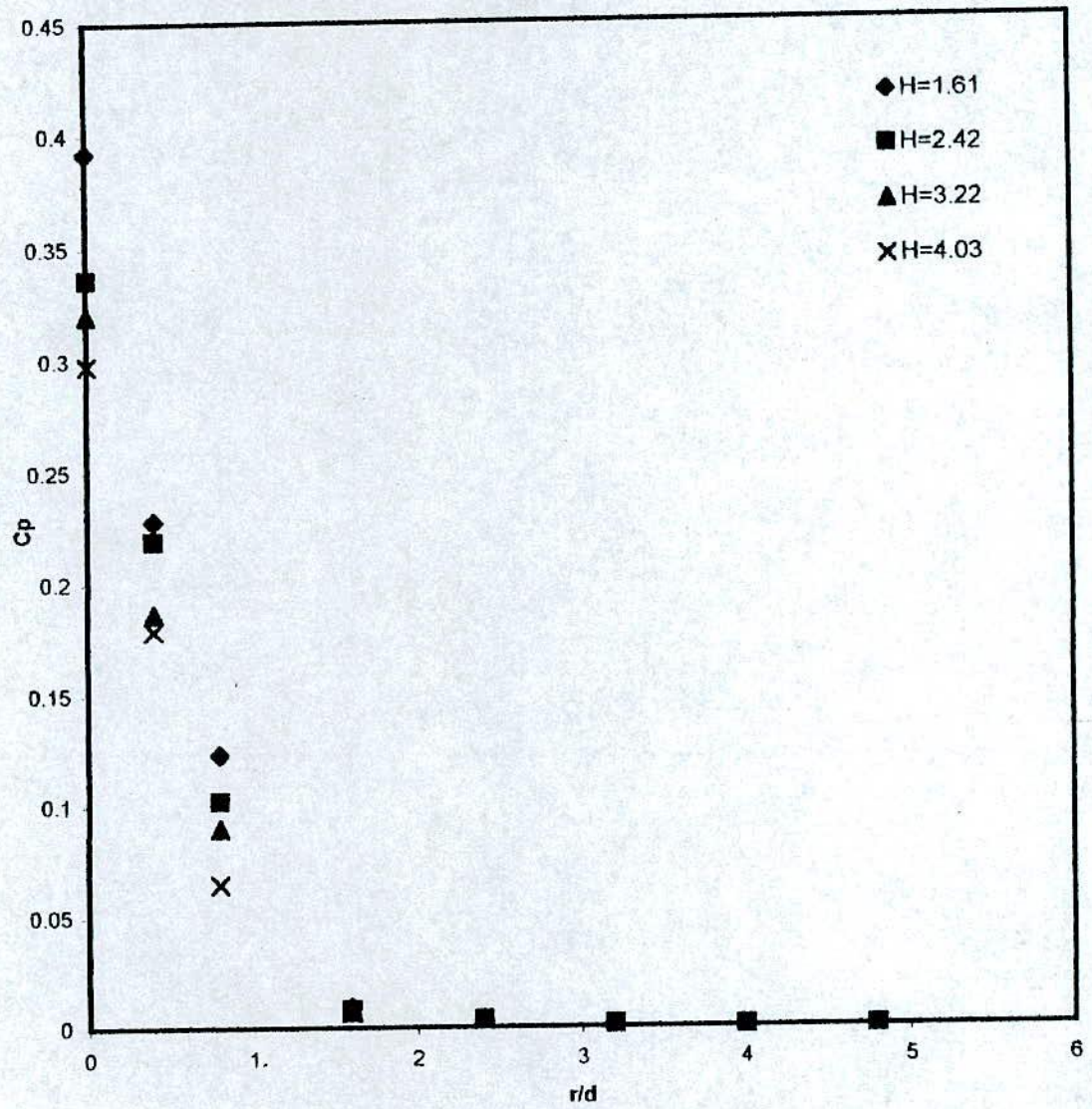


Fig.-5,1,17, Distribution of pressure over the surface of roughness,  $e=,01306$  for different jet-to-plate spacing and at  $Re=16520$ ,

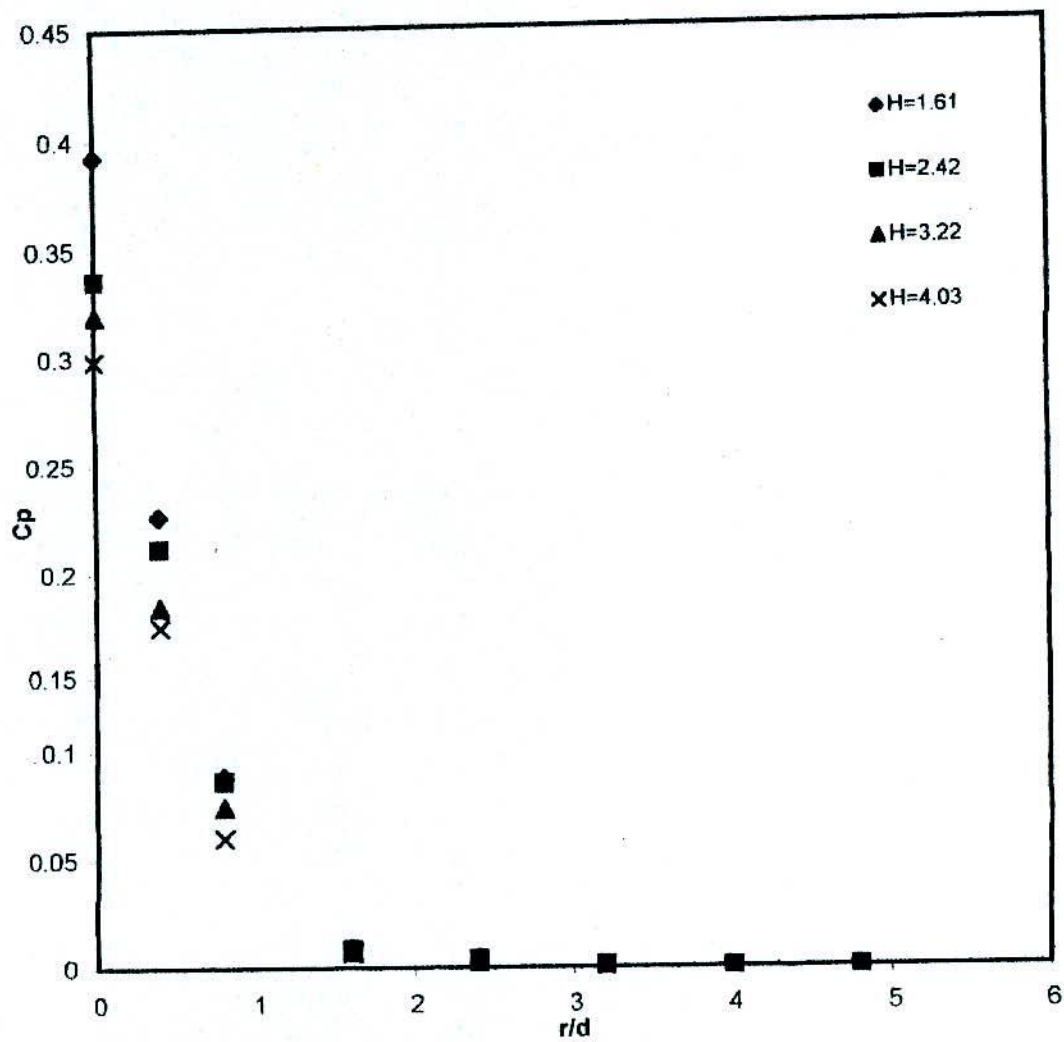


Fig.-5, 1, 18, Distribution of pressure over a surface of roughness,  $\epsilon=.01338$  for different jet-to-plate spacing and at  $Re=16520$ ,

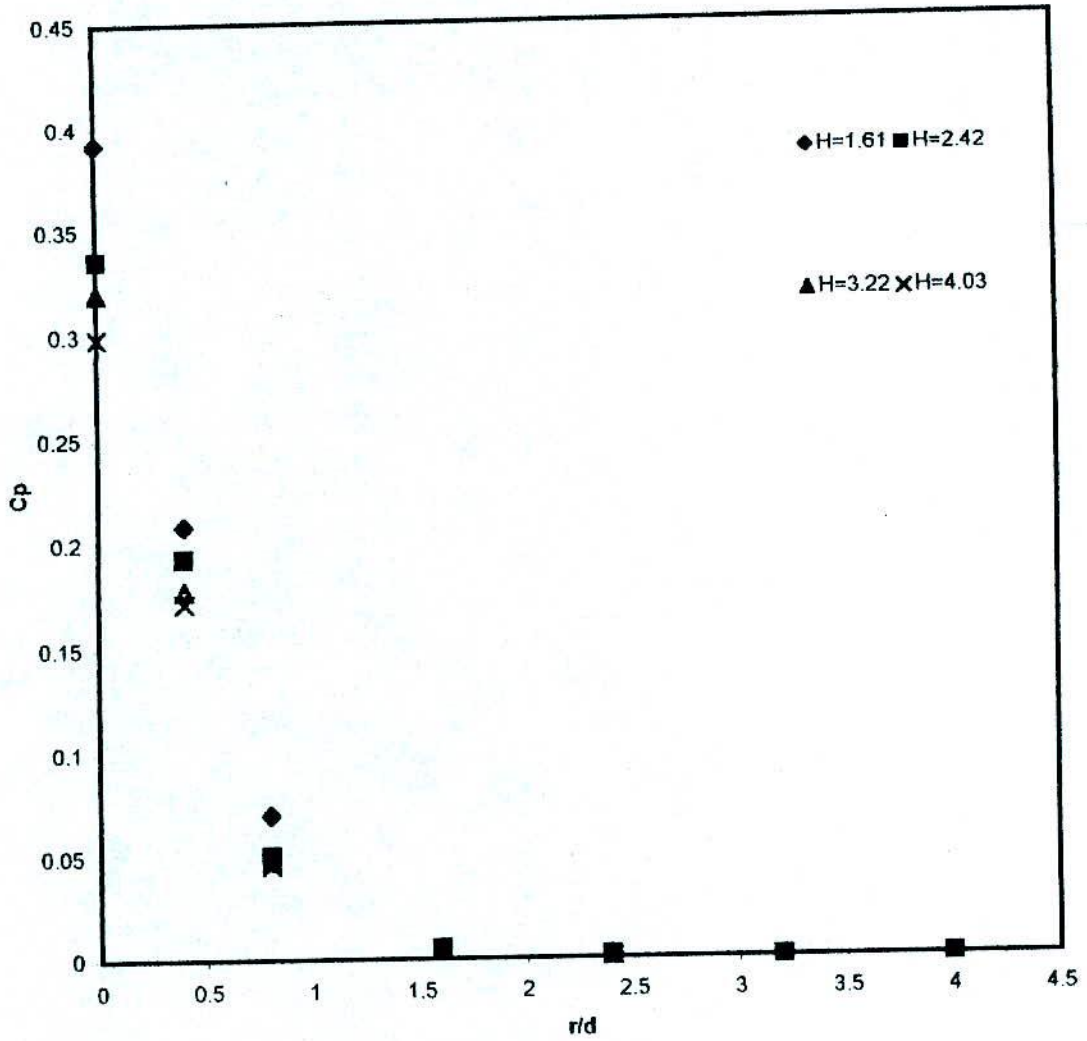


Fig.-5, 1, 19, Distribution of pressure over a surface of roughness,  $e=.01806$  for different jet-to-plate spacing and at  $Re=16520$ ,

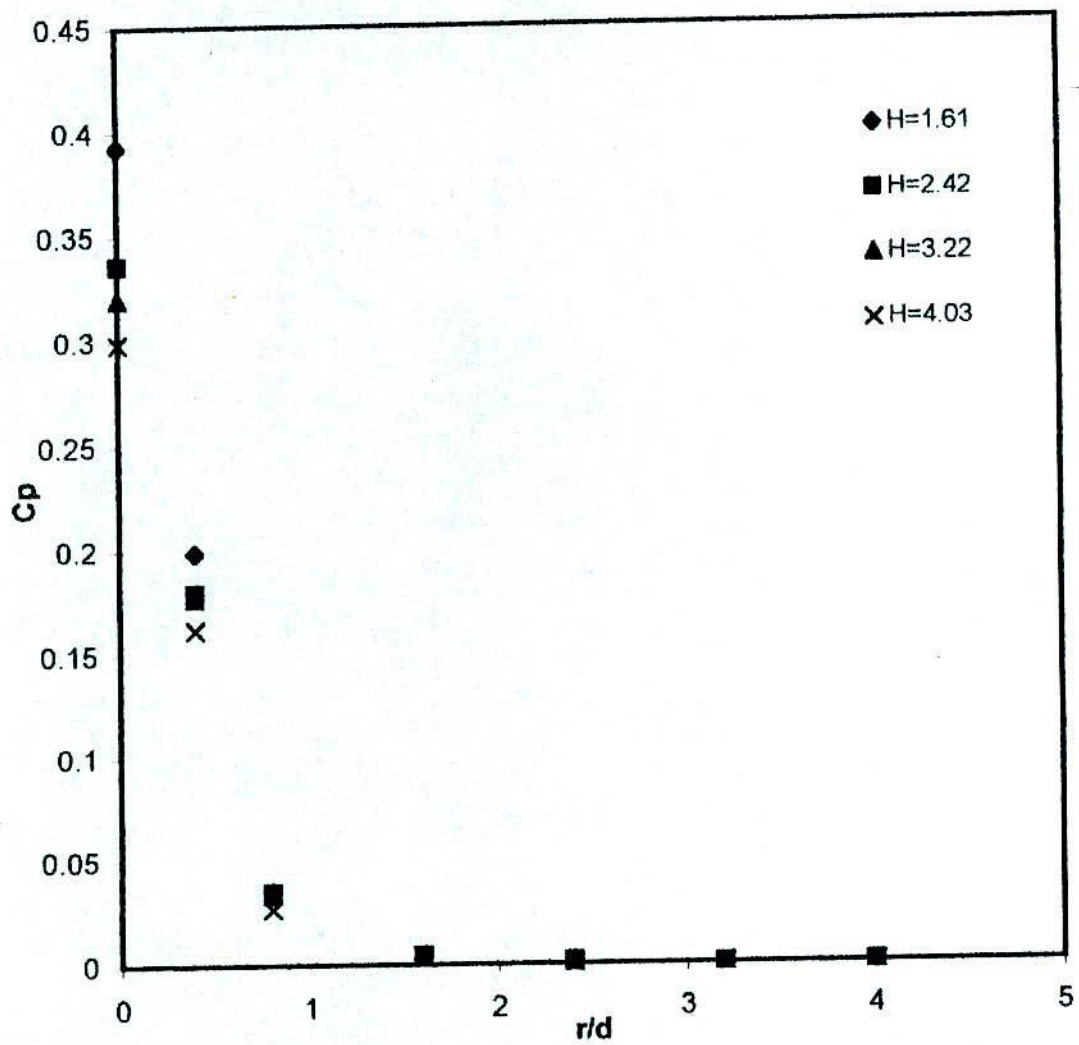


Fig.-5,1,20, Distribution of pressure over a surface of roughness,  $e=0,01952$  for different jet-to-plate spacing and at  $Re=16520$ ,



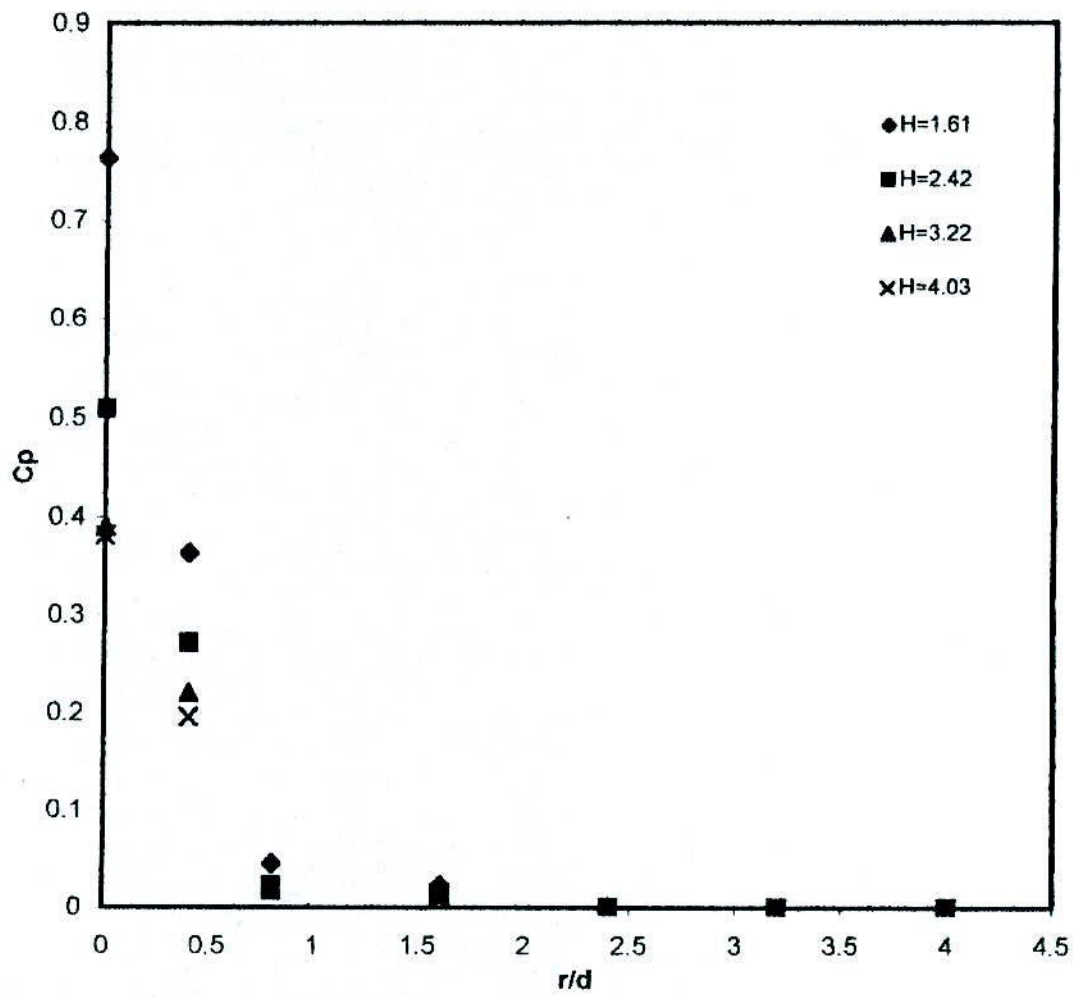


Fig.-5,1,21, Distribution of pressure over a surface of roughness,  $\epsilon=.01806$  for different jet-to-plate spacing and at  $Re=6000$ ,

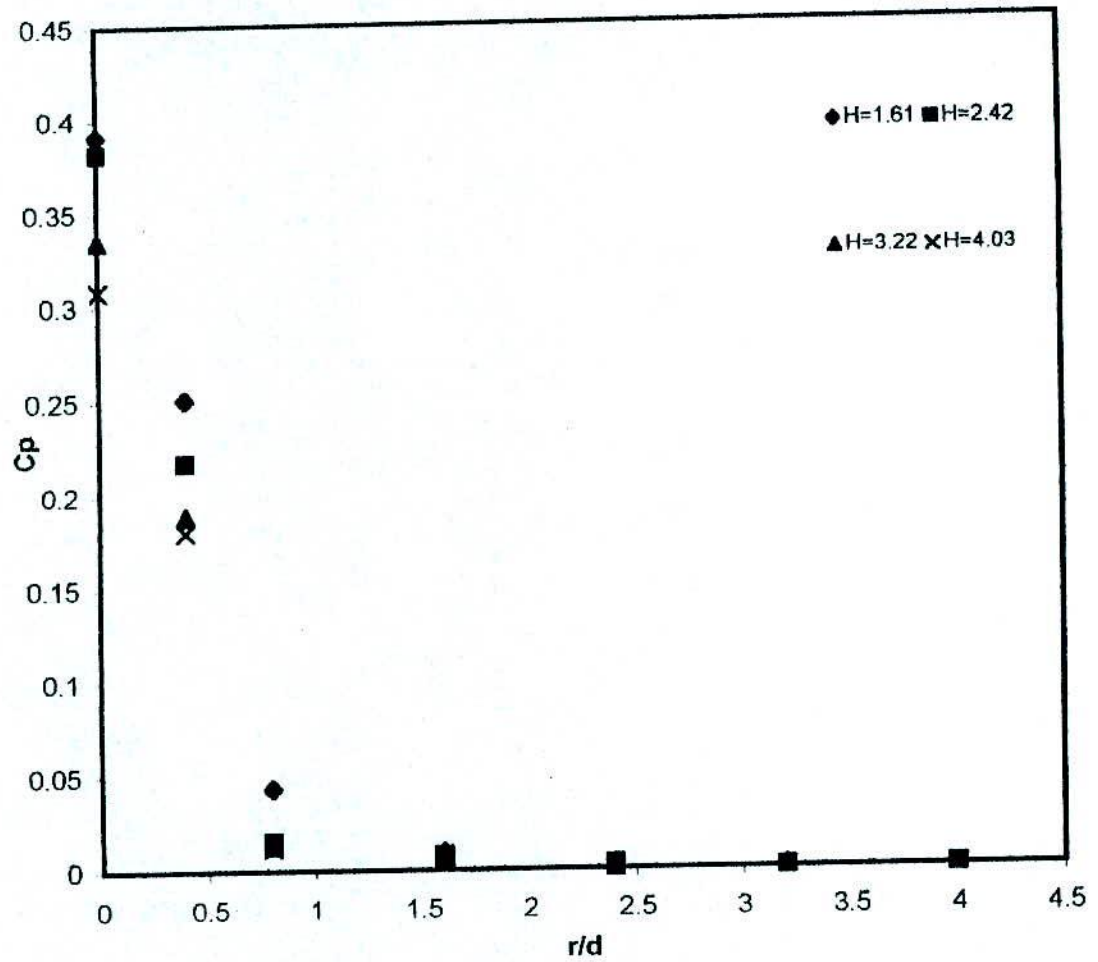


Fig.-5,1,22, Distribution of pressure over a surface of roughness,  $e=,01806$  for different jet-to-plate spacing and at  $Re=8700$ ,

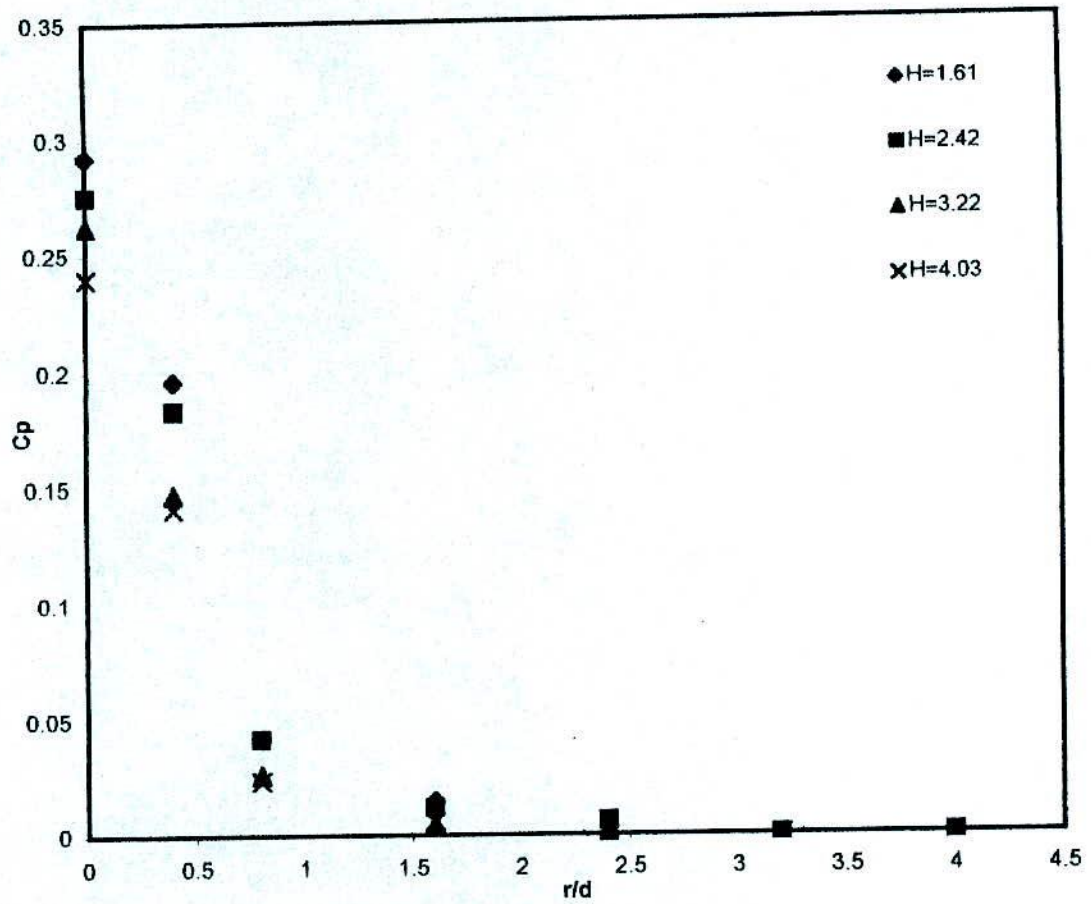


Fig.: 5,1,23, Distribution of pressure over a surface of roughness,  $e=,01806$  for different jet-to-plate spacing and at  $Re=23400$ ,

# NUSSELT NUMBER DISTRIBUTION.

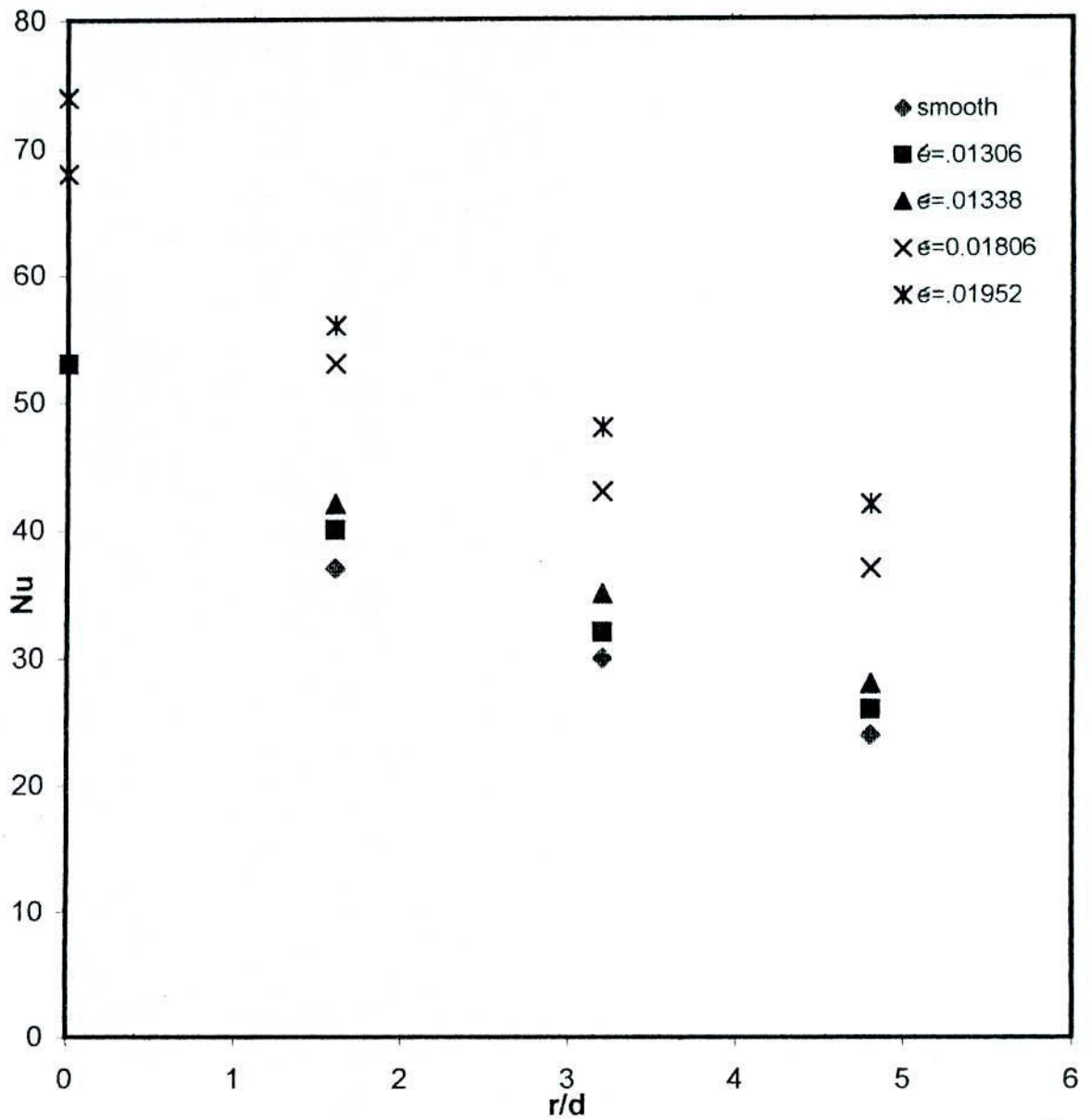


Fig.- 5.2.1. Distribution of Nusselt number over the surfaces of different roughness at  $Re= 6000$  and at jet-to-plate spacing , $H=1.61$ .

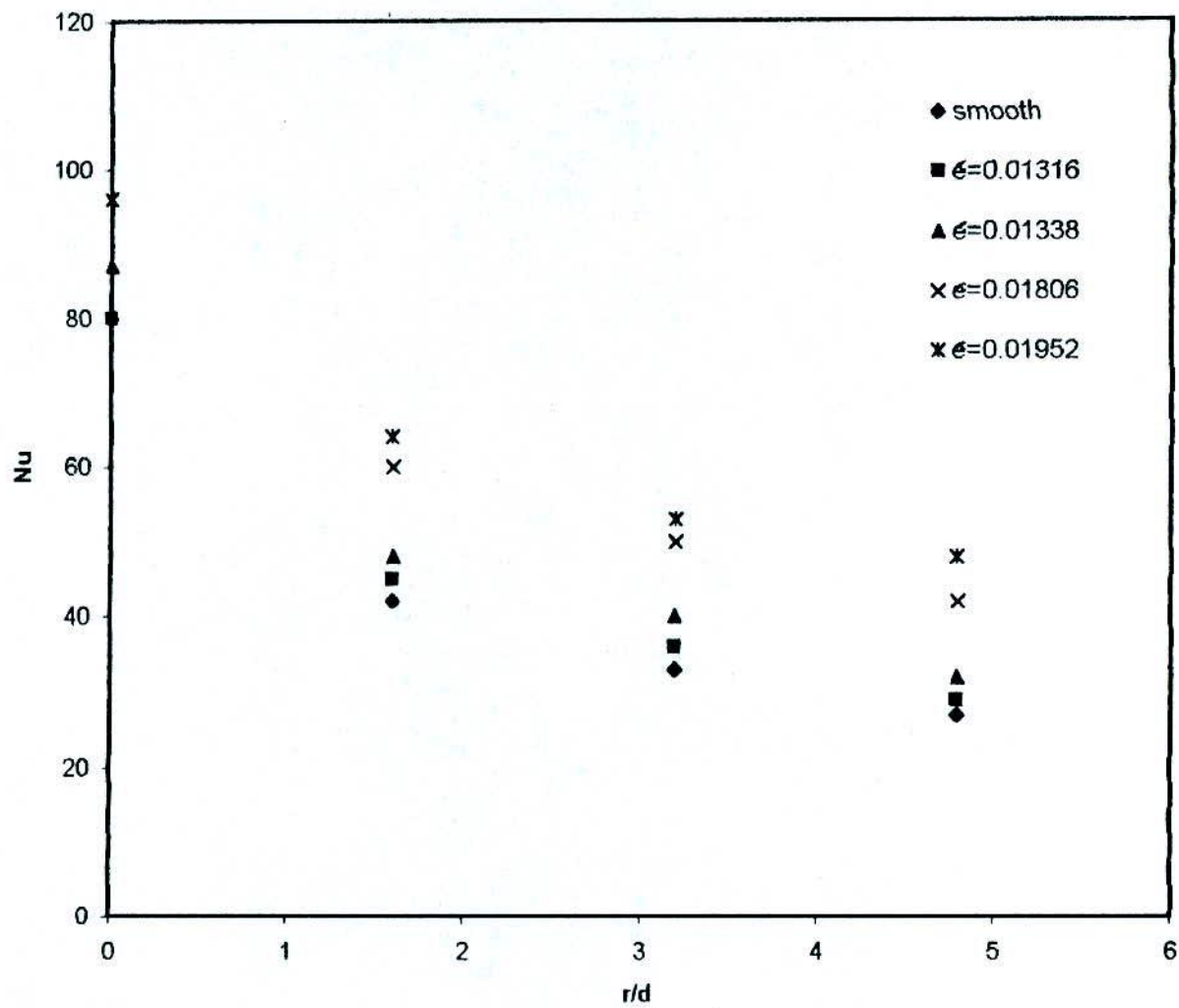


Fig.- 5.2.2. Distribution of Nusselt number over surfaces of different roughness for Re=8700 and at Jet-to-plate spacing, H=1.61.

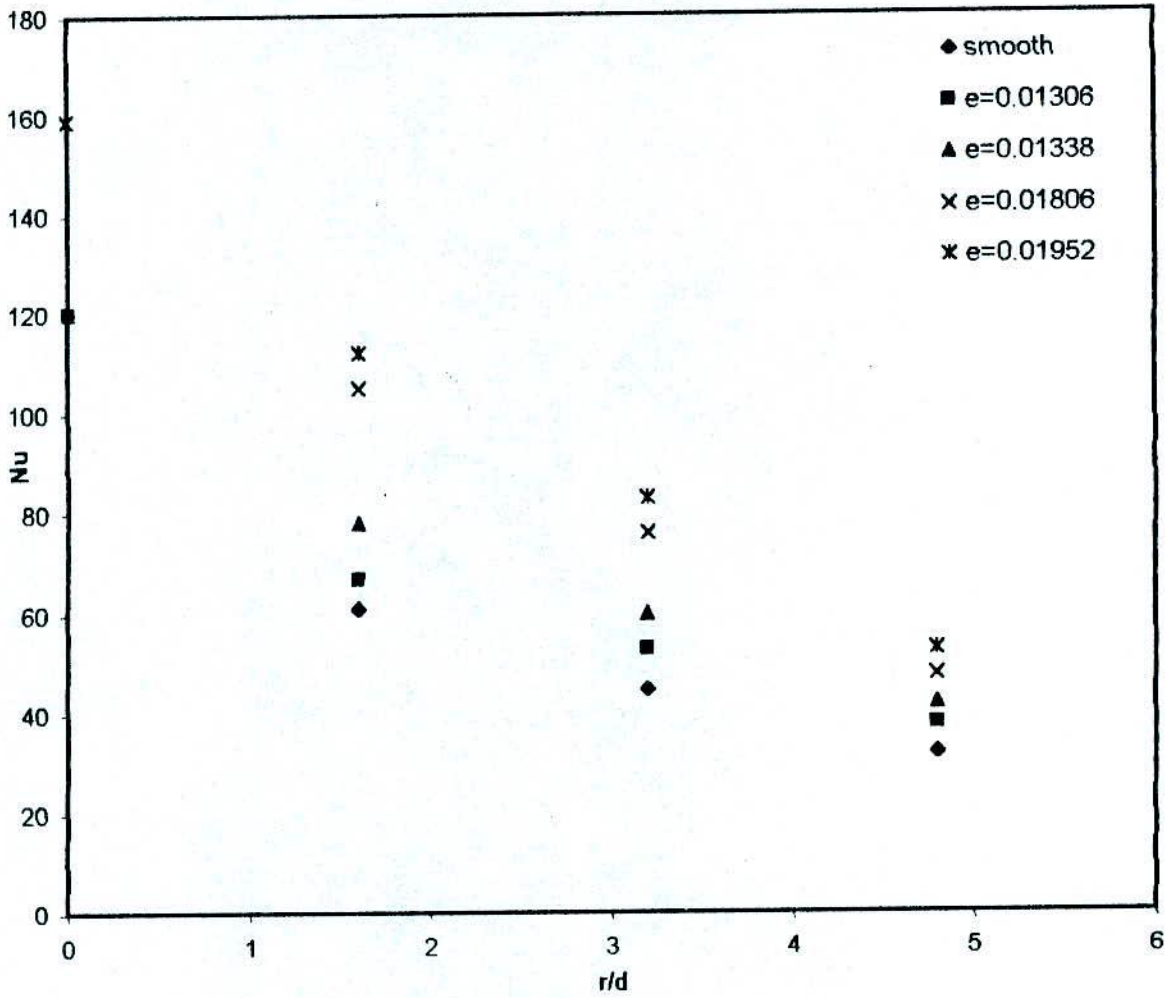


Fig.- 5.2.3 . Distribution of Nusselt number over the surfaces of different roughness at  $Re=16520$  and at Jet-to-plate spacing,  $H=1.61$ .

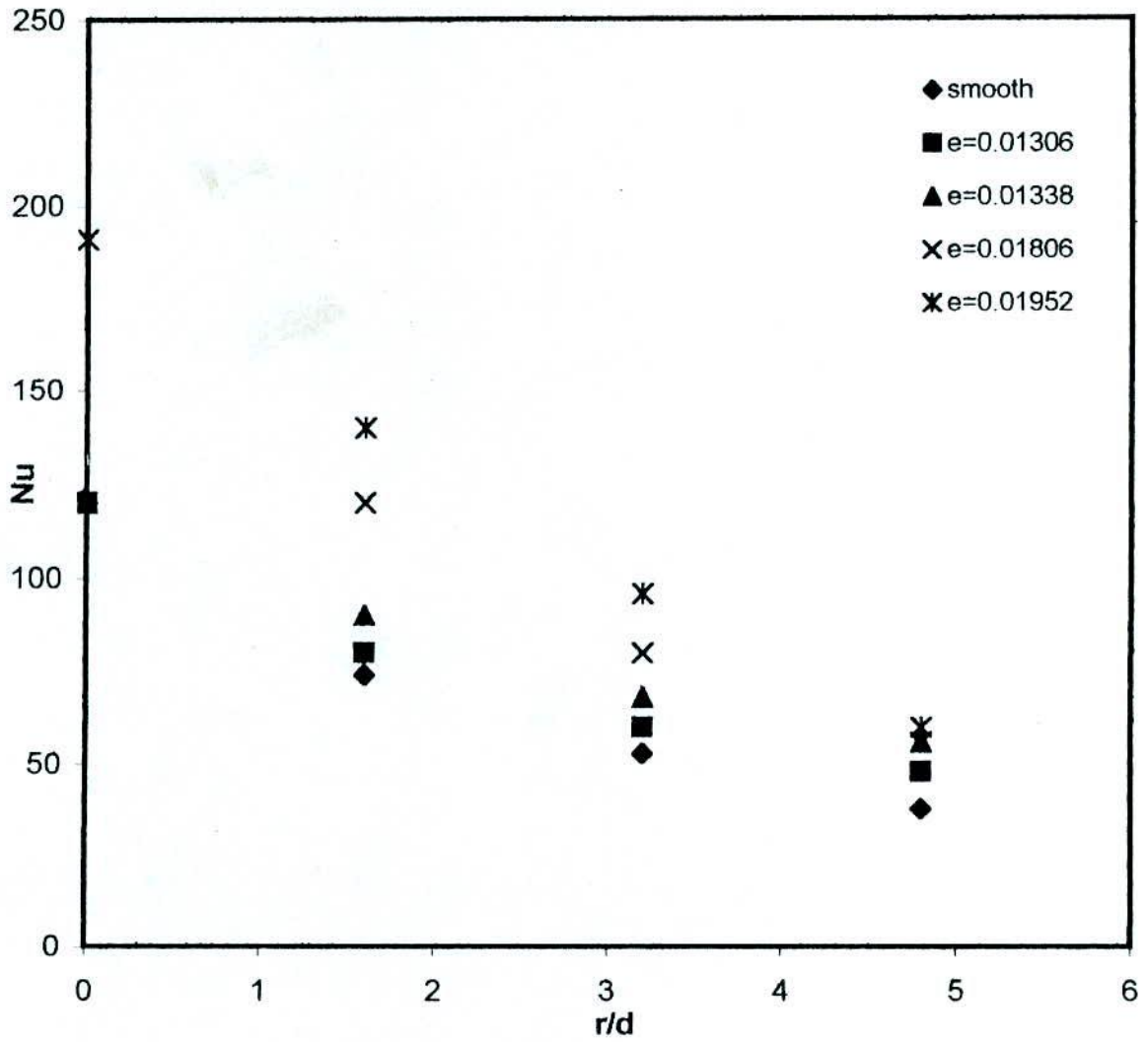


Fig.- 5.2.4. Distribution of Nusselt number over surfaces of different roughness at  $Re=23400$  and at Jet-to-plate spacing,  $H=1.61$ .

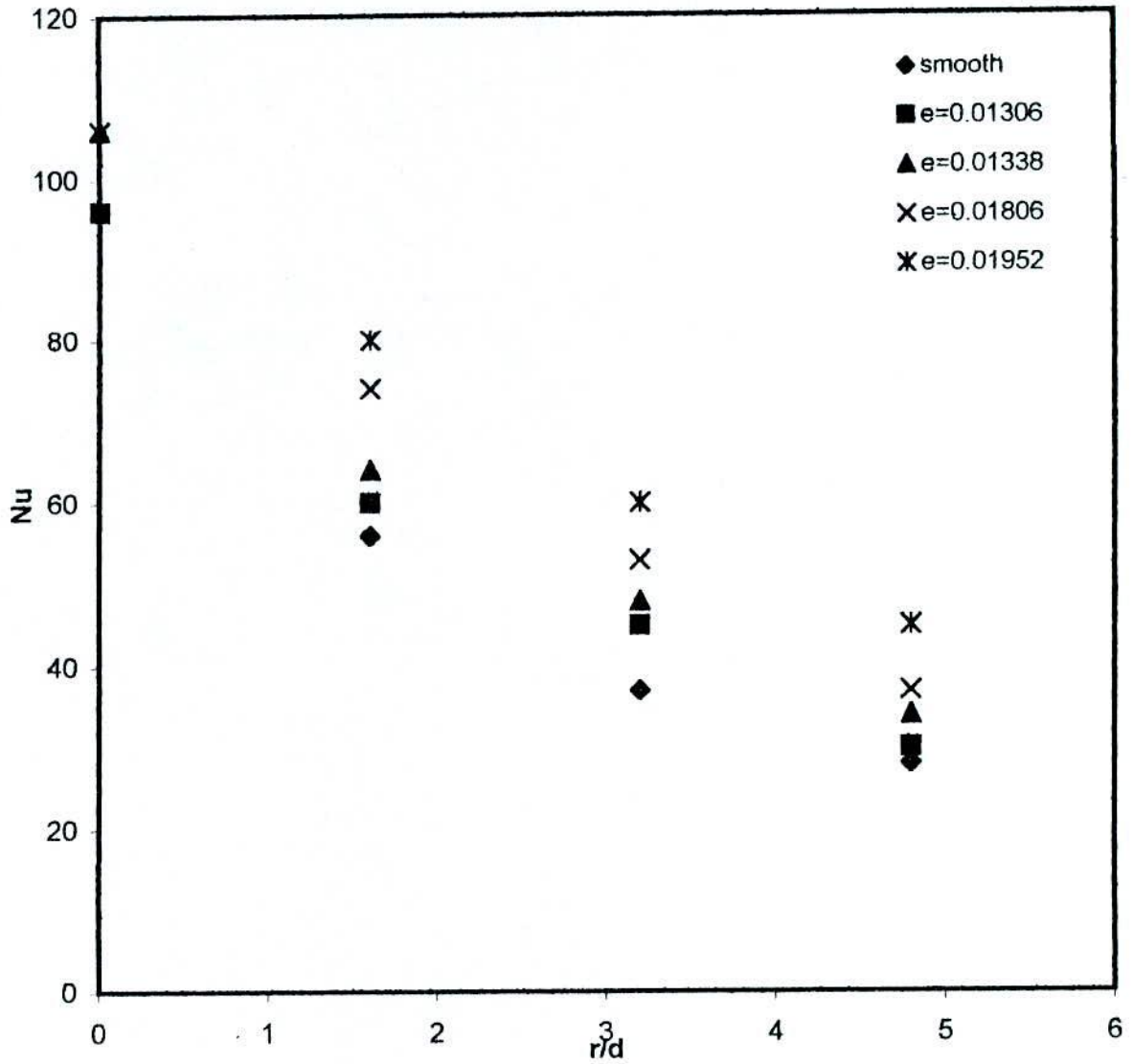


Fig. - 5.2.5. Distribution of Nusselt number over surfaces of different roughness at  $Re=16520$  and at Jet-to-plate spacing,  $H=2.42$ .



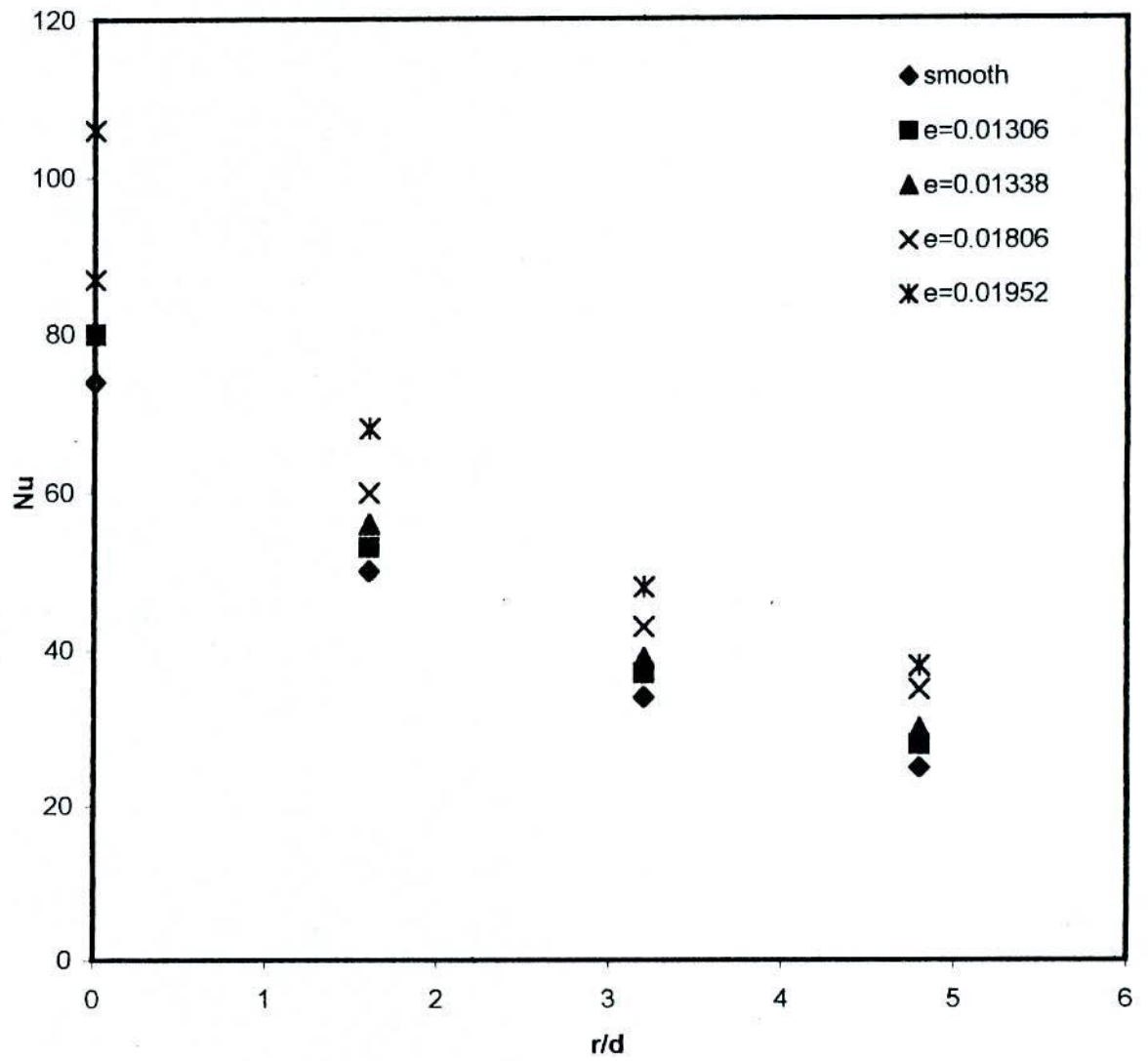


Fig.-5.2.6. Distribution of Nusselt number over surfaces of different roughness at  $Re=16520$  and at Jet-to-plate spacing,  $H=3.22$ .

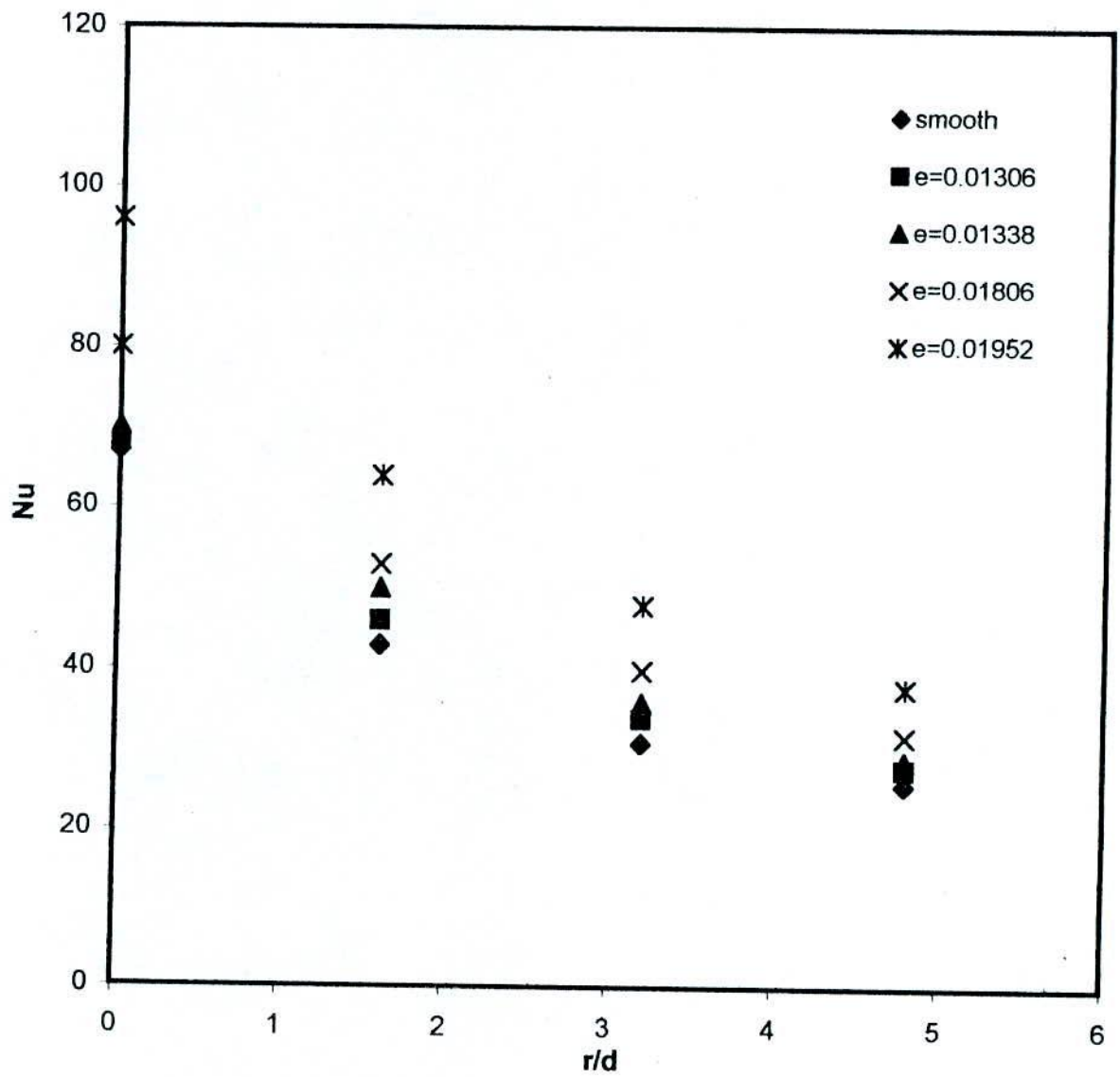


Fig.-5.2.7. Distribution of Nusselt number over surfaces of different roughness at  $Re=16520$  and at jet-to-plate spacing,  $H=4.03$ .

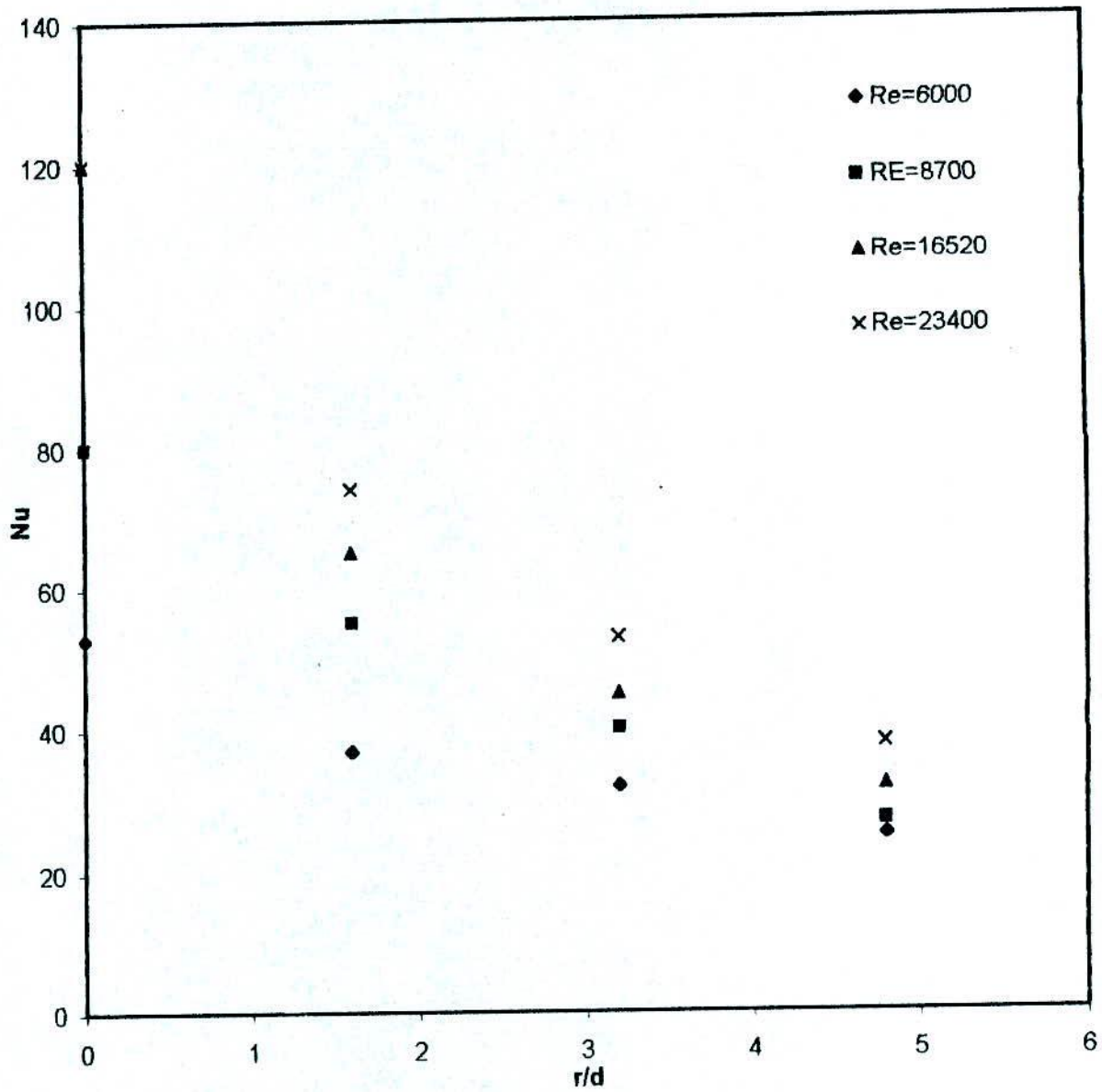


Fig.-5.2.8. Distribution of Nusselt number over smooth surface for different Reynolds number and at Jet-to-plate spacing,  $H=1.61$ .

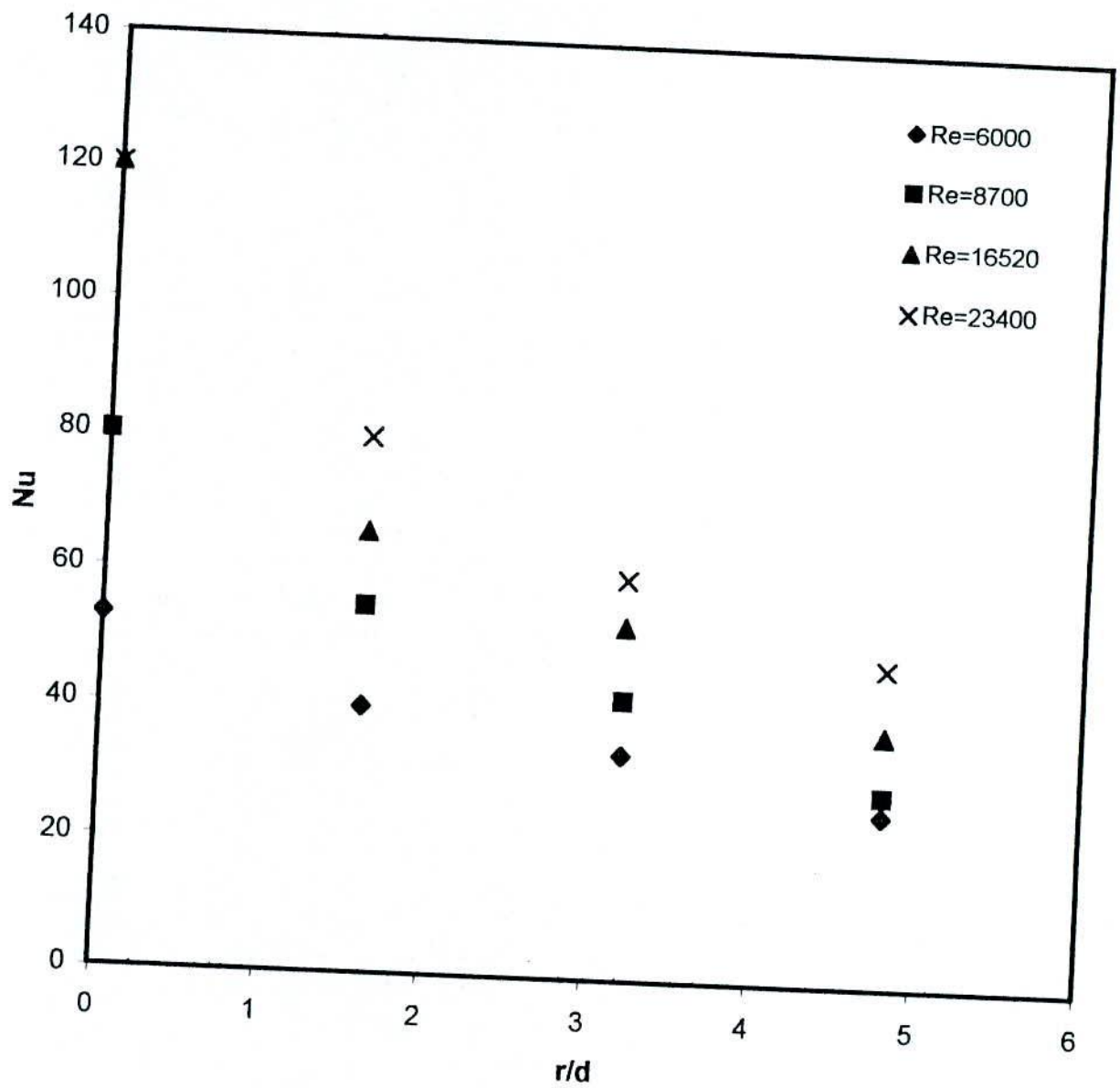
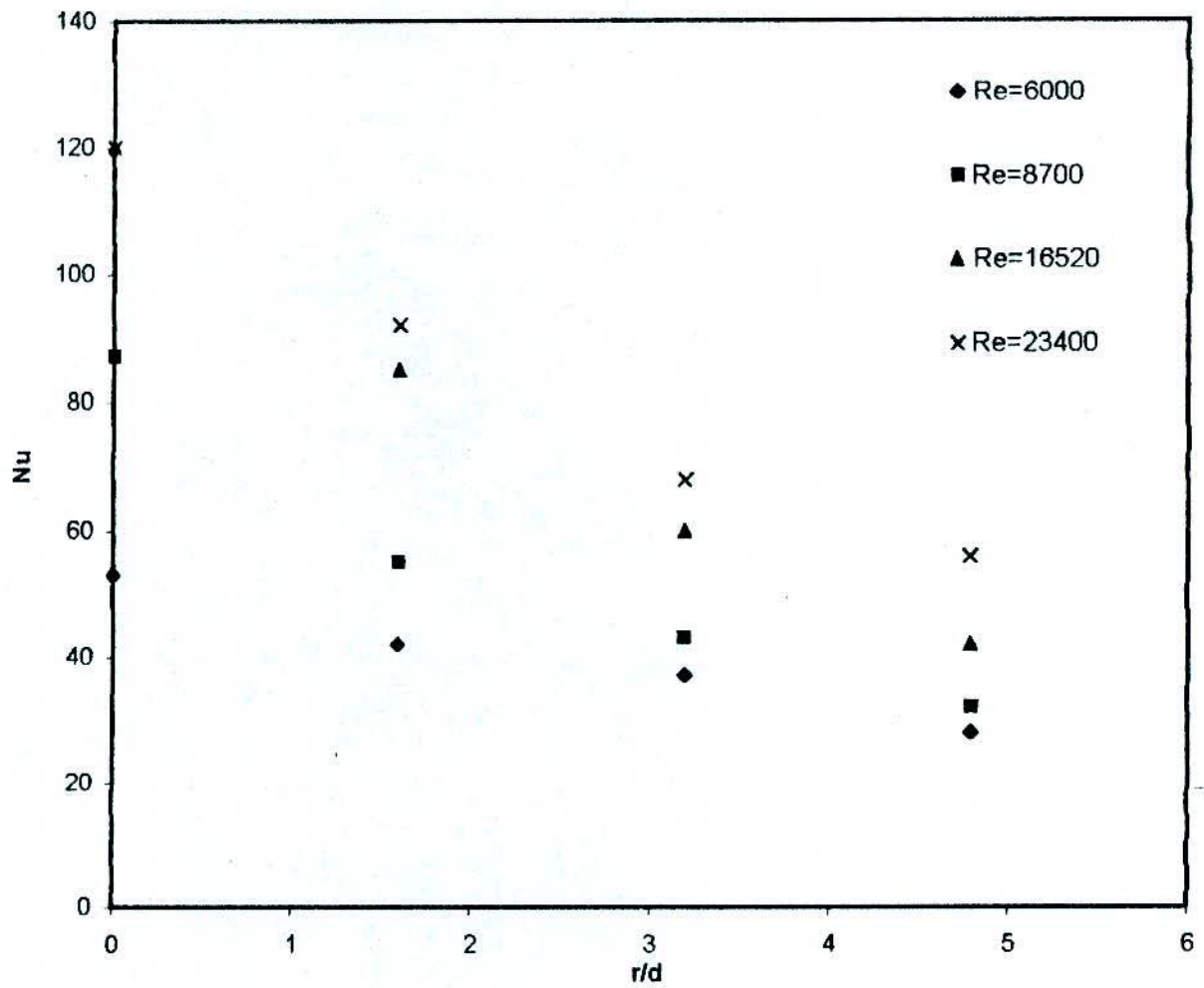


Fig.-5.2.9. Distribution of nusselt number over the surface of roughness,  $e=0.01306$  and at jet-to-plate spacing,  $H=1.61$  for different Reynolds number.



5.2.10. Distribution of Nusselt number over the surface of roughness,  $e=0.01338$  for different Reynolds number and at jet-to-plate spacing,  $H=1.61$ .

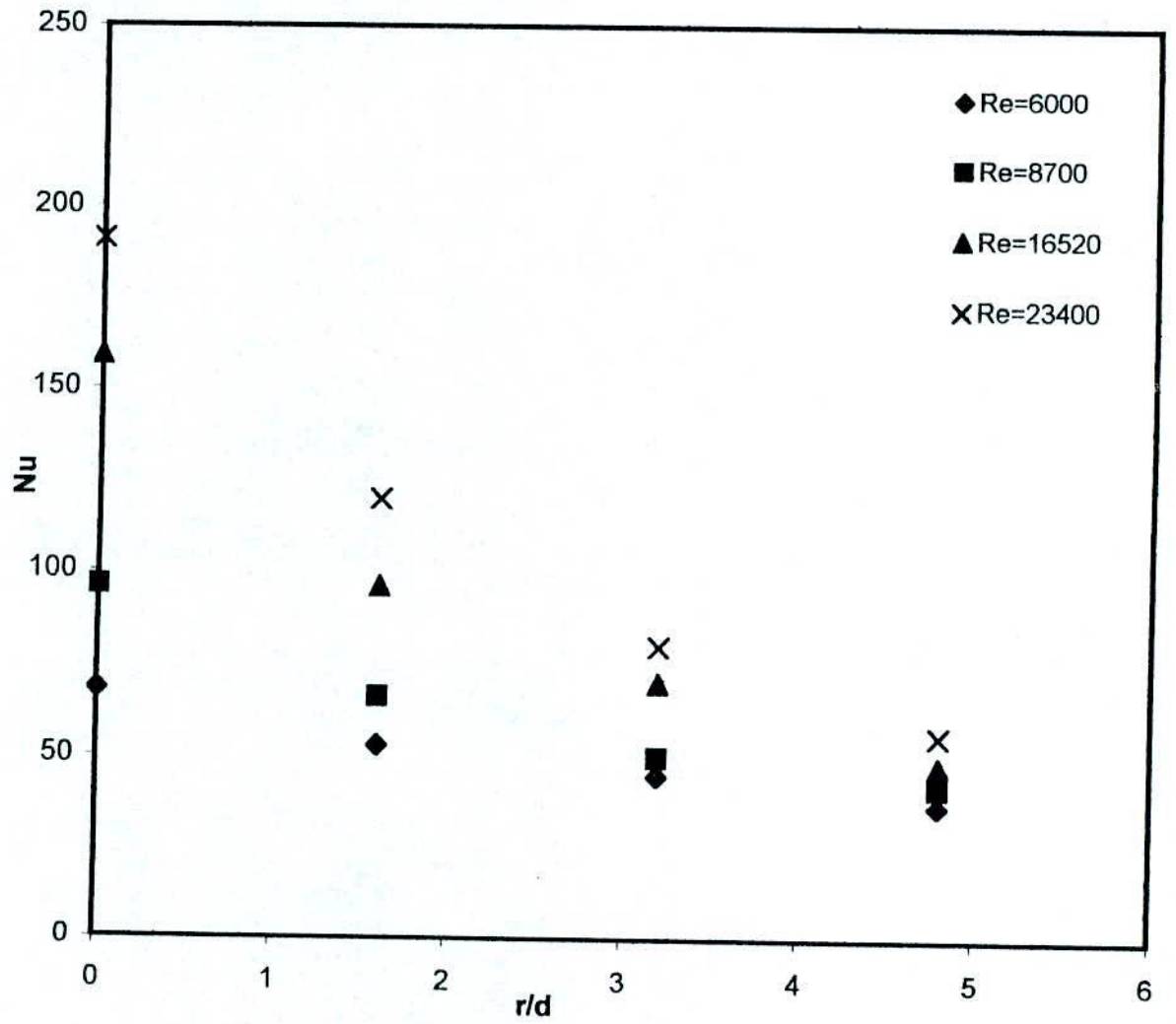


Fig.-5.2.11. Distribution of Nusselt number over the surface of roughness  $e=0.01806$  for different Reynolds number and at jet-to-plate spacing,  $H:$

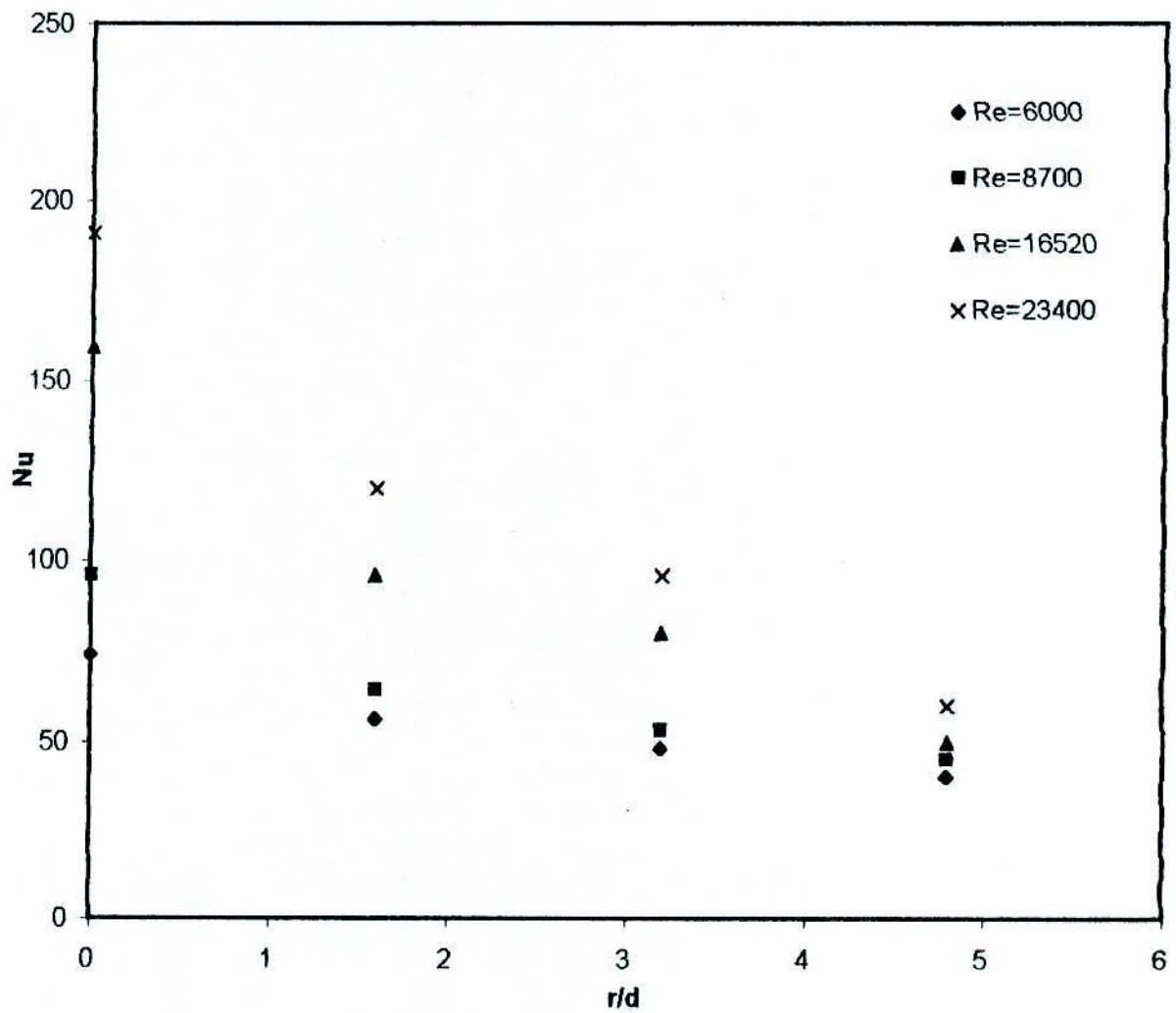


Fig.-5.2.12. Distribution of Nusselt number over the surface of roughness,  $e=0.01952$  for different Reynolds number and at jet-to-plate spacing,  $H=1.61$ .

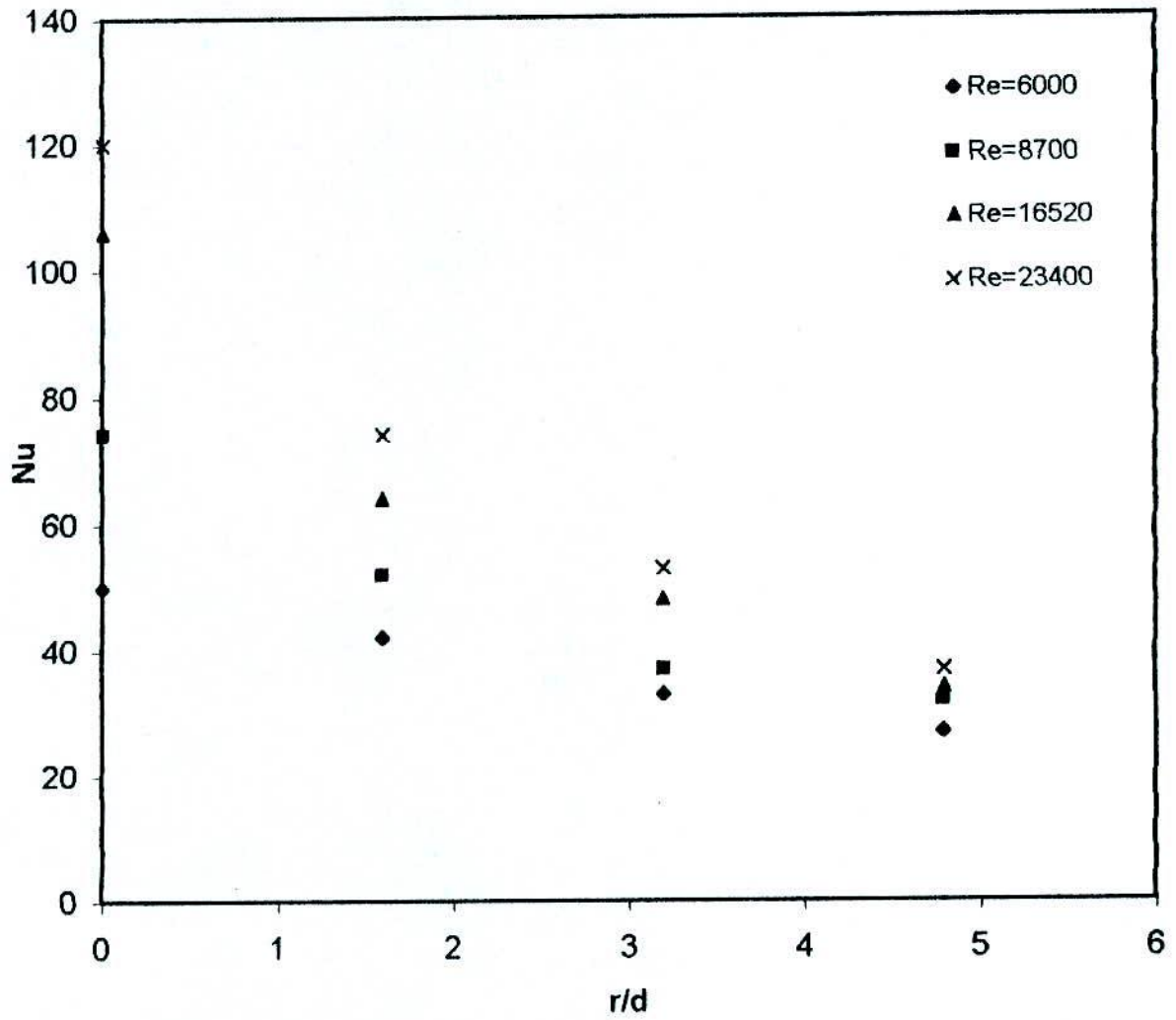


Fig.-5.2.13. Distribution of Nusselt number for different Reynolds number over a surface of roughness,  $\epsilon=0.01338$  and at jet-to-plate spacing,  $H=2.42$ .



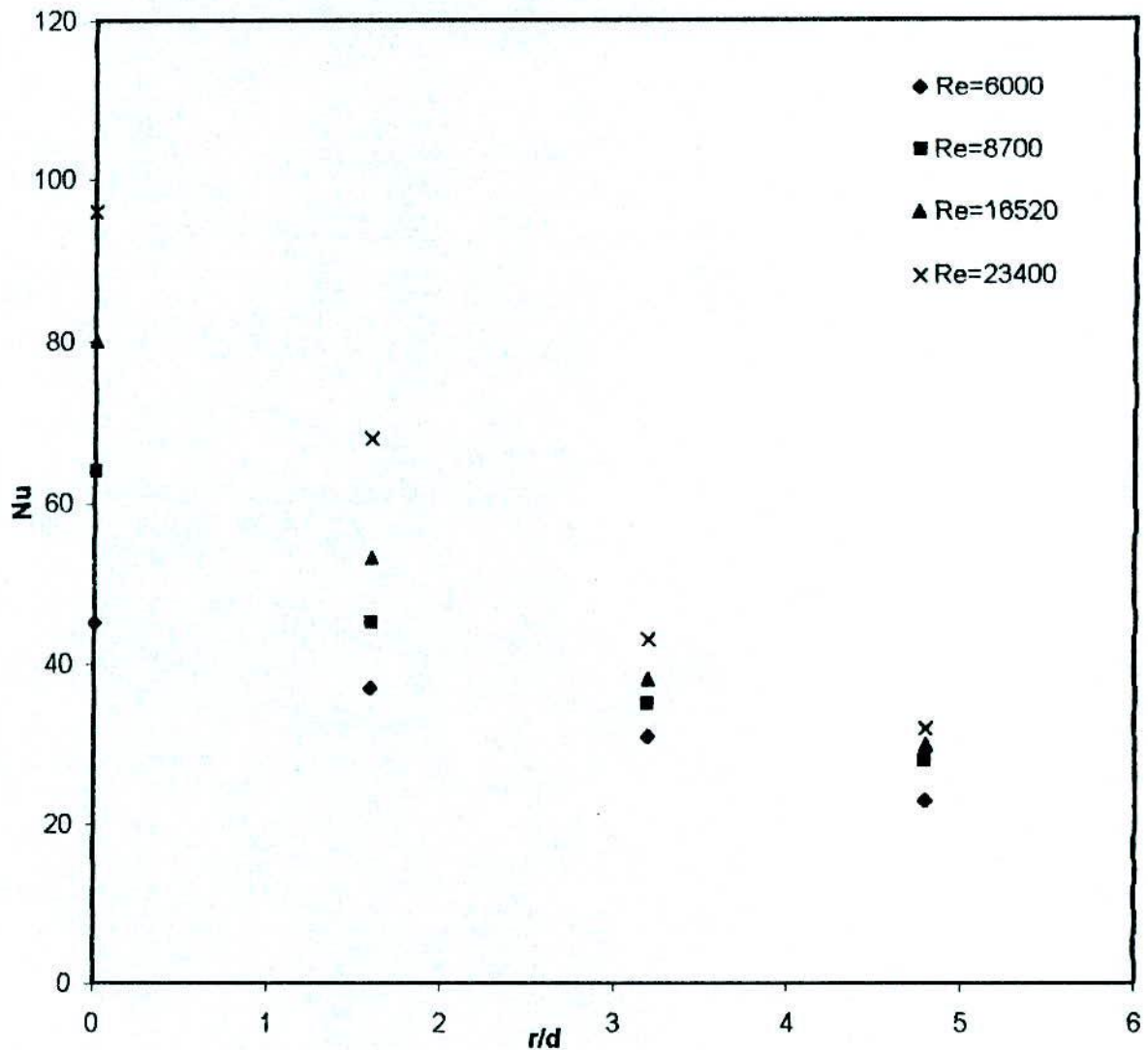


Fig.-5.2.14. Distribution of Nusselt number over the surface of roughness,  $e=0.01338$  for different Reynolds number and at jet-to-plate spacing,  $H=3.22$ .

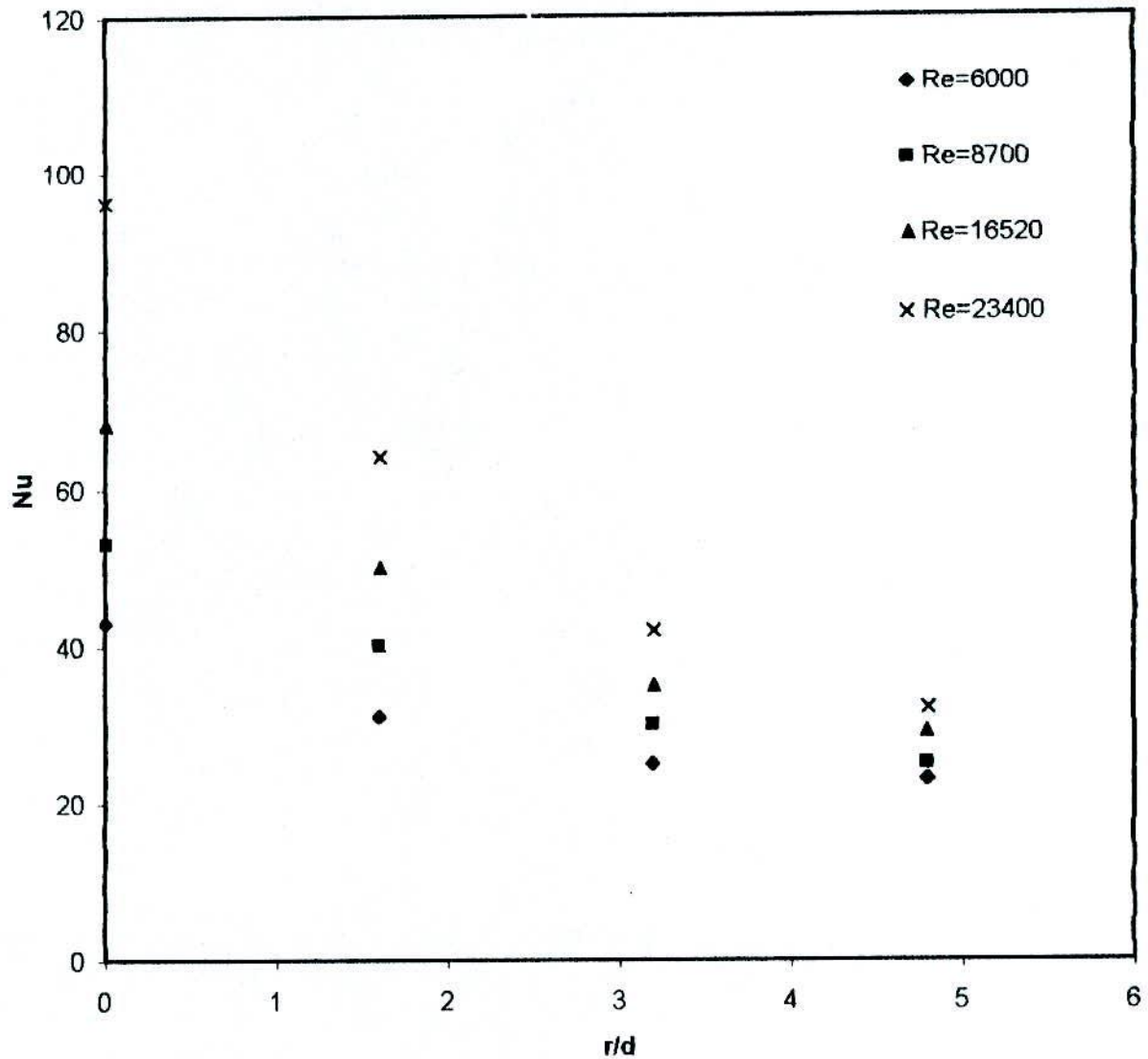


Fig.-5.2.15. Distribution of Nusselt number over the surface of roughness,  $E=0.01338$  for different Reynolds number and at jet-to-plate spacing,  $H=4.03$ .

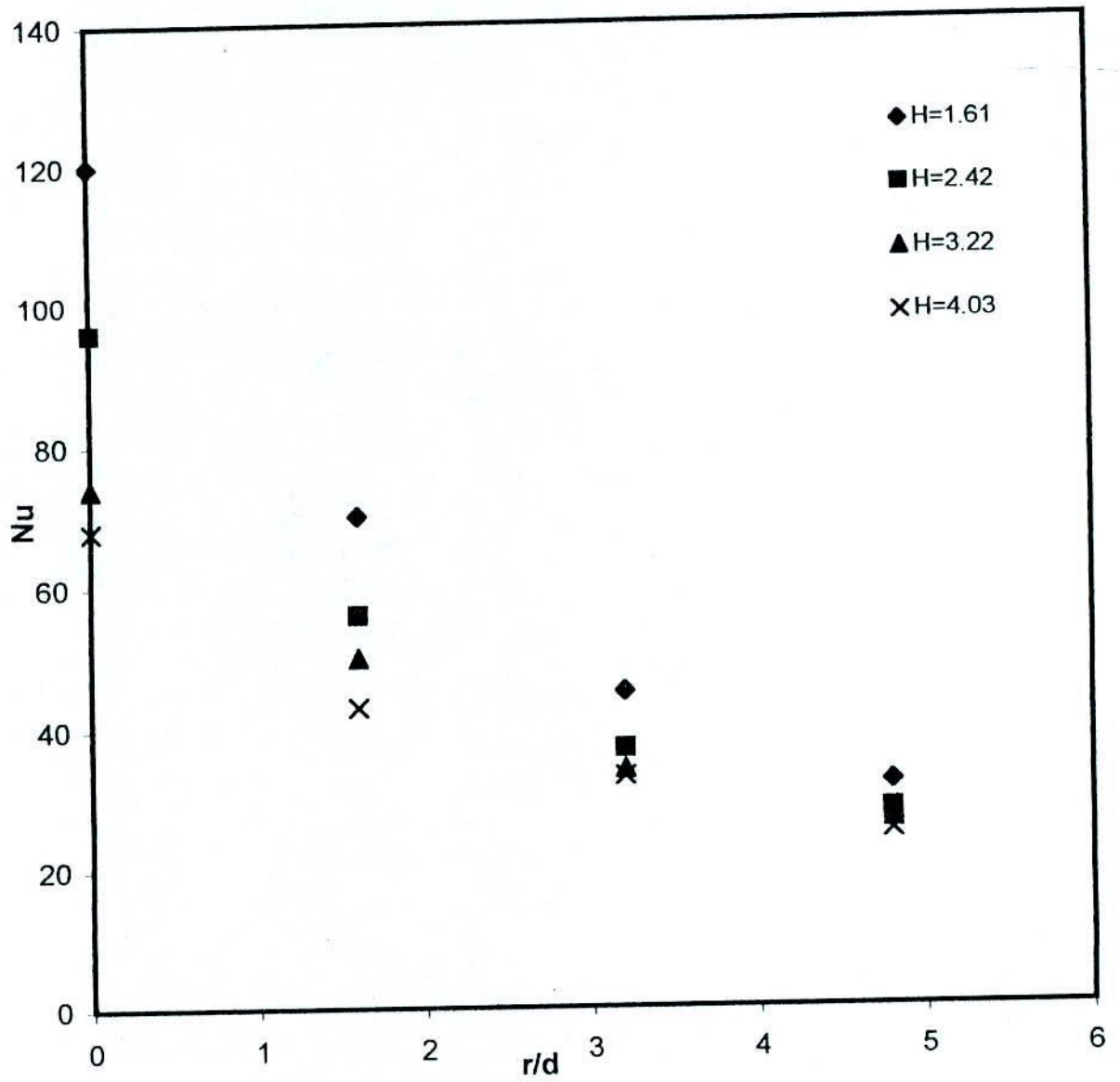


Fig.-5.2.16. Distribution of nusselt number over a smooth surface for different Jet-to-plate spacings and at Re=16520.

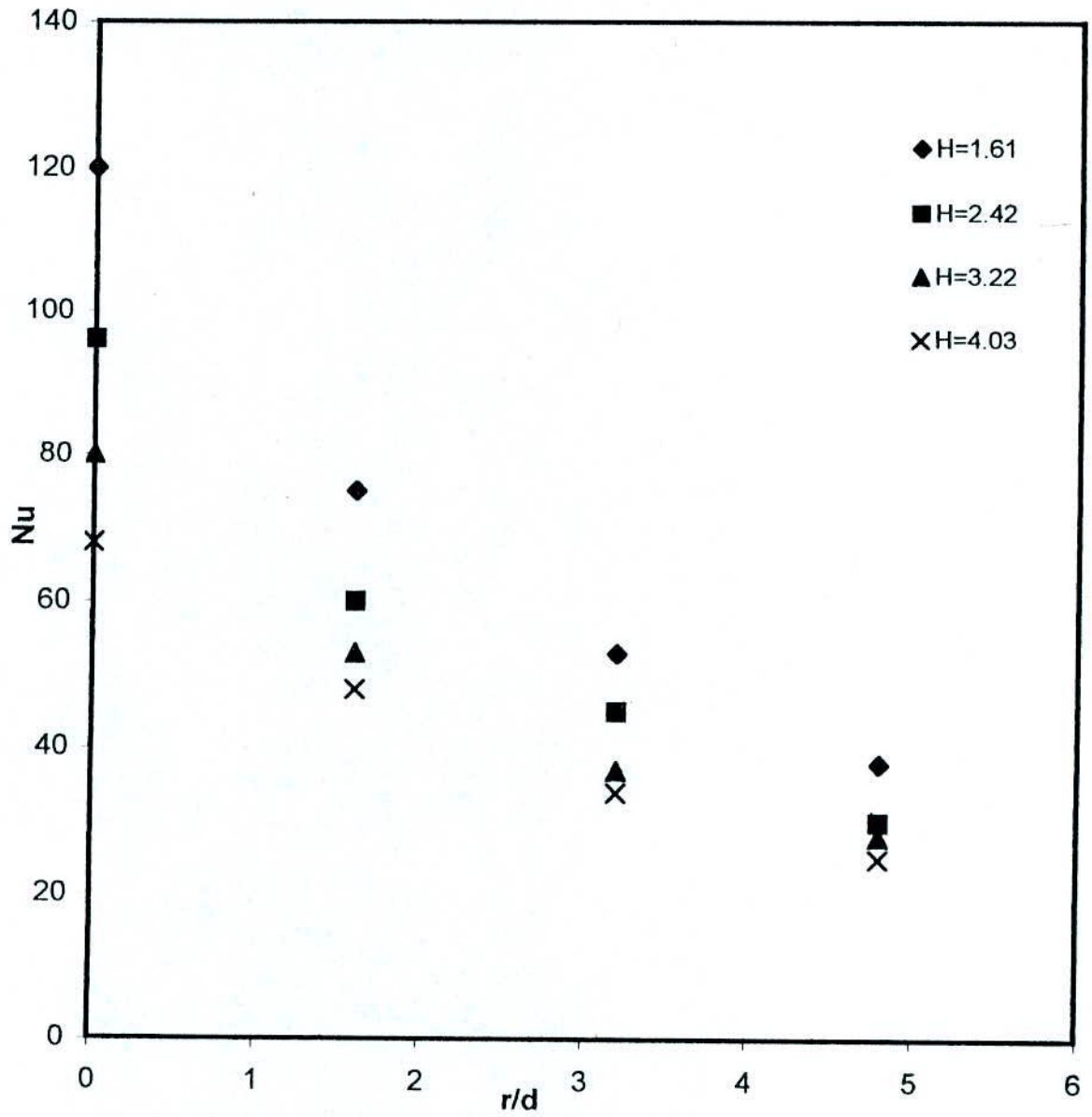


Fig.5.2.17. Distribution of Nusselt number over a surface of roughness,  $e=0.01306$  for different jet-to-plate spacings and at  $Re=16520$ .

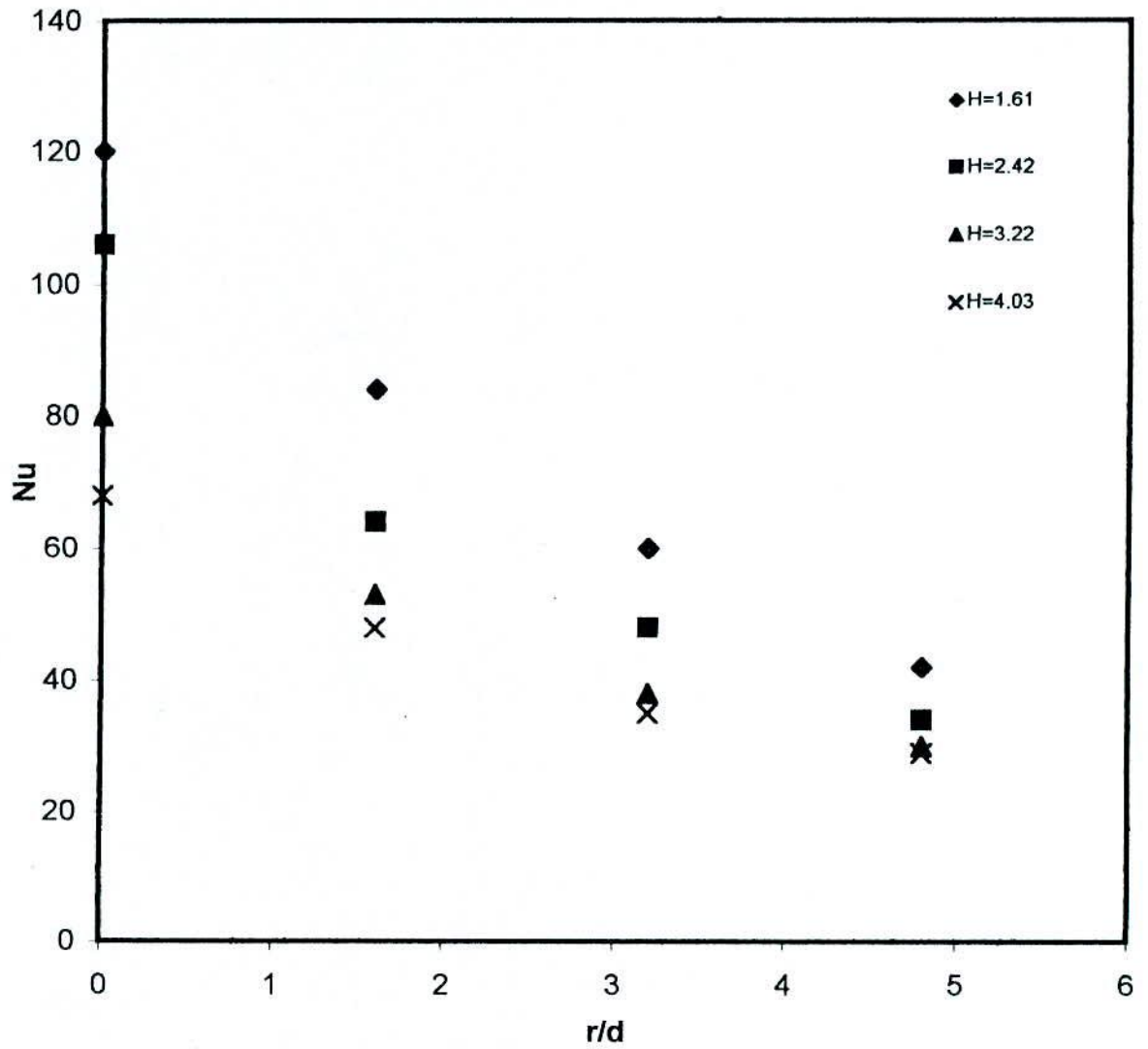


Fig.-5.2.18. Distribution of Nusselt number over a surface of roughness,  $e=0.01338$  for different jet-to-plate spacings and at  $Re=16520$ .

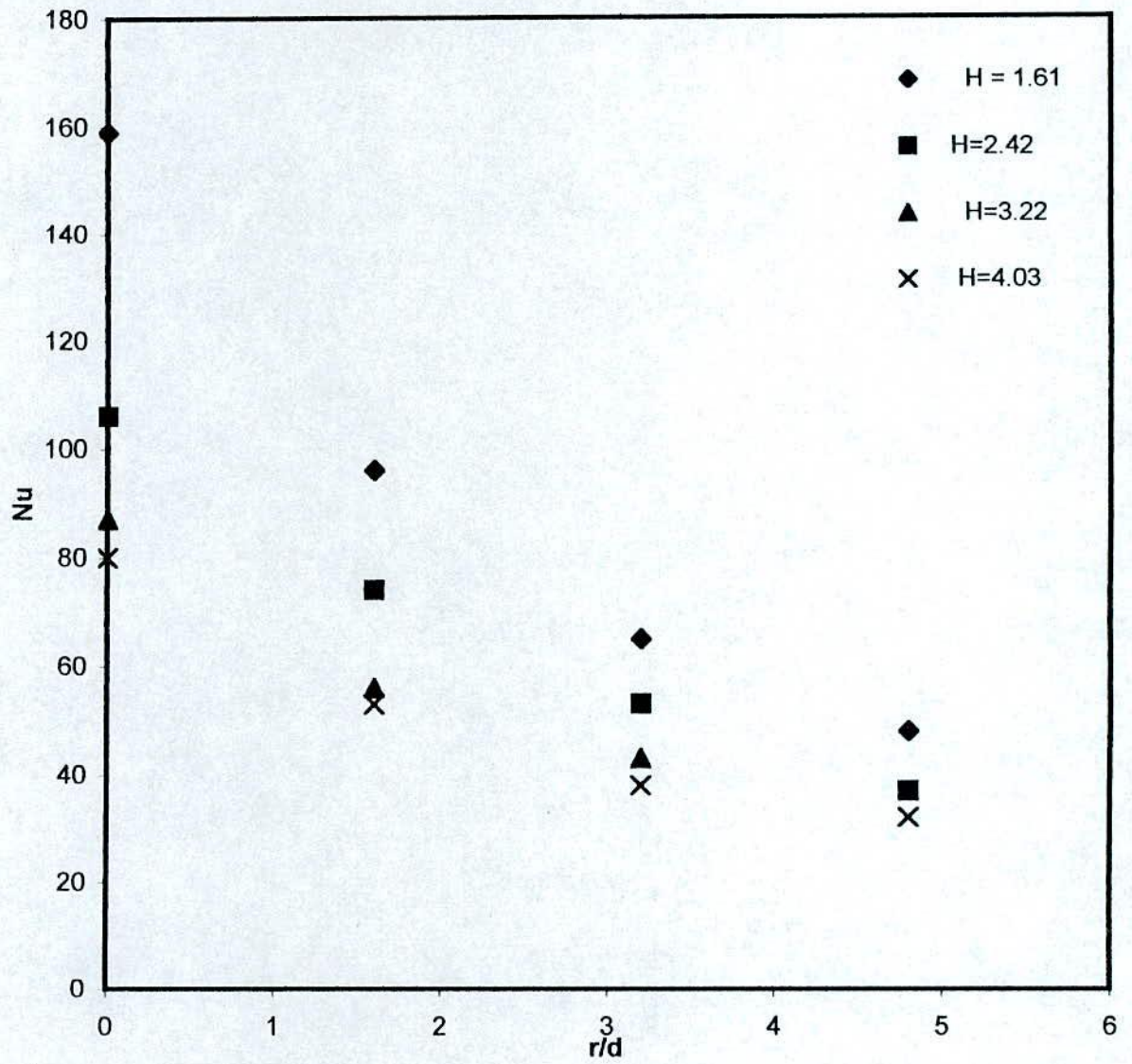


Fig.-5.2.19. Distribution of Nusselt number over a surface of roughness,  $e=0.01806$  for different jet-to-plate spacing and at  $Re=16520$ .

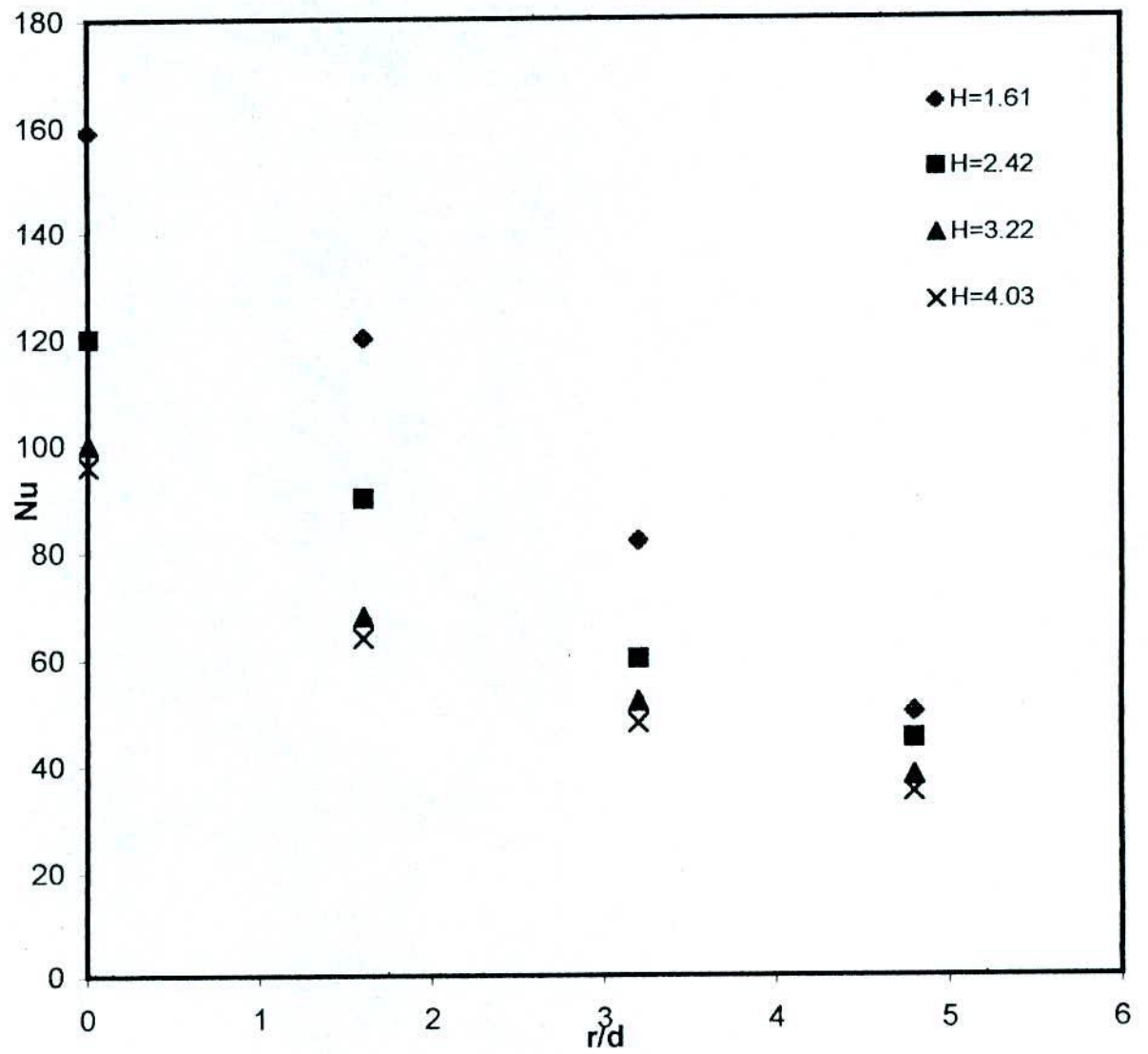


Fig.-5.2.20. Distribution of Nusselt number over a surface of roughness  $e=0.01952$ . for different jet-to-plate spacing and at  $Re=16520$ .

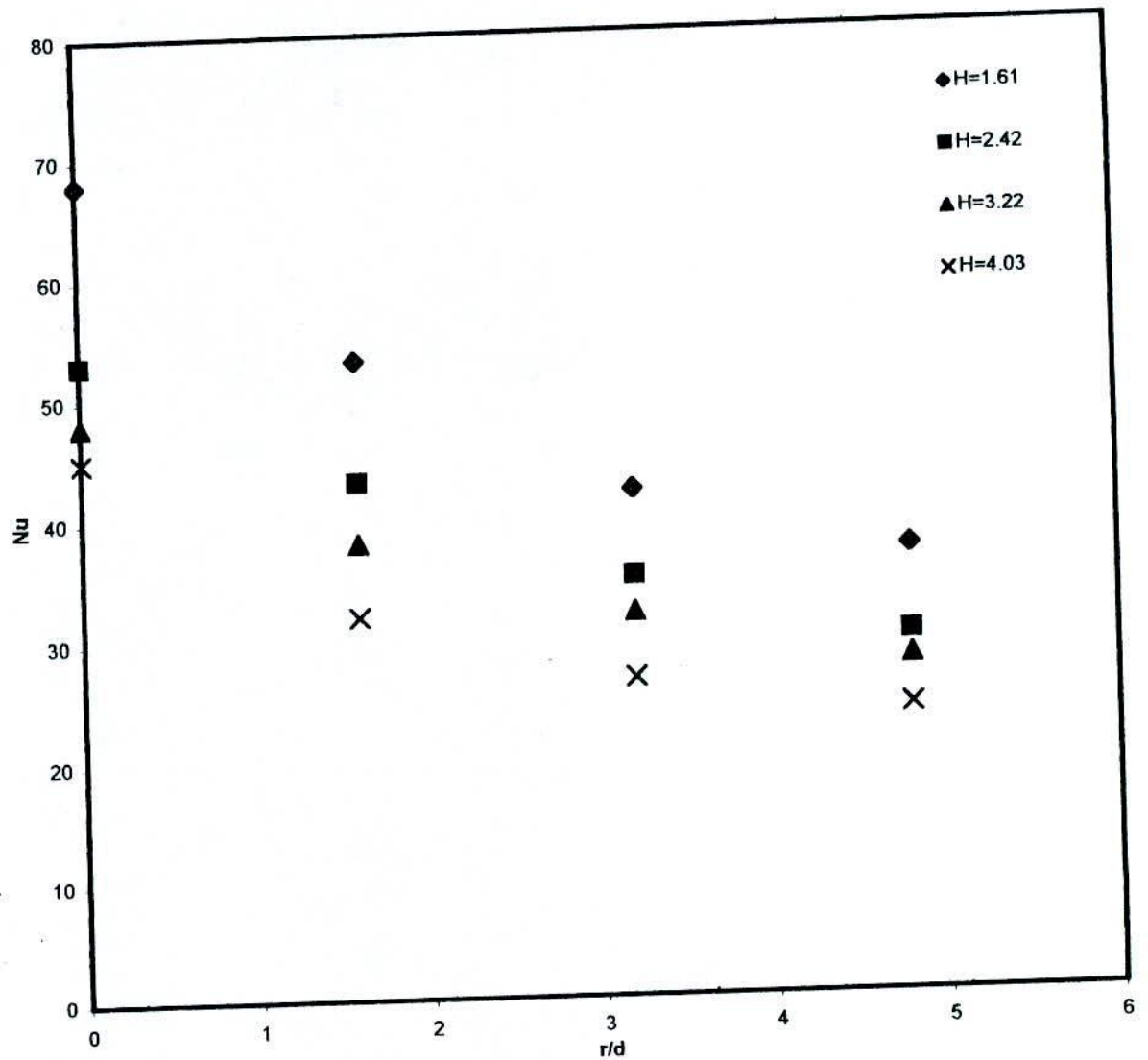


Fig.-5.2.21. Distribution of Nusselt number over a surface of roughness  $e=0.01806$  for different jet-to-plate spacings and at  $Re=6000$ .



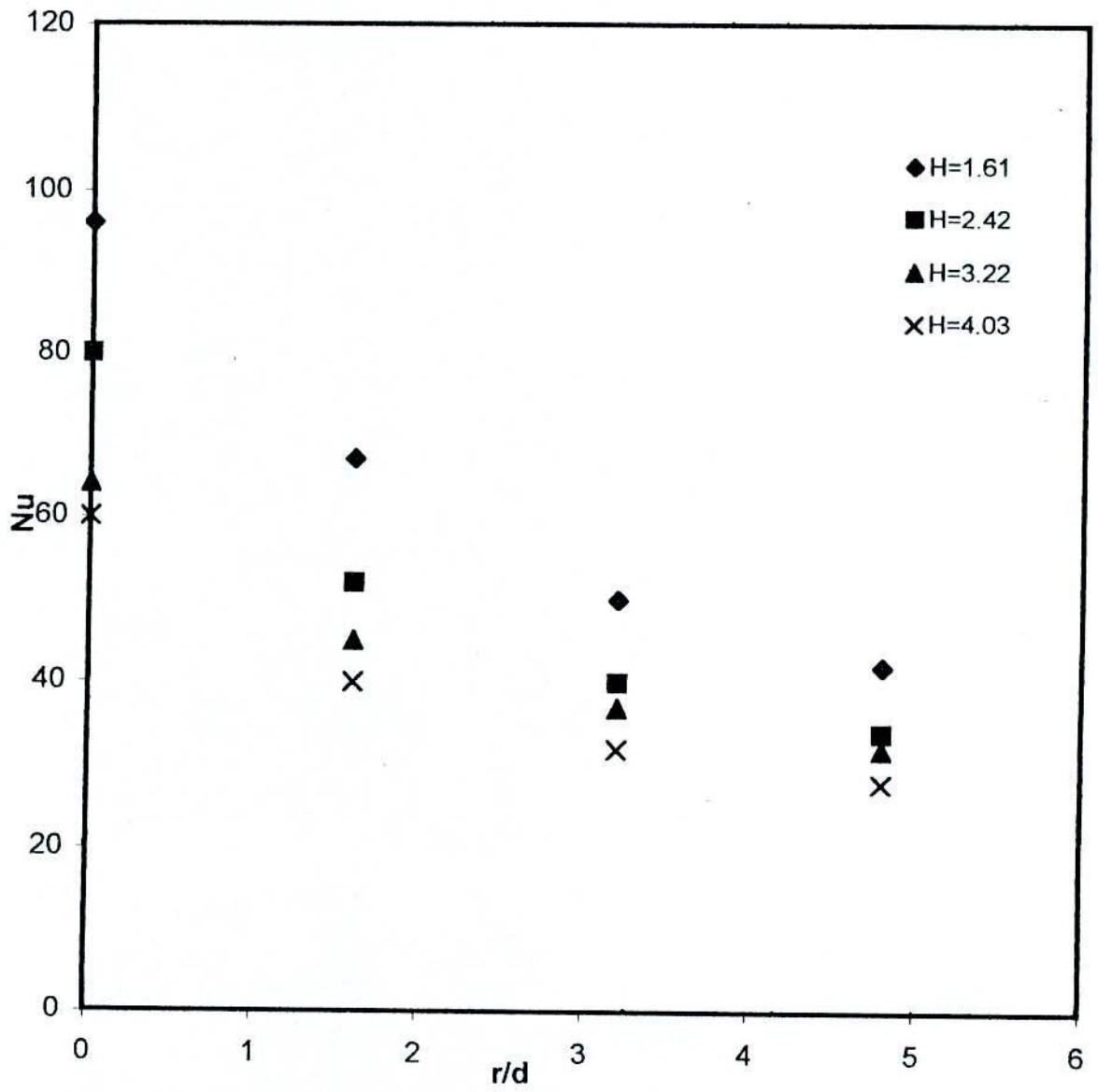


Fig.5.2.22. Distribution of Nusselt number over surface of roughness,  $e=0.01806$  for different jet-to-plate spacing and at  $Re=8700$ .

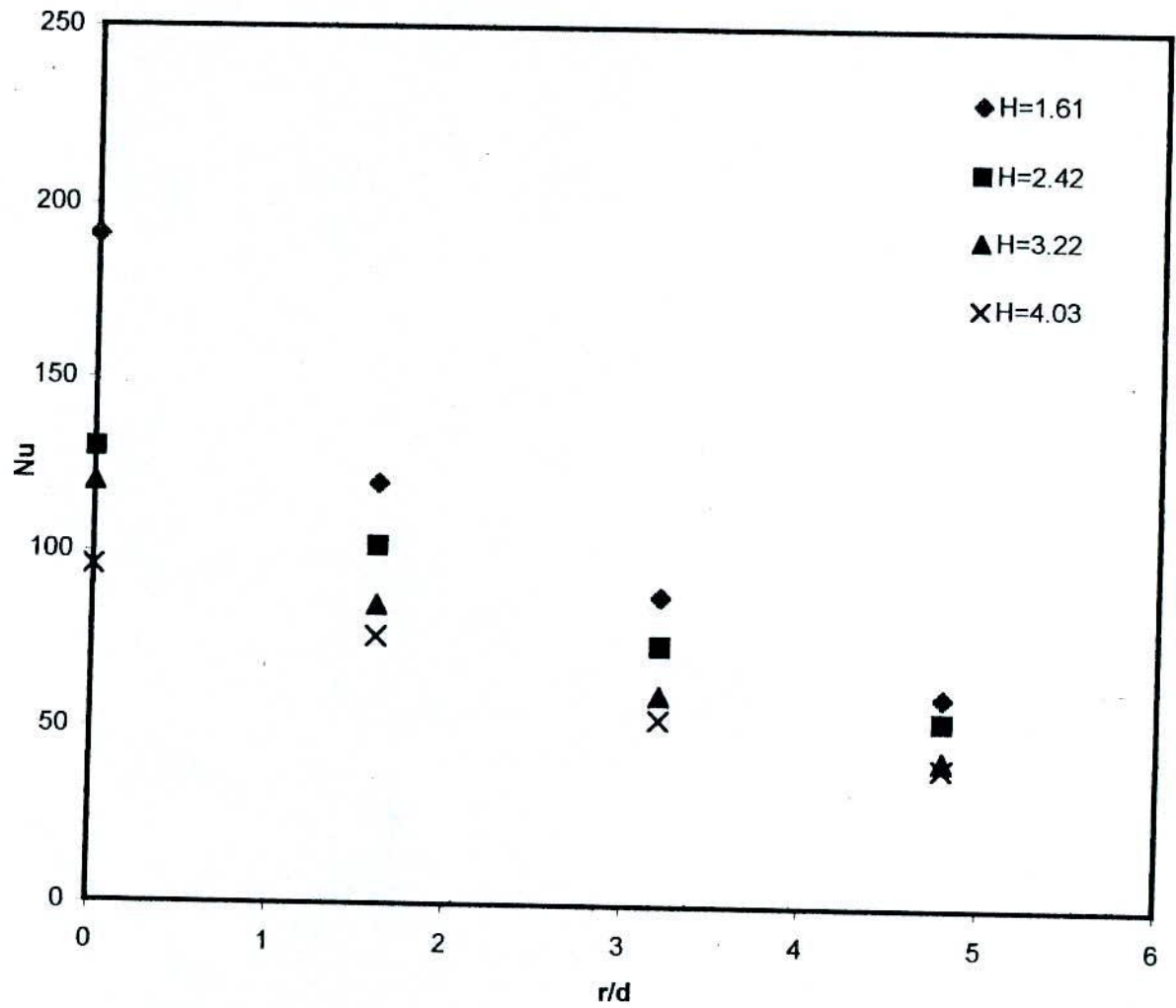


Fig.-5.2.23. Distribution of Nusselt number over a surface of roughness  $e=0.01806$  for different jet-to-plate spacing and at  $Re=23400$ .

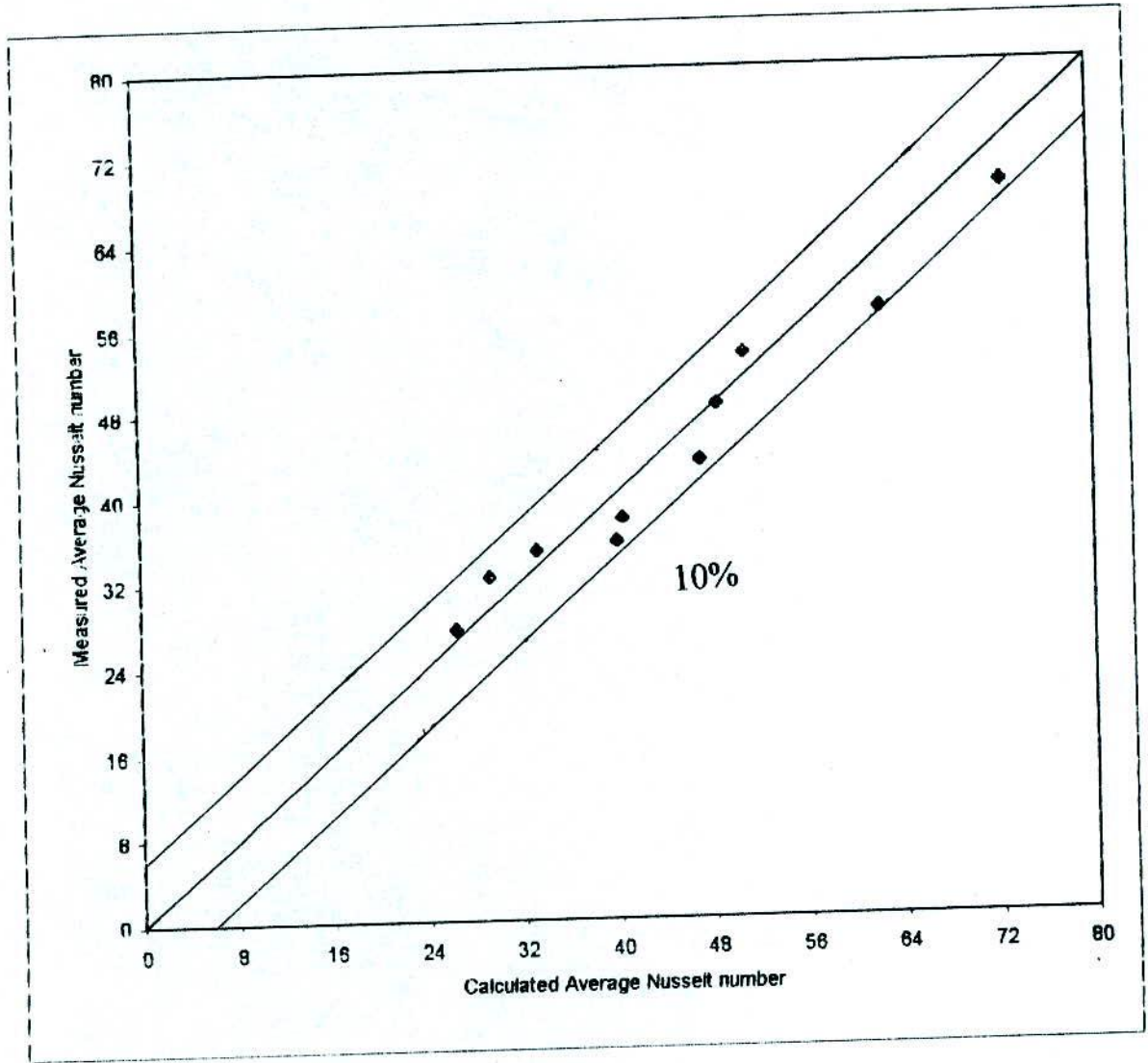


Fig-5.3 Calculated Average Nusselt number Vs. Measured Average Nusselt number.

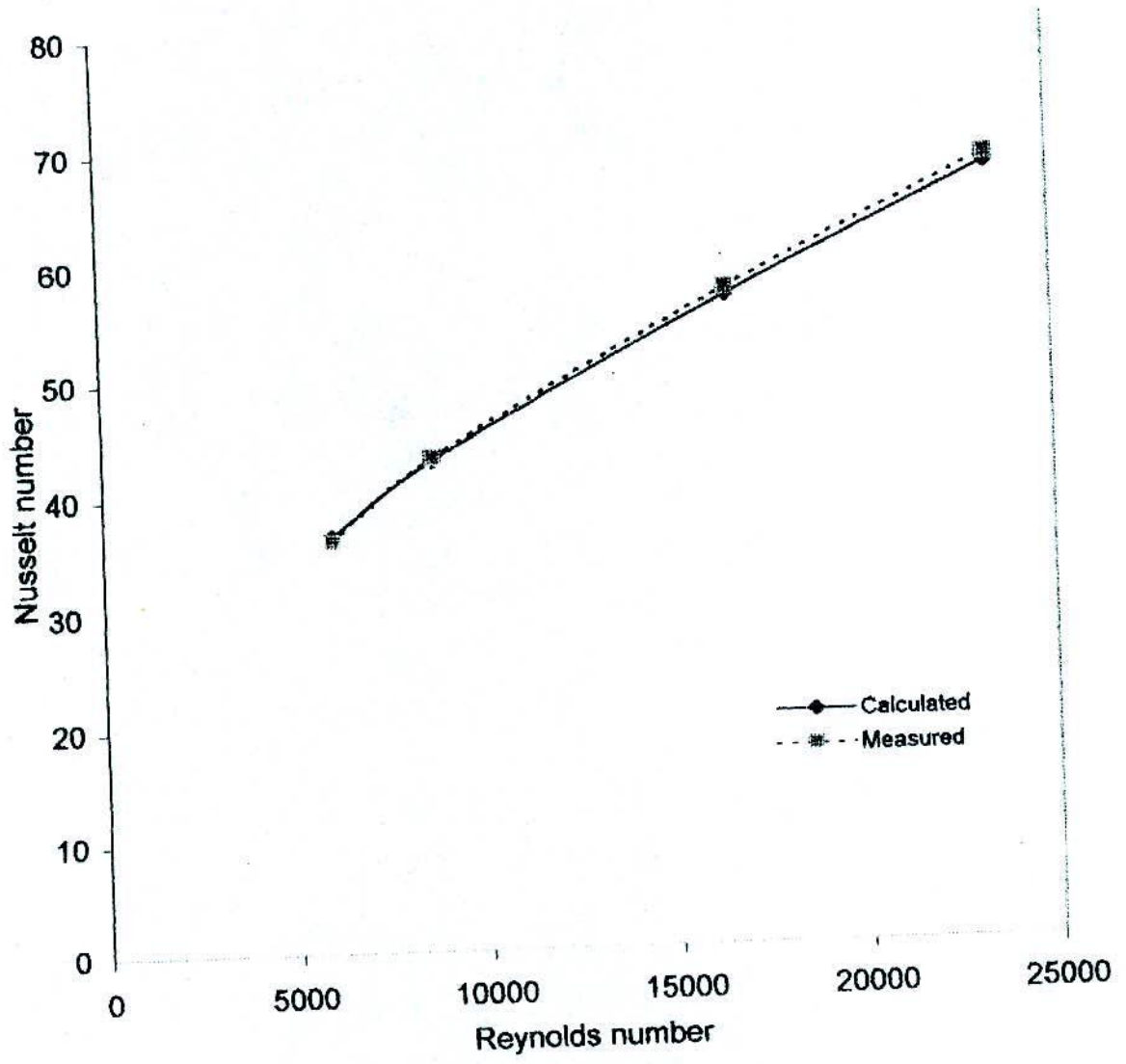


Fig-5.4 Calculated Average Nusselt number Vs. Measured Average Nusselt number.

## APPENDIX A

### [SAMPLE CALCULATION]

**Calculation Method** : Data were obtained to report average Nusselt number,  $\overline{Nu}$  as a function of jet Reynolds number,  $Re$ , relative roughness,  $\epsilon$  and nozzle-to-surface spacings,  $H$ . But jet Reynolds number,  $Re$ , Surface roughness,  $Ra$  Local and Average Nusselt number,  $Nu_x$  and  $\overline{Nu}$  were calculated by the following methods.

#### 3.4.1 Reynolds numbers calculation :-

$$\text{Specific weight of Air} = \gamma_{\text{air}} = \rho \times g = 1.12 \times 9.81 = 10.98 \text{ N/m}^2$$

$$\text{Specific gravity of the manometric fluid} = 0.784$$

$$\begin{aligned} \text{So, specific weight of manometric fluid, } \gamma &= 9810 \times 0.784 \\ &= 7691 \text{ N/m}^3 \end{aligned}$$

$$\text{Kinematic viscosity of air, } \nu = 1.45 \times 10^{-5} \text{ m}^2/\text{sec.}$$

$$\text{Reading from inclined manometer} = \Delta P$$

$$\text{So pressure head, } h_p = \Delta P / \gamma_{\text{air}}$$

$$\text{Velocity of air, } v = \sqrt{2gh_p}$$

$$\text{Reynolds number (Re)} = v d / \nu$$

### 3.4.2. Surface roughness calculation:-

$$\text{Center line average (Ra) in micrometer} = \frac{h_1+h_2+h_3+\dots+h_n}{n}$$

where,  $h_1, h_2, h_3, \dots, h_n$  are the ordinates measured on both sides of the mean line and  $n$  is the number of ordinates.

$$\text{Relative roughness, } \epsilon = R_a / d$$

### 3.4.3 Nusselt number calculation :-

$$\text{Dimensionless temperature, } \theta = (T-T_j)/(T_w-T_j)$$

where,  $T$  - local temperature after impingement

$T_j$  - Temperature of air at jet exit.

$T_w$ - Wall (plate) temperature at steady state.

$$\text{Heat flux, } q = -k_s(T_2-T_1)/dx$$

Here,  $k_s=54\text{w/m.c}$  for Mild Steel ( of 0.5%c) at  $100^0\text{c}$ .

Thus, Average heat flux,  $q=4016.25\text{w/m}^2$ .

$$\text{Local Nusselt number, } Nu_x = q.d/k_a(T-T_j)$$

Here,  $d = 0.0062 \text{ m}$ .

$k_a$ =Thermal conductivity of air at  $30^0 \text{ c}$

$$= 0.026 \text{ w/m.k}$$

$$\text{Average Nusselt number, } Nu = \sum Nu_x \cdot dx/L$$

## REFERENCE

1. Ali khan, M.M., kagasi, K., Hirata, M., and Nishiwaki, 1982, "Heat transfer augmentation in an axisymmetric impinging jet." Proceedings, 7<sup>th</sup> Int. Heat transfer conference, paper FC 6-3. pp-363-368.
2. Ali, M.A.T., Hassan, A., and Islam, M.T. "Turbulent boundary layer growth on a step changed smooth to rough surface." proceedings, 2<sup>nd</sup> annual paper meet, I.E.B., pp-106-122.
3. Ali, M.A.T. and Islam, O. 1982. "development of a turbulent flow in a smooth pipe following a rough pipe." I.E.B. Journal, vol-1 No-2. pp-2.
4. Arora, S.C., and domkundwar, s. "A course in Heat and mass transfer." Danpat Rai & Sons. Delhi.
5. Bouchez, J.P. and Goldstein, R.J., 1995. "Impingement cooling from a circular jet in a crossflow." Int. journal of heat and mass transfer. vol.-18. pp-719-730.
6. Bejan, A. 1993. "Heat transfer." John willy and Sons Inc.
7. Donaldson, C.D., Sndeker, R.S. And Margolis, D.P., 1971. "A study of free jet impingement. Part-2. Free jet turbulent structure and impingement heat transfer." Journal of Fluid mechanics. Vol-45. pp-477-512.
8. Eckert drake. "Heat and Mass transfer." 2<sup>nd</sup> edition. Tata Mcgrew Hill Book Co.
9. Frank, M. White- "Fluid Mechanics" 2<sup>nd</sup> edition Mcgrew Hill book Co. Int edition. 1988.
10. Gardon, R. and Akfirat, J.C. 1965. "The role of turbulence in determining the heat transfer characteristics of impinging jets." International Heat transfer conference. pp-1261-1272.
11. Gardon, R. and Carbonpue. 1961. "Heat transfer between a flat plate and jets of air impinging on it." International Heat transfer conference, part-2, pp-454-460.
12. Goldsten, R..J. and Bhabahni, A.I. "Impingement circular jet with and without crossflow." International journal of Heat and Mass transfer, Vol-25, pp-1377-1382.

13. Garmilla, S. V. and Rice, M. A., 1995, "Confined and submerged liquid jet impingement heat transfer." ASME journal of heat transfer. Vol-117. pp-871-877.
14. Gorshkov, G. I., 1984, "Near wall turbulence in jet impingement on a wall." Journal of applied mechanics, Tech. physics. vol-25. pp-233-241.
15. Huang, L. and EL-Gank, M. S., 1994. "Heat transfer of an impinging jet on a flat surface." International journal of heat and mass transfer, vol-37, pp-1915-1923.
16. Huber, A. M. and Viskent, R., 1994, "Effect of jet-spacing on convective heat transfer to confined, impinging array of axisymmetric air jet." International journal of heat and mass transfer. vol-37. pp-2859-2869.
17. Hollworth, B. R. and Gero, L. R., 1985, "Entrainment effects on impingement heat transfer: part-2.-local heat transfer measured." ASME journal of heat transfer, vol-107, pp-910-915.
18. Hollworth, B. R. and Durbin, M., 1989, "Impingement cooling of electronics." National heat transfer conference. HTD. vol-111. pp-89.
19. Hamadah, T. T., 1989, "Air jet impingement cooling of an array of simulated electronics packages." Proceedings, national heat transfer conference, HTD. vol-111. pp-97-105.
20. Hrycak, P., 1984, "Heat transfer from impinging jets to a flat plate with conical and ring protuberances." International journal of heat and mass transfer. vol-27. pp-2145-2154.
21. Hansen, L. G. and Webb, B. W., 1993, "Air jet impingement heat transfer from modified surfaces." International journal of Heat and mass transfer, vol-1-36. no.-4, pp-989-997.
22. Hossain, K. A. and Arora, R. C., 1997, "Flow characteristics of laminar slot jet impinging over a circular cylinder." Proceedings, 4<sup>th</sup> annual paper meet I.E.B. Mech. division, Paper no.-6, pp-51-57.
23. Hasan Altaf. 1984, "Study of turbulent boundary layer in a step change from smooth to rough surface." M.Sc. thesis, BUET, Dhaka.
24. Jambunathan, K. L. et al, 1992, "A review of heat transfer data for single circular jet impingement." International journal of heat and fluid flow. vol-13, pp-106-115



25. Jung-Yang san et al. ,1997,"Impingement cooling of a confined circular air jet." International journal of heat and mass transfer, vol-40, no-6,pp-1355-1364.
26. Jain, R.K." Mechanical and Industrial measurement." 4<sup>th</sup> edition. Khannapulishers, Delhi, India.
27. Jain,R.K. "Engineering Metrology" 4<sup>th</sup> edition, Khanna publishers, Delhi India.
28. John E. Freund & Ronald E. walpole,1987,"Mathametical statistics.4<sup>th</sup> edition,Prentice hall of India. New Delhi 110001.
29. Kataoka,K.and Mizushina,T.,1974," Local enhancement of the rate of heat transfer in an impinging round jet by free-stream turbulence." proceedings of 5<sup>th</sup> international heat transfer conference, vol-2, paper-FC8,3. pp-305-309.
30. Kline,S.J. and Mc-clintock,F.A.,1953, "Describing uncertainties in single sample Experiment." Mech. Engg.p-3.
31. Living,J.N.B. and Hrycak,P.,1973, "Impingement heat transfer from turbulent air jet to flat plates- a literature survey." NASA TM X-2778.
32. Mihita, 1987, "The effect of surface renewal due to large scale eddies on jet impingement heat transfer." International journal of heat and mass transfer, vol-30, pp-559-567.
33. Nikurades,J., 1950, "Laws of flow in rough pipes." NASA Technical memorandum, p-1292.
34. Obot, N.T.and Trabold, T.A.,1987, "Impingement heat transfer within arrays of circular jets: part-2, effects of cross-flow in the presence of roughness elements, Trans.ASME journal of Turbomachinary, vol-109, pp-594-601.
35. Ozisic "Heat transfer-A basic approach." McGrew Hill book Co.
- 36.Popiel, C.O. and Trass,O.,1982, "The effect of ordered structure of turbulence on momentum, heat and mass transfer of impinging round jets." Proceedings of 7<sup>th</sup> international conference of heat transfer. vol-6, pp-141-146.

37. Sparrow, E.M. et al, 1975, "Effect of nozzle surface separation distance on impingement heat transfer for a jet in a cross flow." ASME journal of heat transfer, vol-97, pp-528-533.
38. Steven, J and Webb, B.W., 1991, "Local heat transfer coefficients under an axisymmetric, single phase liquid jet." ASME journal of heat transfer, vol-113, pp-71-78.
39. ScLising, H., 1968, "Boundary-layer theory." 6<sup>th</sup> edition McGrew Hill Book Co .  
Newyork. USA.
40. Sharp, K.W.B. "Practical Engineering Metrology" Pitman publishers.
41. Tataoka, K., et al, 1978, "Enhancement mechanics of mass transfer in a turbulent impinging jet for high schmidt number." ASME paper no.-78, HF-5.
42. Thasher, L.W. and Binder, R.C., 1957, "A practical application of uncertainty calculation measured data." Transection ASME, pp-373-376.
43. Vennard and Streeter. "Elementary fluid Mechanics." 6<sup>th</sup> edition Jhone Willy and Sons.
44. Whitehead, A.W., 1976, "The effect of surface roughness on fluid flow and heat transfer." Ph.D. thesis. University of London.
45. Webb, B.W. and Lyte, D., 1994, "Air jet impingement heat transfer at low nozzle-plate spacing." International journal of heat and mass transfer. Vol-37, pp-1687-1697.
46. Yuan, S.W., 1967, "Foundation of fluid mechanics practice." -Hall Inc. Englewood cliffs, Newjersey.
-